Fakultät für Medizin

Institut für Zellbiologie des Nervensystems

Remodeling of the axoglial unit during early postnatal development

Mengzhe Wang

Vollständiger Abdruck der von der Fakultät für Medizin der Technischen Universität München zur Erlangung des akademischen Grades eines

Doctor of Philosophy (Ph.D.)

genehmigten Dissertation.

Vorsitzende/r: Prof. Dr. Arthur Konnerth

Betreuer: Prof. Dr. Thomas Misgeld

Prüfer der Dissertation:

1. Prof. Dr. Avraham Yaron

2. Prof. Dr. Stefan Lichtenthaler (schriftliche Beurteilung)

Priv.-Doz. Dr. Tim Czopka (mündliche Prüfung)

Die Dissertation wurde am 18.06.2018 bei der Fakultät für Medizin der Technischen Universität München eingereicht und durch die Fakultät für Medizin am 10.09.2018 angenommen.

ACKNOWLEDGEMENTS

To begin with, I would like to express my sincere gratitude to my supervisor, Prof. Thomas Misgeld, for his continuous support and guidance throughout my PhD study. His passion in science, immense knowledge, visions and creativity have always been immensely inspirational for me. Besides the brilliant scientific expertise, his presentation skills and attention to details have also provided an invaluable lesson for my future career. I could not have imagined having a better advisor and mentor.

My special thanks go to Dr. Monika Brill, who has always been there when I run into questions and difficulties along the way, generously providing help and console. I am sincerely grateful for all her insightful discussions and generous advices.

I would also like to thank the members of my thesis committee, Prof. Stefan Lichtenthaler and Prof. Avraham Yaron, for their valuable suggestions and support. They have always been encouraging and helpful along the way, many of their ideas helped me greatly in moving forward with my PhD project.

My sincere gratitude also goes to our technicians, Manuela and Nebi for taking great care of the mice, Kristina for performing the numerous genotyping, and Yvonne and Alex for taking care of the cloning and solution preparation. Their excellent work and reliable support have made my research experience way more enjoyable and uncomplicated than it otherwise could be.

I am also greatly thankful to the wonderful people I've met along the way, for the generous help they provided and the great fun we've had together: Antoneta, Caro, Eleni, Gabi, Laura, Leanne, Marina, Moni S., Natalia, Nic, Pui Shee, Selin, Shabab, Tatjana. A big thank-you also goes to colleagues in the Czopka, Kerschensteiner and Konnerth lab, for all the great discussions and collaborations we've had.

Finally, I would like to thank my family – my parents, and my husband Jun – for their unwavering love and support through thick and thin. I'm incredibly lucky to have you all in my life.

ABSTRACT

In many axonal populations, neurons first project exuberant branches and form excessive synapses with their target, before the surplus contacts are eliminated in an activity-dependent manner. The cessation of such developmental plasticity correlates with the onset of myelination, forming a precise, efficient and stable neuronal network. How the two processes – myelination and branch loss – relate to each other at the level of single axonal branches, however, remains largely unknown. The aim of my PhD project was to gain insights into this important interaction, by studying synapse elimination and myelination at the developing mouse neuromuscular junction (NMJ). Here excessive axonal branches are removed from multiply innervated NMJs in an activity-dependent manner until single innervation is established, while a simple and invariable myelination pattern forms, with individual glial (Schwann) cells being exclusively dedicated to sheathing one single axonal branch, which thereby becomes fully myelinated.

To investigate this phenomenon, I used pharmacological means, as well as genetic manipulations in knock-out and transgenic mice to screen for factors possibly influencing the remodeling process. Local pharmacological inhibition of cholinergic neurotransmission, which blocks the early stages of synapse elimination, also delayed myelination, suggesting that both processes depend either on each other, or on normal neuromuscular activity. I then used markers for labeling myelination progress, and developed a new assay to measure maturation of the nodes of Ranvier. A more detailed characterization of branch-specific myelination patterns demonstrated that indeed, axon branches that are still engaged in synaptic competition and hence remain plastic show delayed myelination and node maturation. However, when I directly correlated the progress of axon dismantling and myelination at single branches, and induced premature myelination by transgenic overexpression of the pro-myelinating factor, neuregulin (NRG1-III), I found surprisingly that myelination of competing

branches does not significantly affect pruning, and that such myelinating branches can still be dismantled. On the other hand, genetic ablation of the microtubule severing enzyme Spastin, which results in a delay of axon branch removal after competition, led to increased myelination of competing branches, suggesting the possible effect of competition status via microtubule dynamics and axonal transport on myelination. Together the data points to a model of activity-dependent synapse elimination mediated by branch-specific microtubule dynamics, which in turn modulate transport of myelinating factors such as NRG1-III, leading to a coordinated succession of myelination shortly after competition resolves.

ABSTRACT

In vielen axonalen Populationen senden Neuronen zunächst überzählige Verzweigungen in ihr Zielgebiet und bilden überschüssige Synapsen aus bevor diese Kontakte aktivitätsabhängig eliminiert werden. Der Abschluss dieser entwicklungsbedingten Plastizität korreliert mit dem Beginn der Bildung von Myelin (Myelinisierung) und trägt somit zur Ausbildung eines präzisen, effizienten und stabilen neuronalen Netzwerks bei. Wie die beiden Prozesse – Myelinisierung und Synapseneliminierung – auf der Ebene einzelner axonaler Verzweigungen miteinander in Beziehung stehen, ist jedoch weitgehend unbekannt. Das Ziel meiner Doktorarbeit war dementsprechend, Synapseneliminierung und Myelinisierung an der sich entwickelnden neuromuskulären Endplatte (NMJ) der Maus zu untersuchen und Einblicke in diese wichtige Interaktion zu gewinnen. Hier werden überschüssige axonale Äste von multi-innervierten NMJs entfernt während ein einfaches und unveränderliches Myelinmuster entsteht; dabei ummanteln einzelne Gliazellen (Schwann-Zellen) ausschließlich einen einzelnen axonalen Ast, sodass alle axonale Äste einzeln innerviert und vollständig myelinisiert werden.

Ich verwendete sowohl pharmakologische als auch genetische Manipulationen in Knock-out und transgenen Mäusen, um dieses Phänomen und die Faktoren, welche möglicherweise den Remodellierungsprozess beeinflussen, zu untersuchen. Lokale pharmakologische Hemmung von cholinerger Neurotransmission, welches frühe Stadien der Synapseneliminierung beeinflusst, verzögerte auch die Myelinisierung, was darauf hindeutet, dass beide Prozesse entweder voneinander oder von der normalen neuromuskulären Aktivität abhängen. Daraufhin verwendete ich Marker um die Entwicklung von Myelinisierung zu beobachten und entwickelte einen neuen Test zur Messung der Reifung von Ranvier'schen Schnürringen. Diese Untersuchungen ergaben, dass axonale Äste, die immer noch an synaptischer Konkurrenz beteiligt sind

und daher plastisch bleiben, eine verzögerte Myelinisierung und Schnürringreifung zeigten. Wenn ich jedoch den Fortschritt des Axonabbaus und der Myelinisierung von einzelnen Axonzweigen direkt korrelierte und eine vorzeitige Myelinisierung durch Überexpression des pro-myelinisierenden Proteins Neuregulin (NRG1-III) induzierte, fand ich überraschenderweise, dass die Myelinisierung den Synapseneliminierungsprozess nicht signifikant beeinflusst und dass solch myelinisierende Zweige noch abgebaut werden können. Andererseits führte die genetische Ablation des Mikrotubuli-destabilisierenden Enzyms Spastin, welches zu einer Verzögerung des axonalen Abbaus als letztem Schritt der Synapsenelimination führt, zu einer erhöhten Myelinisierung konkurrierender axonaler Äste. Dies deutet darauf hin, dass der Konkurrenzstatus einen Effekt auf die Myelinisierung hat, womöglich über die Dynamik von Mikrotubuli und axonalen Transport. Zusammengefasst deuten die Daten auf ein Modell der aktivitätsabhängigen Synapseneliminierung hin, die durch astspezifische Mikrotubulidynamiken vermittelt wird, die wiederum den Transport von Myelinisierungsfaktoren wie NRG1-III moduliert, was zu einer koordinierten Myelinisierung kurz nach dem Ende der Phase synaptischer Plastizität.

Table of Contents

1. INTRODUCTION 12

1.1. Synaptic pruning during early development 12

1.1.1. Activity-dependent competition 14

1.1.2. Dismantling of the losing axon 15

1.1.3. Removal of retreating axons 20

1.2. Myelination in the peripheral nervous system 24

1.2.1. Composition of Node of Ranvier 24

1.2.2. CNS and PNS myelin formation 26

1.3. Plasticity 27

1.3.1. Experience-dependent synaptic plasticity 27

1.3.2. Experience-dependent myelin plasticity 28

1.4. Aims 30

2. RESULTS 31

2.1. Screen of molecular factors affecting synapse elimination 31

2.1.1. Autophagy-related factor (Atg7) in SCs and neuron 32

2.1.2. Genetic delay of Wallerian degeneration (ΔNLS-Wld^S) 34

2.1.3. Genetic ablation of the caspase activating Bax 36

2.1.4. Engulfment-related factors (Elmo1, Megf10/11, PrS, Gas6) 36

2.1.5. Genetic ablation of the apoptosis-related factor Dr6 40

2.2. Correlation of myelination and synapse elimination 44

2.2.1. Activity blockade delays both synaptic pruning and myelination 44

2.2.2. Synaptic elimination and myelination coincide during development 46

2.2.3. Dynamics of molecular components at nascent nodes 50

2.3. Effects of myelinating factor on synapse elimination: would premature myelination narrow the “window of plasticity”? 55

2.3.1. Effect of premature myelination (Thy1:Nrg1-III) 55

2.3.2. AAV9-mediated Nrg1-III deletion ($Nrg^{FL/FL}$;TdTomato + iCre) 56

2.4. Effects of branch pruning events on myelination: does myelination convey an advantage in competition? 58

2.4.1. Initiation of myelination vs. NMJ territory 58

2.4.2. Initiation of myelination vs. axon diameter 60

2.4.3. Competition status of neighboring branches 62

2.5. How does synapse elimination delay myelination? Potential mechanisms 63

2.5.1. AAV9-mediated Spastin ablation ($Spastin^{FL/FL}$;TdTomato + iCre) 63

2.5.2. Spastin deletion combined with postsynaptic activity block 65

2.5.3. Is axonal transport affecting myelination? 66

3. DISCUSSION 70

3.1. Molecular factors affecting synapse elimination 71

3.1.1. Atg7 deletion did not affect synapse elimination 73

3.1.2. Wallerian degeneration and caspase mediated pruning 75

3.1.3. Engulfment-related factors 76

3.1.4. Apoptosis-related factors 78

3.2. Competition status delays initiation of myelination 80

3.2.1. Activity blockade delays both synapse elimination and myelination 80

3.2.2. Competing branches shows less initiation of myelination 81

3.2.3. Myelination initiation is delayed on competing branches 82

3.2.4. Myelinated axon branches are not favored in competition 83

3.3. Mechanism of synapse elimination and myelination interaction 85

3.3.1. Premature myelination does not affect synaptic pruning 86

3.3.2. Modulated synaptic pruning affect myelination 87

3.3.3. Tools for modulating axonal transport 88

3.4. Model: Activity coordinated myelination following competition 90

3.5. Outlook: Further experiments to consolidate the model 93

3.6. General conclusions 95

4. MATERIALS AND METHODS 97

4.1. Animals 97

4.2. Mouse genotyping 98

4.3. Neonatal AAV-injection (Az55.2-1-54-2532-58-2016) 99

4.4. Western blot 99

4.5. Immunohistochemistry and confocal microscopy 100

4.6. Ex vivo imaging of the triangularis sterni explant 101

4.7. Fluorescence recovery after photobleaching (FRAP) 101

4.8. Image processing and analysis 102

4.9. Statistics 103

4.10. Buffers and solutions 103

5. PUBLICATIONS 106

6. CONTRIBUTIONS TO EXPERIMENTAL WORK 107

7. REFERENCES 108

Abbreviations

AAV9	adeno-associated virus serotype 9
AChR	acetylcholine receptor
ATG	autophagy
ASD	autism spectrum disorders
BAI1	brain angiogenesis inhibitor 1
BTX	bungarotoxin
Caspr	contactin-associated protein
CBD	cargo-binding domain
ChAT	choline acetyltransferase
CNS	central nervous system
CNTN2	contactin-2
din	doubly innervated NMJ
DOCK180	180-kDa protein downstream of CRK
DR6	death receptor 6
ELMO1	Engulfment and cell motility 1
FL	flox
FRAP	fluorescent recovery after photobleaching
GAS6	growth-arrest-specific 6
KHC	kinesin heavy chain
KO	knock-out
MBP	and myelin-basic protein
MEGF10/11	multiple EGF Like Domains 10/11
MFGE8	milk fat globule EGF factor 8 protein
MPZ	myelin protein zero
Nav	voltage-gated sodium channel

NLS	nuclear localizing sequence
NMJ	neuromuscular junction
Nmnat1	nicotinamide mononucleotide adenylyltransferase 1
Nrg1-III	neuregulin 1 type III
rebu	retraction bulb
PNS	peripheral nervous system
PLP	Proteolipid protein
PrS	protein S
Rac1	Ras-related C3 botulinum toxin substrate 1
sin	singly innervated NMJ
(t)SC	(terminal) Schwann cell
WD	Wallerian degeneration

1. INTRODUCTION

The nervous system is one of the most fascinating evolutionary inventions of the multicellular animals, which detects ambient signals, coordinates the animal's behavior in response and allows the animal to adapt rapidly to variations in the environment. On the cellular level, the nervous system consists of the signal-transducing neurons, communicating with their distant target in a rapid and precise manner; and the supporting glial cells, which forms the insulating sheaths, support signaling and provide nutrition and trophic factors for neurons (Kandel, Schwartz and Jessell, 2013). How such coordinated neuron-glia units are established during development and modified in response to environmental signals have long been the focus of research, however, many details of the variable sequence of events and much of the underlying regulation mechanisms remain elusive. With technical advancement in genetic manipulations, fluorescent labeling and light-microscopy imaging, it is now possible to study this immensely complicated process with cellular and even subcellular resolution *in situ*.

1.1. Synaptic pruning during early development

One of the most astounding phenomena of the nervous system is how neurites project long-distances through the body and still connect with high specificity to their targets. Such precise wiring of neurons to their target cells is also of pivotal importance to the proper functioning of the nervous system. How such intricate and specific connection is established has been a fascination for generations of neuroscientists, since the days of Ramon y Cajal (Cajal, 1911) to the present.

One simple and elegant explanation is the chemoaffinity theory (Sperry, 1963), which postulates that neurons, each with their specific assembly of molecular codes, navigate to and recognize their targets via attracting and repulsing local cues (Schuldiner and Yaron, 2015). A variety of such molecular cues have been discovered and validated across different animal models, revealing a sophisticated scenario of

receptor and ligand interactions directing correct wiring during development of the nervous system (Seiradake, Jones and Klein, 2016).

However, accumulating evidence also suggest that neurons do not always connect permanently during the initial attempt at wiring. Rather, as a common strategy, the neurons would first project exuberantly and form excessive synapses with their target, before the surplus contacts are eliminated (or “pruned”) in an activity dependent manner (Cohen-Cory, 2002). This pruning mechanism allows for postnatal refinement and plasticity in the developing and adult nervous systems (Luo and O’Leary, 2005).

One well-studied system for this process is the developing visual system, where input from both eyes converge onto shared target cells in the primary visual cortex at birth, then segregate to different cortical neurons through activity-dependent remodeling during the critical period (Wiesel *et al.*, 1963; Hubel and Wiesel, 1970). Here a crude initial connectivity patterns is first established with the help of guidance cues and intrinsic spontaneous retinal waves, before subsequent refining based on visual experience, resulting in a mature functional network (Sengpiel and Kind, 2002).

To understand this phenomenon at the level of individual synapses, the vertebrate peripheral nervous system (PNS) provides a more readily accessible model compared to the central nervous system (CNS). At the developing mouse neuromuscular junction (NMJ, **Figure 1A**), more than 10 different axonal branches can converge on each endplate immediately after birth (Tapia *et al.*, 2012). During the first two postnatal weeks, most superfluous branches are rapidly removed from the multiply innervated NMJs, until each muscle fiber is innervated by a single terminal branch (**Figure 1B,C,** Balice-Gordon and Lichtman, 1993). Interestingly, time-lapse imaging shows that the excessive axonal branches are not removed through axon retraction or Wallerian-like fragmentation, but rather through axosome shedding, with the remnants engulfed by the surrounding Schwann cells (SC, Bishop *et al.*, 2004). Finally, this process of synapse elimination establishes one-to-one connectivity between axonal branches and

muscle fibers, which will consolidate and remain till adulthood (Keller-Peck *et al.*, 2001; Wyatt and Balice-Gordon, 2003).

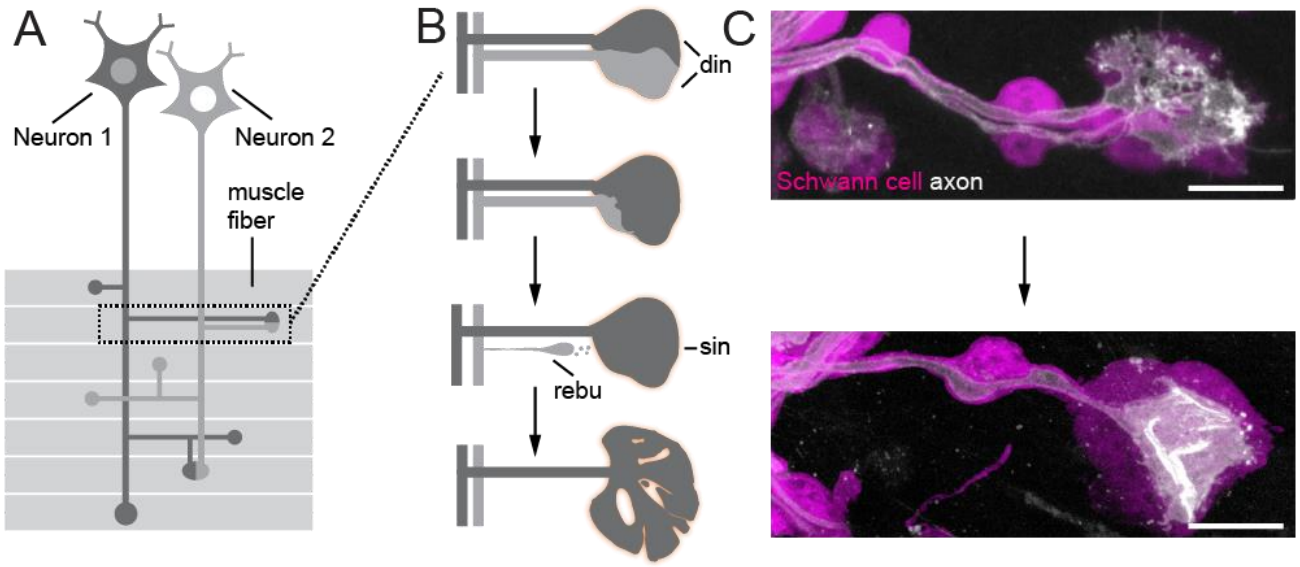

Figure 1: Synaptic pruning at the mouse NMJ during development. **A:** Schematic illustration of two developing motor neurons innervating muscle fibers; **B:** Schematic illustration of two terminal branches converging on the same NMJ (doubly innervated NMJ, or "din"), with one losing its territory to the competing partner and eventually forming a retraction bulb ("rebu") before disappearing, leaving its partner to expand and consolidate the connection NMJ (singly innervated NMJ, or "sin"); **C:** Example of a doubly-innervated (upper) and a singly-innervated NMJ (lower), with axons and terminals (*Thy1:Brainbow 1.1*, white) covered by SCs (*plpGFP*, magenta). Scale bar = 10 µm.

1.1.1. Activity-dependent competition

During the progress of synapse elimination, the proportion of territory occupied by the competing innervating branches shifts towards the winning branch progressively, making the terminal area occupied by each branch an indicator for the likely outcome of competition (Walsh and Lichtman, 2003). The axon diameter of the terminal branches also changes proportionally to the percentage of the respective occupied terminal area, and the losing axon becomes increasingly atrophic before eventually retreating from the terminal (Keller-Peck *et al.*, 2001). The process has been found to depend neuromuscular activity with the stronger input biased to win and lastingly innervate the synapse (Buffelli *et al.*, 2003). Prohibiting neurotransmission activity,

either by curare injection blocking the postsynaptic acetylcholine receptors (AChR, Loeb *et al.*, 2002; Loeb, 2003), or by genetic ablation of choline acetyltransferace (ChAT, Misgeld *et al.*, 2002; Buffelli *et al.*, 2003), results in excessive axonal sprouting and delayed synapse elimination. Genetic overexpression of inward rectifying potassium channels, while increasing axonal conductance, inhibits evoked activity in the muscle fibers, which also leads to persistence of poly-innervation (Favero *et al.*, 2009). Even in adult animals, blocking axonal sodium channel activity with tetrodotoxin was found to induce excessive sprouting and poly-innervation during PNS regeneration after nerve crush (Ribchester, 1993).

How the synaptic strength of the innervating terminals is decoded and compared remains largely unknown. On one hand, terminal branches belonging to the same neuron tend to have the same competition outcome if co-innervating with branches of another motor-unit, and branches of a neuron with larger arborization are more likely to lose against neurons with smaller arborizations, showing that distribution of axonal resources may impact competition outcome (Kasthuri and Lichtman, 2003). On the other hand, intracellular calcium fluxes in the terminal SCs are shown to reflect the relative synaptic strength of the competing branches, suggesting that SCs are capable of decoding neuronal activity and probably actively participate in the eliminating process (Darabid, Arbour and Robitaille, 2013; Darabid, Perez-Gonzalez and Robitaille, 2014). The losing terminal branch undergoes branch-specific microtubule severing and transport loss, before becoming dismantled and engulfed by the surrounding SCs (Brill *et al.*, 2016).

1.1.2. Dismantling of the losing axon

When competition is resolved, one or more of the axons innervating the terminal NMJ become atrophic and are retracted until single innervation is established. The

retraction of inappropriate connecting terminal branches is an active process, and the molecular pathways involved is not yet known. Possibly a lack of trophic signals promotes the distal dismantling of the pruned axons, which is similar to other degenerative processes during pathology, such as Wallerian degeneration (Gillingwater and Ribchester, 2001; Raff, Whitmore and Finn, 2002). The mTOR (mammalian target of rapamycin)-dependent macroautophagy (later referred to as autophagy) is found to correlate with synaptic pruning deficits implicated in autism spectrum disorders (ASDs, Tang *et al.*, 2014). Whether these processes share similar molecular mechanisms remains to be investigated.

1.1.2.1. Autophagy

Autophagy is a highly regulated cellular degradation process in response to nutrient deprivation and cellular stress, and its activation has been implicated in acute neuronal injury as well as various neurodegenerative diseases (Rubinsztein *et al.*, 2005). On the other hand, autophagy is also found to be important for the turn-over of proteins and organelles, thus protective against neurodegeneration in the CNS (Yue, Qing and Komatsu, 2008). It has been reported in children that spine pruning defects were found with autism spectrum disorders (ASD), and the spine pruning deficit shown in the ASD mouse model can be corrected with modulations affecting autophagy (Tang *et al.*, 2014).

The autophagy machinery with various autophagy related proteins (so-called ATGs) was first dissected in yeast, with many of the molecules conserved in higher eukaryotes (Levine and Klionsky, 2004). Specifically in mammals, Unc-51-like kinase1/2 (ULK1/2), negatively regulated by mTOR, forms a complex with ATG13, FIP200 and ATG101 to initiate autophagosome formation; the phosphatidylinositol 3-kinase complex (PI3K) produces phosphatidylinositol 3-phosphate on preautophagosomal structure for initiating vesicle nucleation (Levine and Klionsky, 2004; Mizushima, Yoshimori and

Ohsumi, 2011). Deletion of Beclin1 of the PI3K complex severely alters the autophagy response and affects tumor suppression (Qu *et al.*, 2003; Yue *et al.*, 2003). The two conjugation systems, ATG12-ATG5-ATG16L1/2 and LC3, then enable vesicle expansion and completion, with the E1-like enzyme ATG7 shared between the two systems (**Figure 2**, Mizushima, Yoshimori and Ohsumi, 2011). Ubiquitous knock-out of *Atg5* and *Atg7* in mice results in neonatal mortality, due to severe nutrition and energy deficiency (Kuma *et al.*, 2004; Komatsu *et al.*, 2005). Neuronal deletion of *Atg5* leads to progressive neurodegeneration after 3 weeks, paralleled by intracellular protein aggregation (Hara *et al.*, 2006). Neuronal ablation of *Atg7* causes massive neuronal dystrophy in the CNS, with membrane abnormality and cell death in Purkinje cells and midbrain dopamine neurons (Komatsu *et al.*, 2006, 2007; Friedman *et al.*, 2012), and its deletion in SCs results in myelin clearance delay after peripheral nerve injury (Jang *et al.*, 2016). The autophagosome fuse with lysosome to degrade and eventually recycle the cellular material (Levine and Klionsky, 2004). LC3-positive autolysosomes have been found both in the retreating axon and the associated SCs during synaptic pruning (Song *et al.*, 2008). Autophagy is therefore important both for intracellular degradation under resource constraints, and for long-term maintenance of cellular structures. Whether manipulating the autophagy-related factors in axons and/or SCs affect developmental pruning therefore becomes an intriguing question.

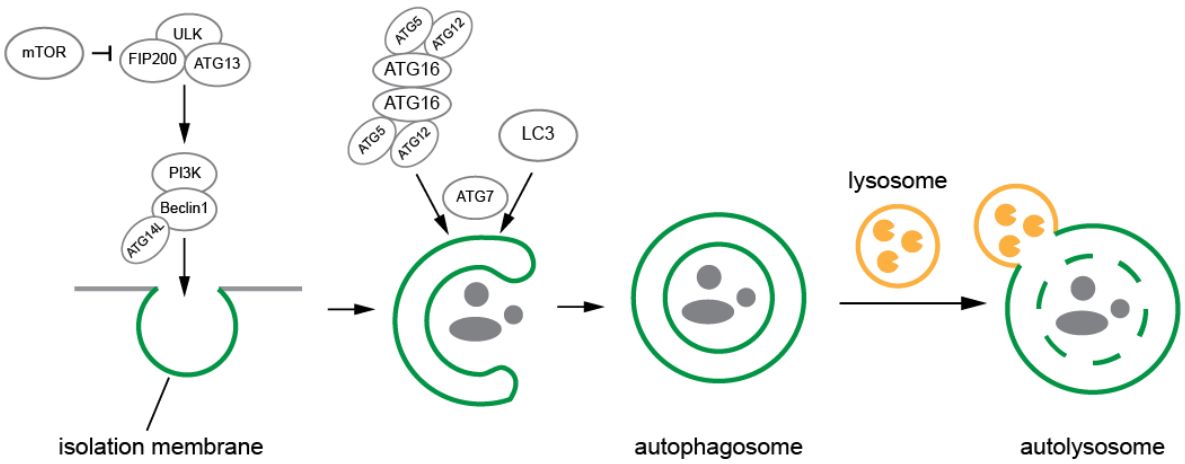

Figure 2: Autophagy pathway and the participating protein complexes (modified from Green and Levine, 2014).

1.1.2.2. Wallerian degeneration

The process of developmental axon branch removal shows some similarities with post-traumatic Wallerian degeneration (WD), which is characterized by axonal fragmentation distal to an axonal transection, followed by breakdown of the myelin sheath and subsequent phagocytosis by SCs and invading macrophages (Gillingwater and Ribchester, 2001). Neoexpression of the of the so-called “Wallerian degeneration slow” protein (Wld^S), a fusion between a fragment of the E4-type ubiquitin ligase, Ube4b, and an enzyme of the nucleotide biosynthetic pathway, nicotinamide mononucleotide adenylyltransferase 1 (*Nmnat1*), substantially delays WD after axotomy in adult mice (Coleman and Freeman, 2010). Despite the similarities between Wallerian degeneration and developmental pruning, in Wld^S mice there is no delay in neuromuscular synapses elimination (Parson, Mackintosh and Ribchester, 1997). Similarly, developmental pruning in the retinocollicular projection and cortical Layer 5 projection is not affected by Wld^S, either (Hoopfer *et al.*, 2006). However, the γ neuron pruning in *Drosophila*, albeit not affected by Wld^S expression, requires the ubiquitin-protease system, similar to the axonal degeneration in response to injury (Watts, Hoopfer and Luo, 2003). Thus, it was concluded that developmental and post-traumatic axon dismantling are regulated by distinct molecular execution programs, although data do not exclude the possibility of common upstream mechanisms that dictate axon-autonomous degeneration, such as the disruption of axonal transport (Gillingwater and Ribchester, 2001; Hoopfer *et al.*, 2006). Interestingly, the expression of *Nmnat1* – which mimics Wld^S – was found to delay axonal degeneration induced by oxidative stress and mitochondrial failure (Press and Milbrandt, 2008). Disruption of mitochondria transport was selectively found in retreating axon branches during developmental synapse elimination (Brill et al., 2016) – thus mitochondrial failure might contribute to developmental axon branch pruning. Since deletion of the nuclear localization sequence (NLS) of Nmnat1 was shown to enhance the neuroprotective

effect of the Wld^S protein (Beirowski et al., 2009), a reexamination of the role of the Wallerian-like pathway in developmental synapse elimination seems timely, taking advantage of expressing the *ΔNLS-Wld^S* construct. We therefore obtained mice carrying the *ΔNLS-Wld^S* allele and expressed it in motor neurons to measure the progress of neuromuscular synapse elimination.

1.1.2.3. Local activation of caspases

Caspases are a family of proteases playing a central role in programmed cell death (more details see Section 1.1.3.2). Here we focus on the non-apoptotic local caspase activation, which has been linked to developmental pruning in various model systems (Miura, 2016). During *Drosophila* metamorphosis, degenerating dendrites undergoing pruning show caspase activity, and suppressing the caspase degradation machinery is found to prevent dendritic removal (Kuo *et al.*, 2006; Williams *et al.*, 2006). Caspase activity is also present locally at branch points of young zebrafish retinal ganglion cells, modulating the arborization remodeling process (Campbell and Okamoto, 2013). In mouse dorsal root ganglion culture, caspase activation is present during neuronal growth factor deprivation induced degeneration, and can be blocked by deleting the upstream regulator *Bax* (Schoenmann *et al.*, 2010).

Bax, a member of the *Bcl-2* family genes, is a potent activator of the intrinsic mitochondrial apoptotic pathway, leading to activation of the executing caspases (Karbowski et al., 2006). Deletion of *Bax* in mice (Knudson et al., 1995) increases the number of neurons or axons in many parts of the nervous system: in the CNS, the dentate gyrus (Sun, 2004), the Purkinje cell layer of the cerebellum (Fan, Favero and Vogel, 2001) and the optic nerves (White et al., 1998); as well as in the PNS, sympathetic (Deckwerth et al., 1996), motor and sensory nerves (White et al., 1998). *Bax* knock-out could also prevent oligomeric β-amyloid induced cell death (Kudo et al., 2012). Specifically during development, *Bax* deletion was found to suppress Caspase-

3 activity during the elimination of embryonic sensory neuron (Schoenmann *et al.*, 2010). The effect of *Bax* deletion on branch pruning at the NMJ remains to be probed.

1.1.3. Removal of retreating axons

Clearance of the axonal remnants ("axosomes") that retreating axons leave behind is part of the final stage of the pruning process, which involves glial SCs engulfing the axosomes (Bishop *et al.*, 2004; Ko and Robitaille, 2015). Whether SCs play an active role monitoring and assisting the dismantling of the retreating branch, or passively react to axonal fragments has yet to be resolved (Luo and O'Leary, 2005). Moreover, since SCs cover all the individual axons before retraction, disappearance of the terminal branches also results in loss of SCs originally wrapped around these stretches of axon. Whether these SCs relocate to persisting branches, are removed by macrophages or other SCs, or undergo apoptosis remains to be investigated.

1.1.3.1. Engulfment

Glial engulfment of axon debris has been observed in various synaptic pruning scenario besides in the mouse NMJ, such as remodeling of γ neuron in the Drosophila mushroom body during metamorphosis (Watts et al., 2004), microglial removal of apoptotic neurons in embryonic zebrafish brains (Mazaheri et al., 2014), and glial clearance of degenerating sensory neurons in the developing mouse dorsal root ganglia (Wu et al., 2009), as well as astrocyte mediated refinement of retinogeniculate connections (Chung et al., 2013).

Various signaling factors have been identified to be relevant for the process. The axonal debris or cell corpses may express surface molecules such as phosphatidylserine, to be bound by soluble bridging molecules, such as the growth-arrest-specific 6 (GAS6) and protein S (PrS), which are then recognized by receptors on the phagocytes (Wu et al., 2005; Hafizi and Dahlbäck, 2006).

After target recognition, an intracellular signaling cascade is activated to reorganize the cytoskeleton of the phagocyte, enabling engulfment. One pathway consists of ELMO1 (Engulfment and cell motility 1) binding to DOCK180 (180-kDa protein downstream of CRK), which activates the small GTPase Rac1 (Ras-related C3 botulinum toxin substrate 1), mobilizing the cytoskeleton to phagocytose the target debris (Ravichandran and Lorenz, 2007). Another engulfment pathway involves MEGF10 (Multiple EGF Like Domains 10) and potentially its isoforms (MEGF11 and 12), the mammalian homolog of nematode CED-1 and *Drosophila* Draper, which interacts with the clathrin assembly protein complex 2 medium chain, inducing protein sorting into endocytic vesicles (**Figure 3**, Suzuki and Nakayama, 2007).

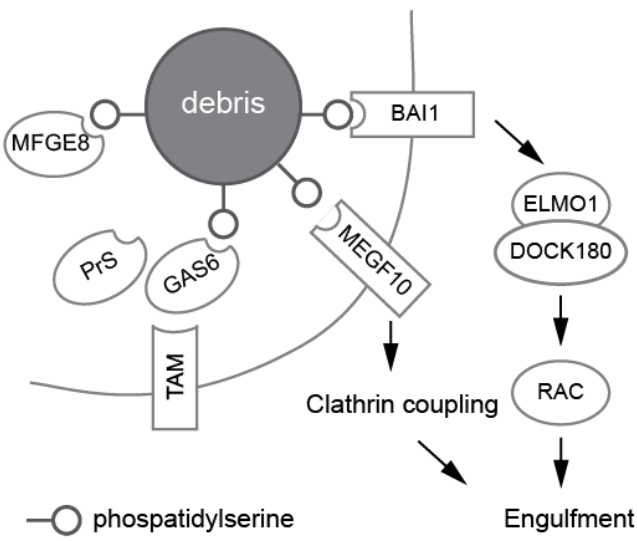

Figure 3: Engulfment pathways with the participating receptors and protein complexes (modified from Ravichandran and Lorenz, 2007).

Among these factors, mice with deletion of *Elmo1*, *Gas6* and *PrS*, as well as *Megf10* and its homolog *Megf11* were obtained, which enabled me to observe how disrupting each of the major engulfment pathways would affect synaptic pruning during development.

1.1.3.2. Apoptosis

Apoptotic death of oligodendrocytes is a common phenomenon during CNS development, due to competition for limited trophic factors (Barres et al., 1992; Raff et al., 1993). Similarly in the PNS, SCs are found to undergo rapid apoptosis in response to denervation in neonates, which can be prevented by glial growth factors (Trachtenberg and Thompson, 1996). During early development, apoptotic SCs in the rat sciatic nerves are occasionally found in the first postnatal weeks, approximately 0.2% on P3, and none were found in adult (Grinspan et al., 1996; Syroid et al., 1996). SCs are sorted along the motor axons so that each axon is wrapped by a chain of individual myelinating SCs, and hence the number of SCs must be tightly controlled to maintain this strict correlation with axons (Syroid et al., 1996). This implies that as exuberant terminal branches are pruned back, the SCs originally covering the pruned axon stretch likely disappear, but the means by which this happens is not known. Three obvious possibilities that I tried to disambiguate are, whether these excessive SCs relocate to surviving branches, undergo apoptosis, or are cleared by other phagocytes.

There are two main pathways of apoptosis, one is the intrinsic pathway responding to various stimuli, regulated by proteins of the Bcl-2 family, which alter mitochondrial membrane permeability, thus controlling cytoplasmic release of the pro-apoptotic factor, cytochrome c; the other is the extrinsic pathway initiated by death receptors, which bind to apoptosis-inducing ligands and then activate Caspase-8. Both pathways lead to the activation of execution caspases such as Caspase-3, ending in DNA fragmentation and cytoskeletal reorganization, forming apoptotic bodies ready for clearance (**Figure 4**, Raff *et al.*, 1993; Elmore, 2007).

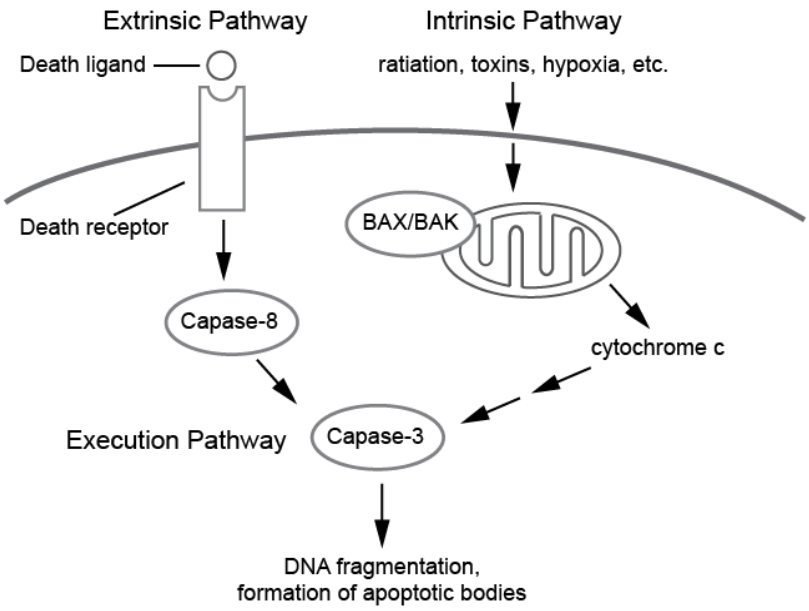

Figure 4: Extrinsic and intrinsic apoptosis pathways with the participating proteins illustrated, activating the execution pathway (modified from Elmore, 2007).

The factor involved in mitochondria-mediated intrinsic pathway leading to apoptosis has been discussed above in Section 1.1.2.3. Since the apoptotic effect of *Bax* is overlapping with *Bak*, and show severe developmental deficits only when both factors are knocked out (Lindsten *et al.*, 2000), we focused on death receptor 6 (*Dr6*) knock-out mice to test for the possible effects of apoptosis on matching SC numbers to remodelling axon branches. DR6 is a member of the death receptor family as well as the TNF receptor superfamily, and is widely expressed in both CNS and PNS neurons and glial cells (Nikolaev et al., 2009; Mi et al., 2011). DR6 has been shown to be required for activation of retinal axon pruning during development (Nikolaev et al., 2009) and Wallerian degeneration after injury (Gamage et al., 2017) while attenuating oligodendrocyte maturation and myelination (Mi et al., 2011). Whether DR6 contributes to SC organization during the developmental pruning process remains to be investigated.

1.2. Myelination in the peripheral nervous system

Another major event of the axoglial remodeling process, besides synaptic elimination, is myelination. The propagation of action potential in unmyelinated axons can be described using the Hodgkin–Huxley model, where conduction velocity is directly proportional to the axonal diameter (Hodgkin and Huxley, 1952), which suffices to enable swift conduction in animals with relatively small body size, such as most invertebrates. Myelination, the formation of an electrically insulating layer by specialized glial cells around axons, is a transformative vertebrate acquisition (Zalc, Goujet and Colman, 2008). The plasma membrane of oligodendrocytes in the CNS, and SCs in the PNS, wraps tightly around stretches of axons forming multi-layered myelin sheath, leaving intervals known as nodes of Ranvier. This allows fast saltatory conduction of action potential, which dramatically improves conduction velocity with limited diameter increase during development (Vabnick and Shrager, 1998) and also reduces energy requirements, thus helping maintain axonal integrity (Simons and Trotter, 2007).

1.2.1. Composition of Node of Ranvier

Myelinated axons are organized into domains with distinct molecular composition: node, paranode, juxtaparanode and internode (**Figure 5**), which also show differences regarding cytoskeleton, organelle distribution and local axonal transport rate (Salzer, 2003). The node of Ranvier is the site where action potentials generated at the axon initial segment are regenerated (Huxley and Stämpeli, 1949), enabled by a 25-fold enrichment of voltage-gated sodium channels (Nav; Hille, 2001). The concentration and retainment of Nav at nodes is ensured by the septate-like junctions in the paranodal region (Rasband and Peles, 2016), where myelinating cells express the 155-kDa isoform of neurofascin (NF-155), forming a complex with contactin and contactin-associated protein (Caspr) anchored in the axonal membrane (Charles *et al.*,

2002). The region next to the innermost paranodal junction is the juxtaparanode, enriched in delayed-rectifier potassium channels (Kv1), which are important for repolarization and maintaining the internodal resting potential (Peles and Salzer, 2000). The axonal complex formed by contactin-2 (also known as TAG-1) and Caspr2 helps ensure the proper clustering of Kv1 (Poliak *et al.*, 2003). The internodal region consists of compact myelin sheaths wrapping around the axolemma, and specific lipid-interacting proteins are required to create and maintain the lipid-rich myelin composition. Proteolipid protein (PLP) and myelin-basic protein (MBP) are major myelin components in the oligodendrocytes (Simons and Trotter, 2007), while myelin protein zero (MPZ) is the most abundant myelin protein in the SCs, responsible for myelin compaction and stability (Giese *et al.*, 1992). Together, the molecular organization of myelin subdomains is hallmark for proper myelination, and is essential for the saltatory action potential propagation of myelinated fibers (Rasband and Shrager, 2000).

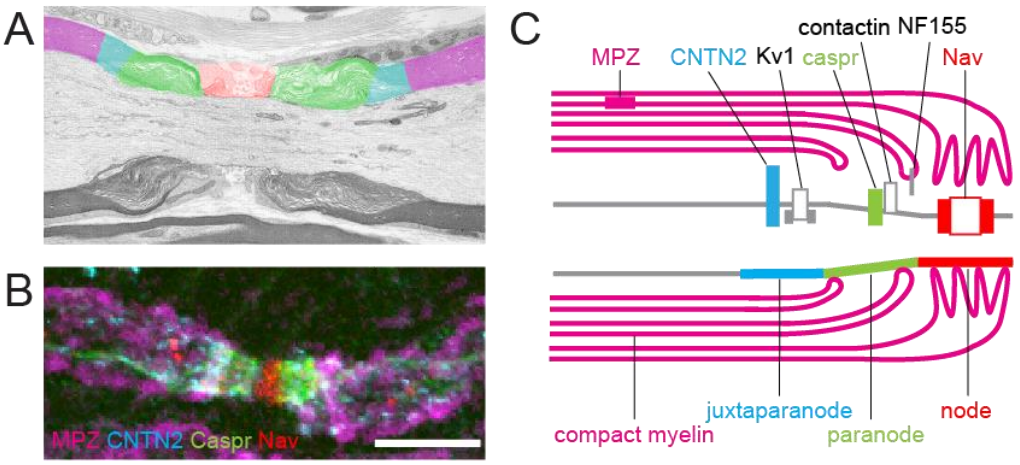

Figure 5: Structure of the node of Ranvier. **A:** Longitudinal view of the Node of Ranvier in the spinal dorsal root of rat, node pseudo-colored in red, paranode in green, juxtaparanode in cyan and internode in magenta; **B:** Immunostaining of nodal structures in an adult mouse *triangularis sterni* motor axon, antibodies against Nav in red, Caspr in green, CNTN2 in cyan and MPZ in magenta (in image); **C:** Schematic illustration of nodal structure and prominent molecular components. Electron micrograph modified from Fields and Stevens-Graham, 2002.

1.2.2. CNS and PNS myelin formation

The CNS and PNS myelin share structural similarities, but also differ in the structural protein composition and the control of myelination, indicating convergent cellular evolution (Nave and Werner, 2014).

In the CNS, oligodendrocyte precursors migrate as oligodendrocyte progenitor cells into the brain and extend numerous processes to myelinate up to 40 separate myelin segments on different axons (Simons and Trotter, 2007). The decision to myelinate for oligodendrocytes is closely correlated to axon diameter. *In vitro* study shows that structures above the threshold of 0.3 ~ 0.4 μm is sufficient to trigger oligodendrocyte wrapping and ensheathing (Lee *et al.*, 2012). But inhibitory signals repellent for oligodendrocyte, or attractive cues to stabilize contact between oligodendrocytes and axons, can potentially regulate myelination in addition to axon diameter (Chang, Redmond and Chan, 2016).

For the PNS, SC precursors develop into immature SCs before birth, and are sorted to individual axons covering the peripheral nerves, which then become myelinating or non-myelinating SCs (Monk, Feltri and Taveggia, 2015). Specifically in motor neurons, each terminal branch is individually wrapped by myelinating axonal SCs, and the endplate is covered by non-myelinating terminal SCs (Trachtenberg and Thompson, 1997). In contrast to oligodendrocytes, SCs typically myelinate axons with diameter larger than 1 μm (Voyvodic, 1989; Peters, Palay and Webster, 1991), and the initiation of myelination is directed by the amount of neuregulin-1 type III (NRG1 type III) present at the axonal surface (Taveggia *et al.*, 2005). Specifically, conditional deletion of ErbB2 in myelinating SCs or reduction of NRG1 type III level in axons inhibit SC myelination (Garratt *et al.*, 2000; Michailov *et al.*, 2004). In converse, overexpression of NRG1 type III in transgenic mice induces hypermyelination (Michailov *et al.*, 2004) and its ectopic expression induces myelination in non-myelinating SCs (Taveggia *et al.*, 2005).

1.3. Plasticity

The nervous system is remarkable in its ability to adapt based on activity-dependent structural changes. Such plasticity underlies disparate phenomena, such as formation of well-adjusted muscle innervation in the PNS, as well as memory formation, learning and adaptation in the CNS. While nervous system plasticity is generally discussed as consequence of synaptic potentiation, depression or remodeling, more recent data suggest that plasticity of axons, and especially their myelin could also substantially contribute to plastic changes in the nervous system (Pajevic, Basser and Fields, 2014; Chang, Redmond and Chan, 2016; Mount and Monje, 2017). However, the mechanisms of such neuro-glial plasticity are still under intensive scrutiny, and much less is known about how they relate to synaptic plasticity and proper remodeling.

1.3.1. Experience-dependent synaptic plasticity

Several kinds of plasticity have been discovered in the recent years, especially in the CNS. To name a few: the Hebbian concept of plasticity proposes that repeated or persistent simultaneous activation of neuron and its target cell increases the synaptic strength between them (Hebb, 1949). This principle has been demonstrated in various systems, such as the eye-specific segregation of cortical neurons (Wiesel *et al.*, 1963; Hubel and Wiesel, 1970; Feller, 2002), long-term potentiation of excitatory synapses in the hippocampus, and the maturation of neuromuscular junctions in the PNS (Bliss and Gardner-Medwin, 1973; Bliss and Lømo, 1973). Additional forms of synaptic plasticity include the homeostatic plasticity, or synaptic scaling, where the strength of all of a neuron's excitatory synapses are adjusted in a negative feedback system to stabilize firing (Turrigiano, 1999), which has been shown in spinal, neocortical and hippocampal pyramidal excitatory neurons (Turrigiano, 2008). Another possibility is metaplasticity, a change in the ability of the neuron to undergo subsequent synaptic plasticity, or "the plasticity of synaptic plasticity" (Abraham and Bear, 1996). This form

of plasticity has been demonstrated in hippocampal CA1 neurons, dentate gyrus and the lateral performant path (Abraham, 2008).

In the synaptic elimination process of the peripheral system, however, the less active connections are punished and dismantled, leaving the whole terminal to its more active competitor, in contrast to the Hebbian competition (Lichtman and Balice‐Gordon, 1990; Sanes and Lichtman, 1999). The microtubule in the losing terminal branch becomes severed and the axonal transport halted, progressively lose its connecting territory (Brill *et al.*, 2016), while the diameter and synaptic territory of the more active branch grow until covering the whole NMJ (Keller-Peck *et al.*, 2001; Walsh and Lichtman, 2003). The molecular mechanisms behind the detection and comparison of local input strength remains to be dissected. It has been shown that calcium signals in the terminal SCs reflects the relative synaptic strength of the competing branches, suggesting that SCs may play an active role in the decoding and decision making of branch elimination (Darabid, Arbour and Robitaille, 2013; Darabid, Perez-Gonzalez and Robitaille, 2014; Ko and Robitaille, 2015).

1.3.2. Experience-dependent myelin plasticity

The stability of myelin is crucial to ensure rapid conduction of action potential and axonal integrity, while delayed myelination can lead to developmental delay of motor and cognitive functions in children (Pujol *et al.*, 2004). It has been shown that in the mature brain, myelination can consolidate neural circuitry by suppressing plasticity (McGee *et al.*, 2005). However, oligogenesis and formation of new myelin is found to continue well into adulthood (Richardson *et al.*, 2011), with myelination in the prefrontal cortex even into the third decade of human life (Yakovlev and Lecours, 1967). Instead of a static structure to maximize conduction speed, myelin can be responsive to the activity of individual axons, or even stretches of axons, and modify its wrapping pattern to achieve functional optimization in neural circuits (Chang, Redmond and Chan, 2016).

Experience-dependent myelin modifications have been documented in both the human and murine nervous system. Neuroimaging studies demonstrated regional white matter plasticity in response to a variety of tasks, such as piano performance (Oztürk *et al.*, 2002; Bengtsson *et al.*, 2005), the game of Go (Lee *et al.*, 2010), juggling training (Scholz *et al.*, 2009), or extensive language course (Schlegel, Rudelson and Tse, 2012). In murine models, both juvenile and adult mice deprived of social interactions show decreased myelin gene expression, especially in the prefrontal cortex, correlating with behavioral and cognitive deficits (Liu *et al.*, 2012; Makinodan *et al.*, 2012). At the same time, enriched environments induce oligodendrocyte proliferation in the rat visual cortex (Szeligo and Leblond, 1977; Sirevaag and Greenough, 1987), and increases myelin volume in the corpus callosum (Zhao *et al.*, 2012).

There are a variety of possibilities how myelination could be regulated in response to functionality needs, such as i) timing of myelination; ii) internodal length; iii) myelin pattern; iv) myelin thickness *etc*.

Myelination can be delayed until the neuronal circuit is finalized, such as in the delay line axons of barn owl *nucleus laminaris*, where myelination is delayed until after the head reaches the adult animal's width (Cheng and Carr, 2007). Myelin can also be specifically regulated in terms of internodal length for functional purposes. In both avian and mammalian auditory system, internodal myelin length and axon diameter are coordinated to ensure the isochronicity of conduction time between the binaural paths with microsecond precision (Seidl, Rubel and Harris, 2010; Seidl and Rubel, 2016). The presence of myelin is not an all-or-nothing decision, but intricately regulated in the CNS, providing possibility of fine-tuning and plasticity (de Hoz and Simons, 2015). High-throughput electron microscopy reconstruction of the mouse neocortex has shown that individual neurons exhibit highly diverse longitudinal myelination pattern, with long unmyelinated stretches between myelinated segments (Tomassy *et al.*,

2014). The mechanism of functional activity influencing myelination is not yet known (Fields, 2015), but it has been shown that optogenetic stimulation of premotor cortex in mice alone suffices to promote the proliferation and differentiation of oligodendrocytes, and leads to increased myelin sheath thickness (Gibson *et al.*, 2014).

1.4. Aims

My PhD project aims to gain insights into the process and mechanism of axonal remodeling at the level of single axons, using the developing mouse neuromuscular junction (NMJ) as a model, which involves the achievement of the following objectives:

1) Screen for molecules possibly involved in the synapse elimination process. Using genetic manipulations of factors possibly influencing neuronal maintenance and maturation, disassembling of retreating axonal structures, SC engulfment of debris and apoptosis, to analyze the respective innervation phenotype.

2) Investigate the process of myelination and synapse elimination during early development. Immunofluorescent staining and FRAP experiment were used to determine the time-course and protein turn-over rate in the wild-type situation.

3) Focus on the influence of myelination on synapse elimination, using genetic manipulations of myelin-regulating factor to examine the effect of myelination progress on synapse elimination.

4) Examine, in converse, the effect of synapse elimination on myelination, using pharmacological and genetic manipulations that affect synapse elimination to study the possible mechanism behind the process.

2. RESULTS

To understand the important interaction between glial cells and neurons during developmental synapse elimination, a genetic screen was first carried out to search for factors potentially affecting axoglial remodeling. The concurrent pruning and myelination process was then scrutinized under physiological conditions, and genetic manipulations were performed to uncover the possible mechanisms behind the intricate coordination of the two processes.

Note: Sections 2.2 – 2.5 of the Results part of this thesis are modified from my first author manuscript, which we are currently preparing for submission (Wang et al., *in preparation*). Section 2.1.5 is a modified version of my contribution to the publication *"Non-cell-autonomous function of DR6 in SC proliferation"* (Colombo *et al.*, 2018). And section 2.5 includes modified parts of my inputs to the publication *"Branch-specific microtubule destabilization mediates axon branch loss during neuromuscular synapse elimination"* (Brill *et al.*, 2016).

2.1. Screen of molecular factors affecting synapse elimination

During the first two postnatal weeks, exuberant branches are rapidly removed from multiply innervated NMJs, until single innervation is established (Balice-Gordon and Lichtman, 1993). This extensive remodeling process involves the maintenance and maturation of surviving terminal branches, disassembling of retreating axonal structures and axosome shedding (Bishop *et al.*, 2004), before engulfment of debris by the SCs (Brill *et al.*, 2011; Ko and Robitaille, 2015). To understand the molecular mechanism behind this process better, a series of neuronal and glial molecules possibly influencing the above aspects were inspected – selected based on hypotheses generated from previous work in the lab that had shown the importance of regulated axon branch fragmentation and subsequent glial engulfment (Bishop *et al.*, 2004), lysosome-mediated degradation (Song *et al.*, 2008) and SC dynamism (Brill *et*

al., 2011). Specifically, conditional *Atg7* knock-out mice were studied to examine the role of autophagy in the maintenance and turnover of axonal and glial cells; *ΔNLS-Wld*^{S} to probe the possible involvement of Wallerian-like degeneration in axon pruning; conditional *Elmo1* knock-out and *Megf10/11* deletions for involvement of specific SC engulfment receptors; *Bax* and *Dr6* knock-out for apoptosis-related factors. Here the innervation status (*i.e.* frequency of double innervation at specific ages), as well as – in selected cases – on SC numbers, of the animals depleted of the respective factors were analyzed. Given the stereotypical anatomy of the NMJ, these parameters provide a sensitive readout of the progress of synapse elimination and of the functionality of the intercellular interactions involved.

2.1.1. Autophagy-related factor (*Atg7*) in SCs and neuron

Autophagy is a highly regulated intracellular process for degrading and recycling proteins and organelles, which occurs in response to both extracellular and intracellular stress, which involves dynamically rearranging intracellular membrane to form autophagosomes (Levine and Klionsky, 2004). Autophagosome formation is regulated by a series of ATG and ATG-related proteins. Among these, ATG7 is an E1-like enzyme that activate both the ATG12 and ATG8/LC3 conjugation system, important for the elongation of membrane during the formation of autophagosomes (Mizushima, Yoshimori and Ohsumi, 2011). ATG7 deficiency in the mouse CNS led to massive neurodegeneration in the cortices and behavior abnormalities, as well as premature death of the animals (Komatsu *et al.*, 2006). Specific loss of ATG7 in Purkinje cells caused axonal dystrophic swelling, membrane structure aberrations, followed by cell death and behavioral deficits (Komatsu *et al.*, 2007). Since ATG7 deficiency appears to be an efficient means to block a central autophagy pathway, we checked if the deletion of this autophagy factor in either neurons or glial cells can affect the pruning progress.

2.1.1.1. Genetic ablation of *Atg7* in SCs (*plpCreERT* x *Atg7*^{FL} x *TdTomato*)

To analyze the effect on glial cells, *Atg7* conditional knock-out mice (Komatsu *et al.*, 2005) were first crossed to *plpCreERT* animals, and injected with tamoxifen (5mg/ml, 20 µl) on postnatal day 3 to induce SC specific deletion. The *TdTomato* reporter (*Rosa26-STOP-tdTomato*) was used to control for the effectiveness of Cre induction. However, given that the *TdTomato* reporter allele is located on the same chromosome (6) as the floxed *Atg7* allele, induction could only be verified in the heterozygous controls, where the tamoxifen dosage applied induced expression in ~100% SCs (**Figure 6A, B**). No significant difference in double-innervation was detected on P7 and P9 (**Figure 6C**, poly-innervation on P7 in WT/FL = 39.8 ± 0.06%, in FL/FL = 40.0 ± 0.01%, Mann-Whitney test p = 0.83; on P9 in FL/WT = 27.4 ± 0.05%, in FL/FL = 22.5 ± 0.02%, Mann-Whitney test p = 0.40; number of axon per animal ≥ 50, animal per group ≥ 3; throughout this thesis, results are given as Mean ± SEM).

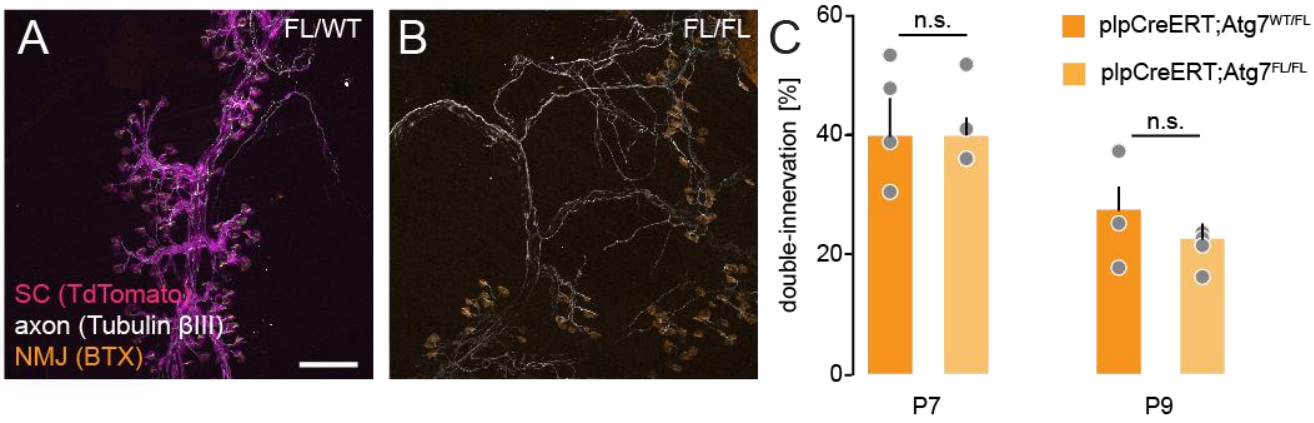

Figure 6: SC deletion of *Atg7* did not affect synapse elimination. **A:** heterozygous control animal; **B:** homozygous SC deletion of *Atg7*. Littermate controlled, 20µl 5 mg/ml tamoxifen injection on P3. Magenta: *TdTomato* positive SCs; white: axonal Tubulinβ-III staining; orange: BTX staining of NMJ. Scale bar = 100µm. **C:** quantification of synaptic elimination of ATG7 SC deletion.

2.1.1.2. Genetic ablation of *Atg7* in neurons (SLICK-3 x *Atg7*^{FL} x *TdTomato*)

For determining the function of *Atg7* in motor-neurons, we generated mice with neuronal deletion of *Atg7* with the SLICK-3 animals (Young *et al.*, 2008), and tamoxifen (5mg/ml, 20 µl) was injected on postnatal day 3 to induce neuronal specific deletion.

The SLICK-3 insertion includes a YFP reporter to indicate presence of the tamoxifen-inducible Cre construct, and *TdTomato* was used to control for the effectiveness of tamoxifen induction. Due to the same chromosomal conflict described above, the Cre efficiency could only be verified in the heterozygous controls, where the dosage induced a close to ~100% expression in motor neurons (**Figure 7A, B**). No significant difference in double-innervation was detected on P7 and P9 (**Figure 7C**, poly-innervation on P7 in WT/FL = 28.0 ± 0.06%, in FL/FL = 25.0 ± 0.03%, Mann-Whitney test $p = 0.89$; on P9 in FL/WT = 15.6 ± 0.04%, in FL/FL = 14.9 ± 0.03%, Mann-Whitney test $p = 0.7143$; number of axon per animal ≥ 50, animal per group ≥ 3).

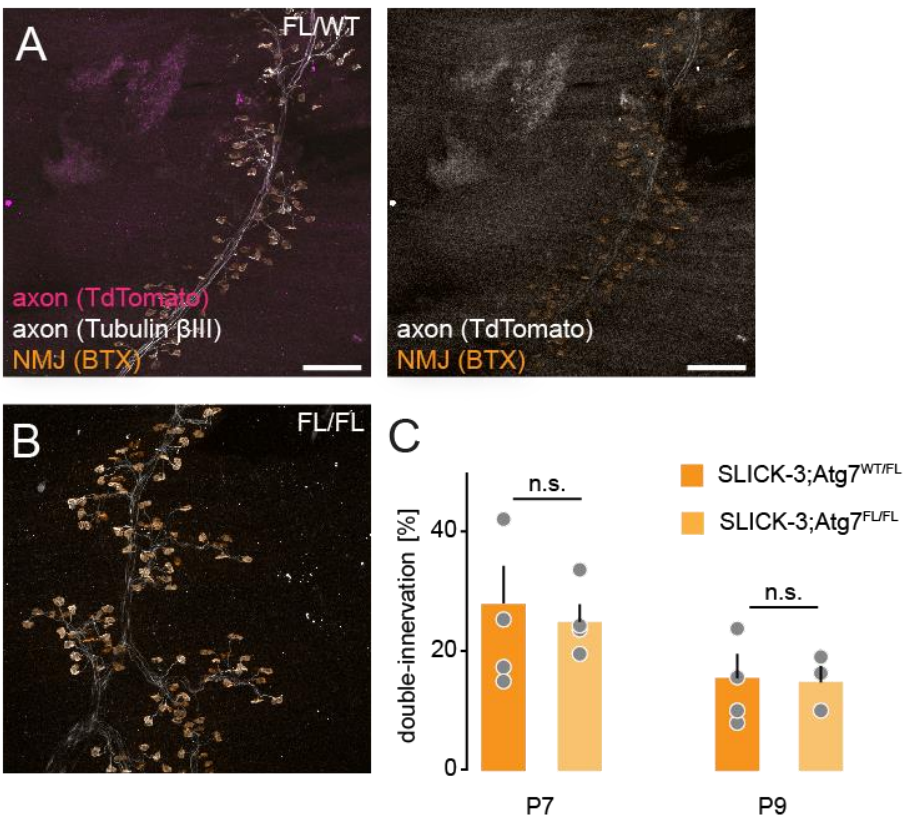

Figure 7: Neuronal deletion of *Atg7* did not affect synapse elimination. **A:** heterozygous control animal; **B:** homozygous motor neuron deletion of *Atg7*. Littermate controlled, 20µl 5 mg/ml tamoxifen injection on P3. Magenta: *TdTomato* positive axons; white: axonal Tubulinβ-III staining; orange: BTX staining of NMJ. Scale bar = 100µm. **C:** quantification of synaptic elimination of *Atg7* motor neuron deletion.

2.1.2. Genetic delay of Wallerian degeneration (*ΔNLS-Wld^S*)

Wallerian degeneration refers to the process of axon-autonomous degeneration distal to the injury site (Waller, 1850), which involves active axon fragmentation and

degeneration, with the debris cleared by glial cells and macrophages (Coleman and Freeman, 2010). Deletion of the nuclear localization sequence (NLS) of one part of the slow Wallerian degeneration protein (Wld^S) fusion protein, Nmnat1, was shown to enhance enhance axon import and the axon-protective effect of the protein (Beirowski *et al.*, 2009). To determine whether – in contrast to prior work with the conventional, weaker allele (Parson, Mackintosh and Ribchester, 1997; Hoopfer *et al.*, 2006) – such enhanced protection might affect synapse elimination during development, *ΔNLS-Wld*^{S} expressing (heterozygote) mice were analyzed for innervation patterns (**Figure 8A, B**) on P9 and P11, since a delayed degradation phenotype was expected here and the effect could be more obvious at a later timepoint. No significant difference on P9 and P11 was found compared to wild-type littermates, confirming that synaptic pruning in the mammalian system is through a mechanism distinctive from Wallerian degeneration (poly-innervation in WT/WT = 20.8 ± 8.3%, in WT/TG = 24.0 ± 8.3%, Mann-Whitney test $p = 0.54$; on P11 in WT/WT = 2.0 ± 0.4%, in WT/TG = 1.7 ± 0.9%, Mann-Whitney test $p = 0.70$; number of axon per animal ≥ 50, animal per group ≥ 3).

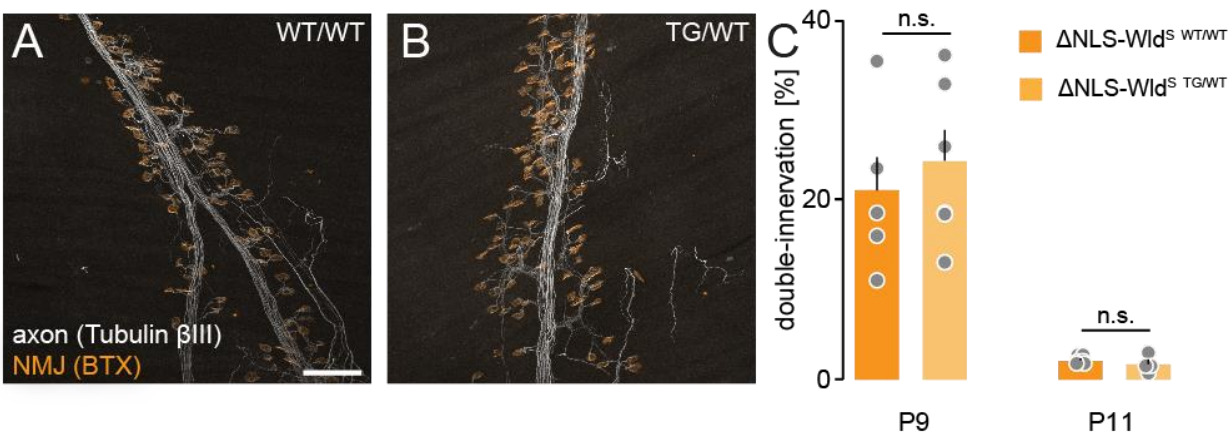

Figure 8: *ΔNLS-Wld*^{S} mice did not show a synapse elimination phenotype. **A:** homozygous wild-type control animal; **B:** heterozygous transgenic *ΔNLS-Wld*^{S} animal. Littermate controlled, White: axonal Tubulinβ-III staining; orange: BTX staining of NMJ. Scale bar = 100µm. **C:** quantification of synaptic elimination of *ΔNLS-Wld*^{S} innervation on P9 and P11.

2.1.3. Genetic ablation of the caspase activating *Bax*

Since local caspase activity has been found to play a role in the pruning process of various systems (Kuo *et al.*, 2006; Williams *et al.*, 2006; Campbell and Okamoto, 2013; Miura, 2016), I investigated the role of the upstream regulator BAX, which has been shown to be a key element in inducing caspase activity during synaptic pruning, as well as mediating axonal degradation after axotomy and/or deprivation of trophic factors (Schoenmann *et al.*, 2010).

To verify the effect of local caspase activation during synapse elimination, $Bax^{KO/WT}$ animals (Knudson *et al.*, 1995) were crossed to generate general littermate controlled $Bax^{WT/WT}$ and $Bax^{KO/KO}$ animals (**Figure 9A, B**). However, *Bax* KO animals did not show any significant difference from the wildtype controls both on P7 and P9 (**Figure 9C**, poly-innervation in P7 WT = 26.2 ± 1.9%, in KO = 31.5 ± 4.7%, Mann-Whitney test $p = 0.63$; in P9 WT = 12.7 ± 2.8%, in KO = 11.85 ± 4.16%, Mann-Whitney test $p = 0.73$; number of axon per animal ≥ 50, animal number per group ≥ 3).

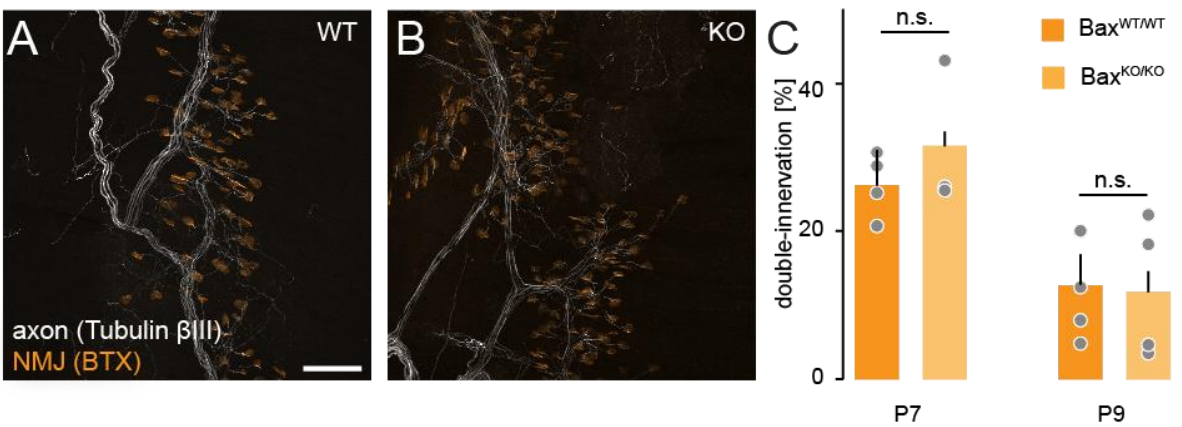

Figure 9: *Bax* KO did not affect synapse elimination. **A:** wild-type control animal; **B:** *Bax* homozygous KO animal. Littermate controlled, white: axonal Tubulinβ-III staining; orange: BTX staining of NMJ. Scale bar = 100µm. **C:** quantification of synaptic elimination in *Bax* WT vs. KO animals.

2.1.4. Engulfment-related factors (*Elmo1*, *Megf10/11, PrS, Gas6*)

The final stage of the pruning of exuberant axons is the engulfment of remnant retreating axons. Retreating axonal branches undergo axosome shedding (Bishop *et*

al., 2004), and the debris is engulfed by the non-myelinating terminal SCs covering the NMJ monitor synaptic (Brill *et al.*, 2011; Ko and Robitaille, 2015) – moreover in flies (Awasaki *et al.*, 2006) and in mammalian cortex (Chung *et al.*, 2013), it has been shown that interference with the engulfment process is found to preserve immature innervation patterns. Therefore, it is of interest to investigate possible effects of engulfment factors on the synaptic pruning process at the NMJ.

2.1.4.1. Genetic ablation of *Elmo1* in SCs (*plpCreERT* x *Elmo1*^{FL} x *TdTomato*)

ELMO1 is part of the ELMO/Dock180 protein complex functioning as a guanine nucleotide exchange factor for the small GTPase Rac, which is evolutionarily conserved, functioning downstream of the phosphatidylserine receptor BAI1, for regulating the actin cytoskeleton during engulfment of apoptotic cell debris (Gumienny *et al.*, 2001; Brugnera *et al.*, 2002; Park *et al.*, 2007).

Conditional knock-out animals were generated by crossing the *Elmo1*$^{FL/FL}$ mouse-line (Elliott *et al.*, 2010) to *plpCreERT* and injecting the pups with tamoxifen (5mg/ml, 20 µl on postnatal day 3). The *TdTomato* reporter was used to illustrate the effectiveness of Cre induction, and the dosage induced a close to ~100% expression in SCs. Littermates heterozygous for the *Elmo1* deletion were used as controls (**Figure 10A, B**). No significant difference in double-innervation was detected on P7 and P9 (**Figure 10C**, poly-innervation on P7 in WT/FL = 45.8 ± 0.03 %, in FL/FL = 48.1 ± 0.09%; number of axon per animal ≥ 50, animal per group ≥ 3, Mann-Whitney test p = 0.97; on P9 in FL/WT = 14.2 ± 0.03 %, in FL/FL = 8.5 ± 0.01%, Mann-Whitney test p = 0.20; number of axon per animal ≥ 50, animal per group = 4).

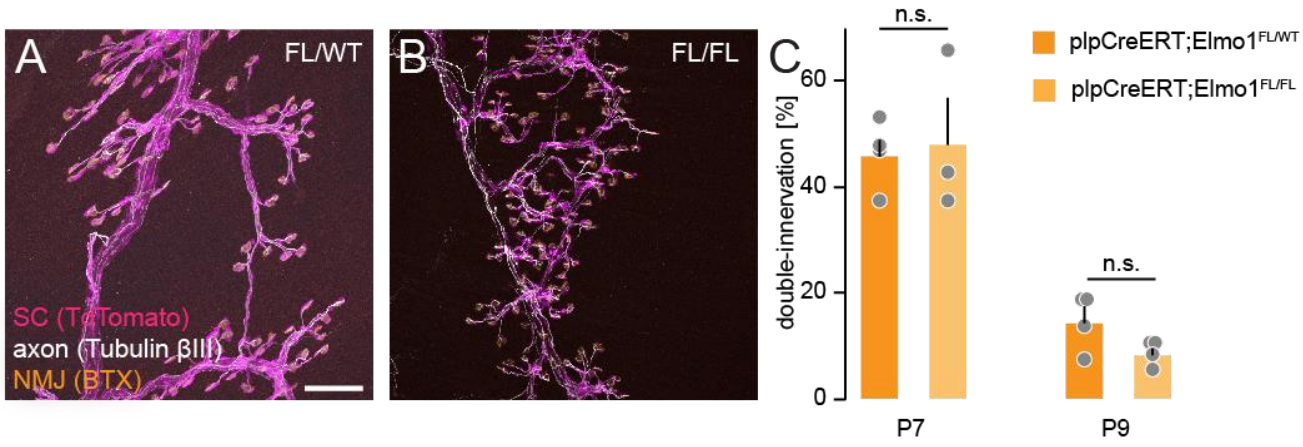

Figure 10: SC deletion of *Elmo1* did not affect synapse elimination. **A:** heterozygous control animal; **B:** homozygous SC deletion of *Elmo1*. Littermate controlled, 20µl 5 mg/ml tamoxifen injection on P3. Magenta: *TdTomato* positive SCs; white: axonal Tubulinβ-III staining; orange: BTX staining of NMJ. Scale bar = 100µm. **C:** quantification of synaptic elimination of *Elmo1* deletion.

2.1.4.2. Genetic double ablation of *Megf10/11*

MEGF10 and MEGF11 belong to a family of transmembrane phagocytic receptors that are homologs to *Draper* in *Drosophila* and CED-1 in *Caenorhabditis elegans* (Wu *et al.*, 2009). While our analysis was in progress, MEGF10 was found to be critically required by astrocyte during the activity-dependent pruning of retinogeniculate connections (Chung *et al.*, 2013). MEGF10/11 also play an important role in the mosaic spacing of starburst amacrine cells and horizontal cells in the mouse retina (Kay, Chu and Sanes, 2012).

Megf10 and *Megf11* knockout mice (Kay, Chu and Sanes, 2012) were crossed to generate WT and double KO animals. Here heterozygous animals were used as controls (*Megf10*$^{KO/WT}$; *Megf*11$^{KO/WT}$, **Figure 11A, B**), and a significant increase in double innervation was found in *Megf10/11* double KO compared to heterozygous animals on P7 (**Figure 11C**, poly-innervation in double WT/KO = 21.5 ± 0.05%, in double KO/KO = 38.4 ± 0.03%; number of axon per animal ≥ 50, animal per group ≥ 3, Kruskal-Wallis test with Dunn's multiple comparisons test p = 0.03), but not on P9 (number of axon per animal ≥ 50, animal per group ≥ 3, Kruskal-Wallis test p = 0.78), indicating a possibly transient effect on synaptic elimination.

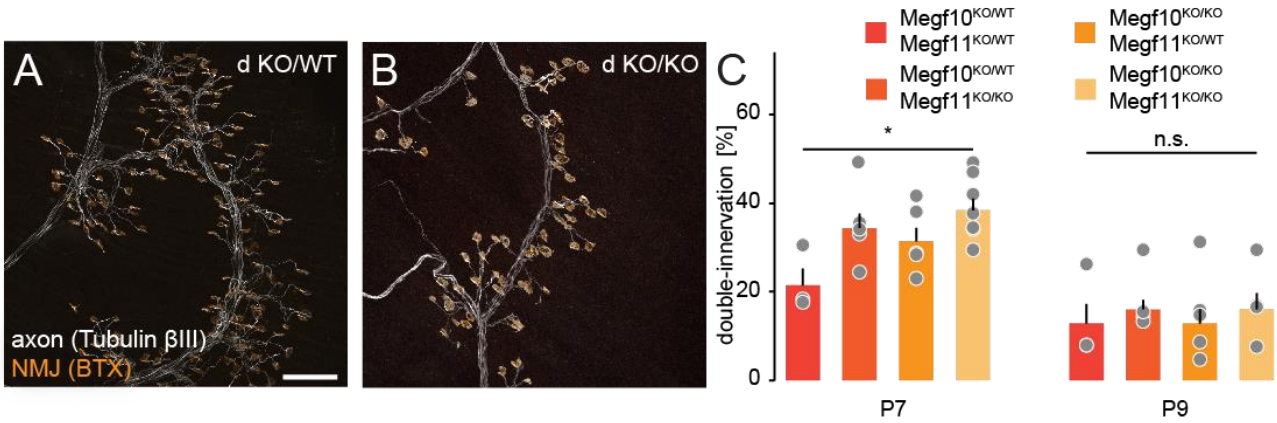

Figure 11: *Megf10/11* double KO affect synapse elimination. **A:** *Megf10/11* heterozygous control animal; **B:** *Megf10/11* homozygous KO animal. Littermate controlled, white: axonal Tubulinβ-III staining; orange: BTX staining of NMJ. Scale bar = 100µm. **C:** quantification of synaptic elimination in *Megf10/11* KO animals.

2.1.4.3. Genetic double ablation of *PrS* and *Gas6*

The vitamin K-dependent protein S (PrS) and growth arrest-specific gene 6 protein (GAS6) are main ligands of the TAM (Tyro3, Axl and MerTK) family of tyrosine kinase receptors (Stitt *et al.*, 1995), and have been shown to regulate engulfment of apoptotic cells (Wu *et al.*, 2005; Hafizi and Dahlbäck, 2006).

PrS (Burstyn-Cohen, Heeb and Lemke, 2009) and *Gas6* (Angelillo-Scherrer *et al.*, 2001) knock-out animals were crossed by our collaborators (A. Yaron, Weizmann Institute) to produce the double knock-out animals (**Figure 12A, B**). When I examined double knock-out animal muscles at P9, I did detect any significant difference in double innervation from wildtype controls (**Figure 12C**, poly-innervation in WT = 27.5 ± 2.5 %, dKO = 27.6 ± 0.8%, number of axon per animal ≥ 50, animal number WT = 2, double KO = 3, Mann-Whitney test $p > 0.99$).

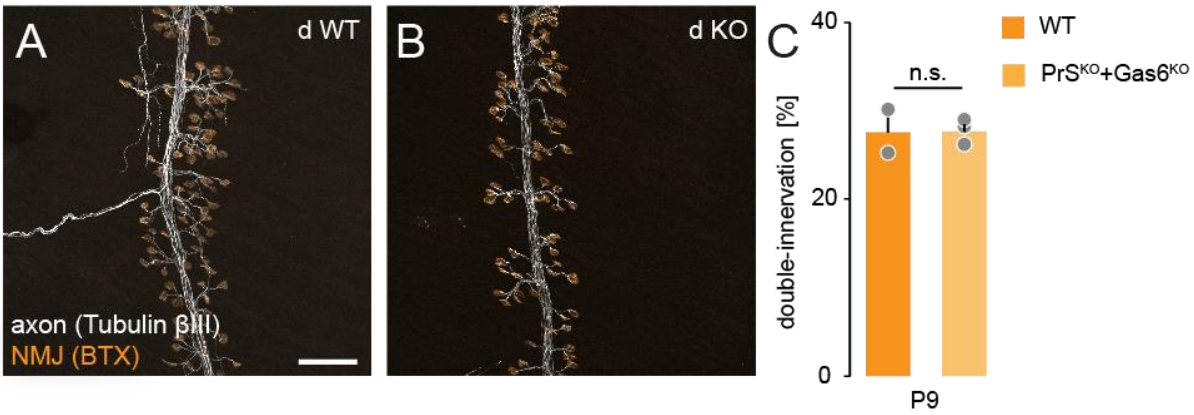

Figure 12: *PrS* and *Gas6* double KO did not affect synapse elimination. **A:** wild-type control animal; **B:** *PrS* and *Gas6* homozygous KO animal. Littermate controlled, white: axonal Tubulinβ-III staining; orange: BTX staining of NMJ. Scale bar = 100µm. **C:** quantification of synaptic elimination in PrS and *Gas6* WT vs. KO animals.

2.1.5. Genetic ablation of the apoptosis-related factor *Dr6*

After removal of retreating branches, the SCs originally covering the pruned axon stretch disappear. To determine if this process involves apoptosis – *i.e.* a form of programmed cell death – antibody against cleaved Caspase-3 was used to detect apoptotic cells during development in the *triangularis sterni* muscle. Only very rarely were any SCs detected to be positive for cleaved Caspase-3 (data not shown). However, further morphological study and analysis of knock-out animals showed a more intricate regulation of apoptosis-related factors on SCs during synapse elimination.

To be noted, the terminal SCs (tSC) covering the NMJ on immature competing branches intermingle and do not segregate to territories occupied by individual axons (Brill *et al.*, 2011). Interestingly, shortly before the terminal branch retreats and forms a retraction bulb, one SC could often be observed to form a long, thin and tube-like structure along the retreating axon, with the SC's nucleus still associated with the endplate (**Figure 13A**, white arrowhead). The structure was also preserved when the retraction bulb was pruned back (**Figure 13B**, white arrowhead). Indeed, the number of terminal SCs on a singly innervating NMJ ("sin") was found to be on average one

cell less than on doubly innervating NMJs (“din”) on the same postnatal day from P5 to P11 (**Figure 13C**, 0.8 ± 0.1, ≥ 30 axons from 5 animals analyzed per group). Even more strikingly, a freshly singly innervated NMJ (“young sin”), defined as a singly innervating branch with a retraction bulb nearby (**Figure 13B**, black arrowhead), which indicates recent completion of competition (Walsh and Lichtman, 2003), was also found to have approximately one cell less on the terminal than the average doubly innervated NMJ (**Figure 13C**, 0.9 ± 0.1, ≥ 30 axons from 5 animals analyzed per group). It appears that on the *triangularis sterni* muscle, one of the tSCs is eventually assigned to the retreating terminal branch. It prunes back the retraction bulb, leaving the NMJ to the remaining tSCs.

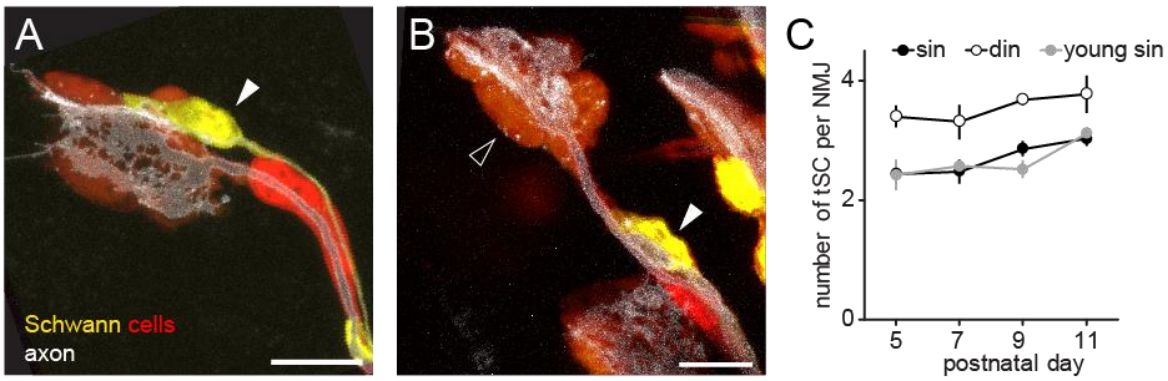

Figure 13: Terminal SC withdrawing from NMJ as a terminal branch prunes back. **A:** sequential bleaching reveals tSC morphology on a terminal branch shortly before retreating, the tube-like SC (yellow, with white arrowhead) with its nucleus still associates with the terminal, axon (*Thy1:OFP3*) in white and the other SCs in red; **B:** A recently established singly innervating axon (black arrowhead) in adjacent to a retraction bulb (white arrowhead); **C:** Quantification of tSC number associated with the endplate when the NMJ is singly/doubly innervated, or singly innervated but with a retraction bulb nearby.

Death receptor 6 (DR6) has been shown to promote apoptosis when overexpressed (Pan *et al.*, 1998), and is found to function through a unique pathway involving *Bax* translocation and cytochrome c release (Zeng *et al.*, 2012). *Dr6* deletion affect retinal axon pruning (Nikolaev *et al.*, 2009) and Wallerian degeneration (Gamage *et al.*, 2017) as well as oligodendrocyte maturation and myelination (Mi *et al.*, 2011). To understand whether DR6 affect the SC reorganization after synaptic pruning, *Dr6*

knock-out mice (Zhao *et al.*, 2001) were crossed to the PLP-GFP line (Mallon *et al.*, 2002) for SC labeling in DR6 deletion. The effect of *Dr6* deletion was quantified by determining terminal SCs number and axonal SC length, as well as the onset of myelination on terminal branches (**Figure 14A**). Depletion of DR6 significantly increased the number of terminal SCs covering the NMJ on P11 (2.6 ± 0.1 in WT vs. 3.2 ± 0.05 in KO, Mann-Whitney test $p < 0.01$, NMJ analyzed per animal ≥ 30, number of animal per group ≥ 5), while NMJ area and axonal length remained similar compared to WT (**Figure 14B**). The length of axonal SCs is significantly shorter in *Dr6* KO animals than in controls (**Figure 14C**, 32.5 ± 2.6 µm in WT vs. 24.2 ± 1.2 µm in KO, Mann-Whitney test $p = 0.02$, terminal branch analyzed per animal ≥ 30, number of animal per group ≥ 5). The myelination status was also more advanced in *Dr6* KO animals compared to WT on P9 as assessed by Caspr stainings (**Figure 14D, E,** 27.4 ± 3.8% in WT vs. 38.2 ± 2.4% in KO, Mann-Whitney test $p = 0.04$, terminal branch analyzed per animal ≥ 24, number of animal per group ≥ 6). The effect is transient since by P21, all terminal branches become fully myelinated (**Figure 14F**). Together the data suggests that *Dr6* negatively regulates SC proliferation and myelination in the PNS (Colombo *et al.*, 2018).

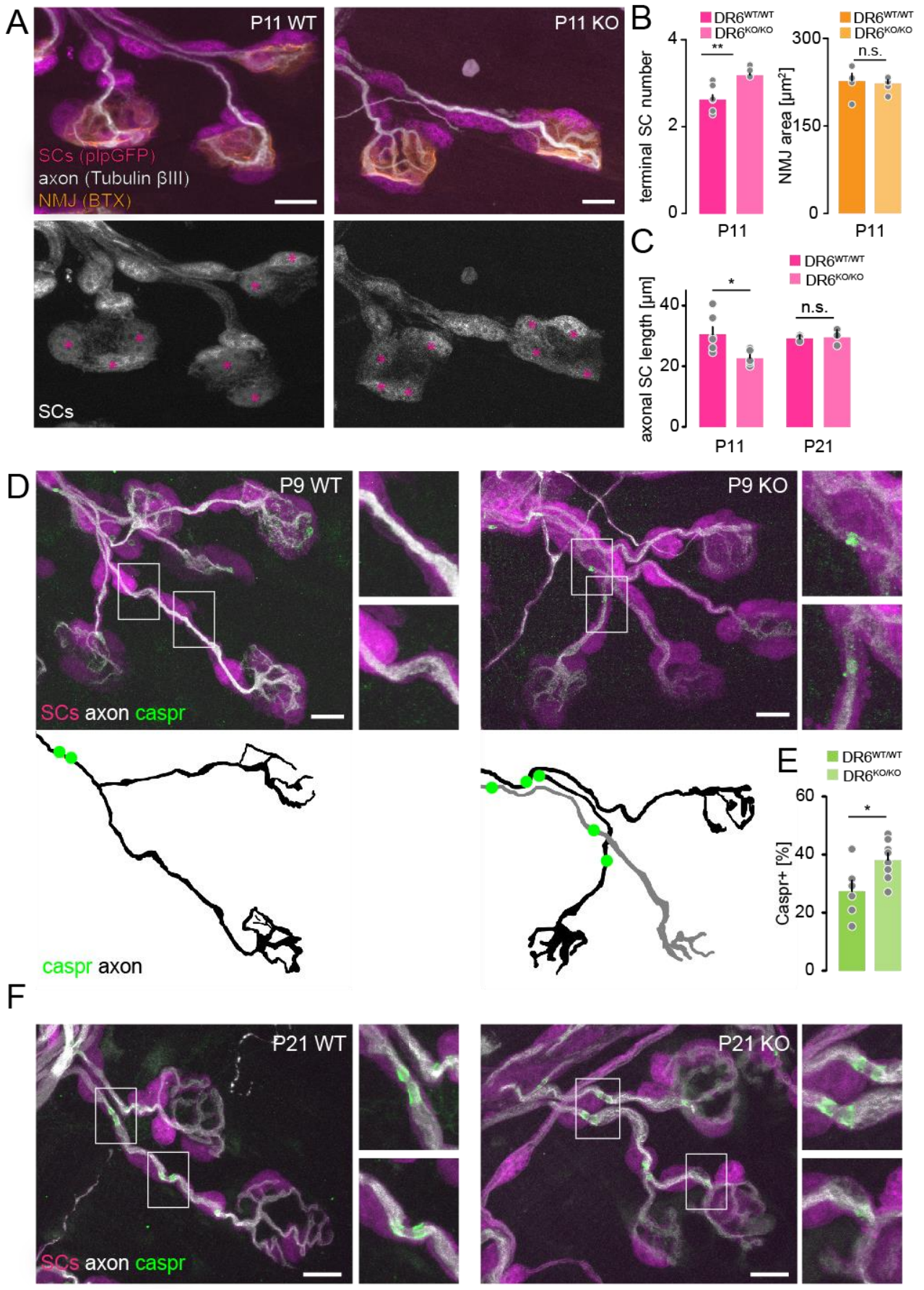

Figure 14: *Dr6* negatively regulates SC number and myelination. **A:** P11 DR6 WT vs. KO. Magenta (above) / grey (below): plp-GFP labeled SCs; white: axonal Tubulinβ-III staining; orange: BTX staining of NMJ. Terminal SCs are marked with magenta asterisks. **B:** Terminal SC numbers increased in P11

DR6 KO mice compared to littermate WT controls, whereas the sizes of NMJ (right panel) did not change. **C:** Axonal SC length was decreased in NMJ of P11 DR6 KO mice compared to littermate WT controls. **D:** P9 terminal branches in WT or DR6 KO with paranodal Caspr staining (green). To the right are higher magnification of the regions in white boxes and below are the outlines of axonal branches. **E:** Caspr-positive terminal branches increased in P9 KO. **F:** P21 terminal branches in WT or DR6 KO, where all branches were positive for Caspr. Scale bars = 10 µm. (Modified from Colombo *et al.*, 2018)

Overall, the experiments showed a surprising robustness of the stereotypical synapse elimination process against genetic manipulations. Factors involved in neuronal and glial maintenance, engulfment and clearance, as well as apoptosis, appear to have at most mild effects on the pruning process during development of the mouse peripheral NMJ.

2.2. Correlation of myelination and synapse elimination

The onset of myelination correlates in many axonal populations with cessation of developmental plasticity (Luo and O'Leary, 2005; Simons and Trotter, 2007). In the mouse NMJ system, excessive axonal branches are removed from multiply innervated NMJs until single innervation is established (Tapia *et al.*, 2012). At the same time, a simple and invariable myelination pattern forms, with individual glial (Schwann) cells being exclusively dedicated to sheathing one single axon branch (Salzer, Brophy and Peles, 2008). The correlation of these two processes were first demonstrated with bungarotoxin induced activity blockade, then the myelination and innervation status of single branches were investigated with immunofluorescence staining. FRAP assay was performed to analyze the turn-over rate of developing nodal structures in relation to their respective competition states.

2.2.1. Activity blockade delays both synaptic pruning and myelination

Synapse elimination at the NMJ was shown to be an activity-dependent process, with the more powerful input strongly favored over its weaker competitor (Buffelli *et al.*,

2003), where neurotransmission was reduced in a subset of neurons with genetic depletion of the choline acetyltransferase (ChAT) by crossing crossing a mice carrying a floxed allele of ChAT (*ChAT*$^{FL/FL}$) to mice that ubiquitously express a tamoxifen-dependent version of cre recombinase (*CAG-CreER*). ChAT was then deleted in a subset of motor axons by low dose treatment with tamoxifen on P0. On P11, the competition status was examined and the branches positive for ChAT staining were overwhelmingly found to prevail in competition outcome when pitted against branches that had lost ChAT.

To influence competition in a similar manner, while avoiding effects that presynaptic blockade of neurotransmission could have on myelination (Misgeld *et al.*, 2002), fluorescently-conjugated bungarotoxin was locally injected to one side of the thoracic muscle of P7 mice. The injected pups were viable and active after the treatment, not distinguishable from untreated controls. BTX was allowed to take effect for two days before analysis. Typically, the injected side of the thorax would show distinct fluorescence compared to the uninjected side of the same animal, providing an internal control for the developmental assays (**Figure 15A, B**). It has been reported that focal application of BTX in adult mice causes permanent loss of the blocked part of the NMJ, while blockade of the whole junction does not cause synapse elimination (Balice-Gordon and Lichtman, 1994). Here all the analyzed BTX-positive terminals were 100% blocked, and no denervated terminals were found. As expected, the branches with BTX-positive endplates showed a significant delay in the elimination of excessive branches (**Figure 15C**, double-innervation in BTX-negative control = 22.1 ± 3.2%, in BTX-positive = 34.0 ± 4.2%, Wilcoxon test $p < 0.01$; number of axon per animal ≥ 50, animal per group = 8). Interestingly, the 2-day BTX blockade also delayed the initiation of myelination on terminal branches, marked by the presence of Caspr positive paranodes, compared to unaffected NMJs (**Figure 15D**, Caspr positive single

innervation in BTX-negative control = 27.4 ± 3.5%, in BTX-positive = 14.3 ± 4.3%; Wilcoxon test p = 0.03, animal per group = 6). This outcome suggests that both synaptic pruning and myelination might be under the influence of neurotransmission, neurotransmission and potentially retrograde signaling from muscle. Moreover, the counter-correlation of both developmental processes could indicate that they represent mutually exclusive programs – a hypothesis that I set out to test in more detail.

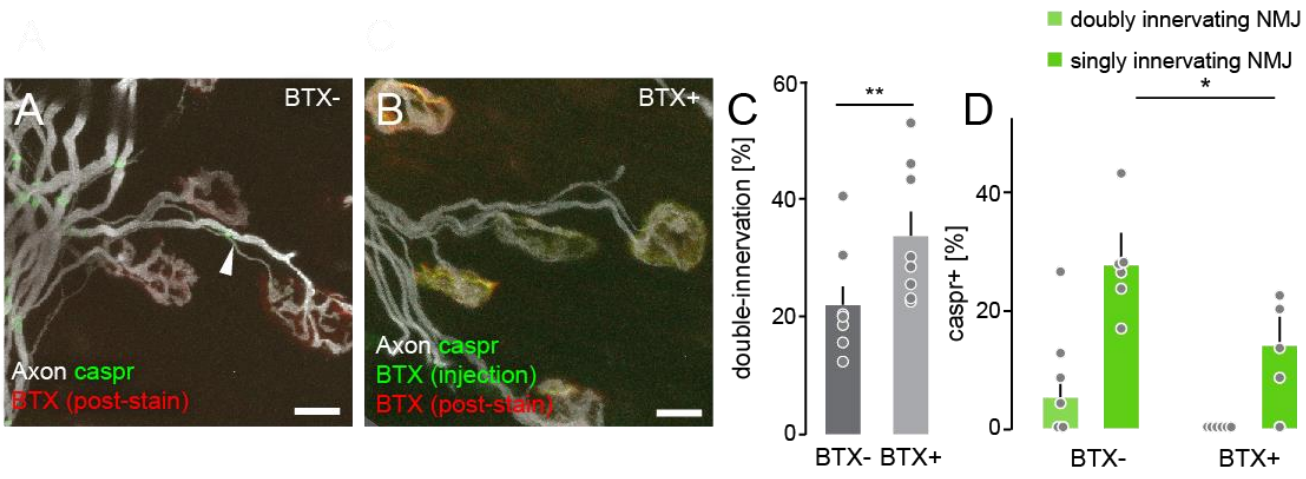

Figure 15: Activity blockade with injected BTX significantly delay both synaptic elimination and myelination. **A:** P9 *Trangularis sterni* muscle on the uninjected side of the thorax, arrowhead point to a Caspr positive paranode on a doubly innervating branch; **B:** *Trangularis sterni* muscle on the injected side of the thorax, from the same animal as in (**A**). **C:** Quantification of synaptic elimination status on P9; **D:** Quantification of myelin initiation status on P9.

2.2.2. Synaptic elimination and myelination coincide during development

To understand the concurrent process of synaptic pruning and myelination under physiological circumstances, a series of morphological observations were carried out in mice with genetically labelled neuron and/or glial cells. Individual SC morphology was delineated through sequential photobleaching (Brill *et al.*, 2011), and immunofluorescent antibody staining was used to illustrate nodal and myelin components. The dynamics of nodal proteins during node formation were analyzed using the fluorescent recovery after photobleaching (FRAP) assay.

2.2.2.1. Schwann cell morphology

From birth, motor neurons and their endplates are covered with SCs, with myelinating SCs wrapping around the axons, and non-myelinating terminal SCs associated with the NMJ (**Figure 16A**, Ko & Robitaille, 2015). Individual SCs can be distinguished by laser photobleaching of neighboring SCs (**Figure 16A-C**, Brill *et al.*, 2011). Early during development, axonal SCs start forming myelin and in the second week after birth, the structures of the node of Ranvier can be found along some of the terminal branches innervating the *triangularis sterni* muscle, illustrated using immunostaining of Caspr, (**Figure 16C, D**).

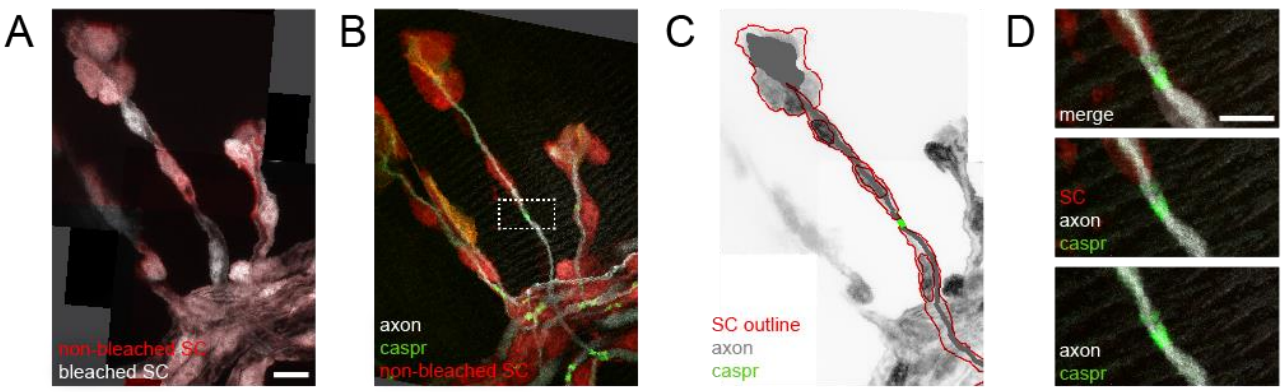

Figure 16: SCs on terminal branches start myelinating during the second postnatal week. **A:** SCs covering the motor axons and endplates, with individual SCs in red or white to visualize the territories, Scale bar = 10 µm; **B:** Partially myelinated terminal branches, with axons in white, Caspr in green, and non-bleached SCs in red; **C:** Outlined axon showing SC and Caspr in relation to each other; **D:** Enlarged view of dashed box in B, with forming paranodal Caspr stained at either ends of SCs. Scale bar = 5 µm.

2.2.2.2. Caspr as a representative myelination marker

To analyze the formation of myelin on terminal branches, I detected various myelin and node of Ranvier structures using immunostaining of the respective markers (**Figure 17A**). Specifically, the compact myelin sheath was marked for myelin protein zero (MPZ), the juxtaparanodal region for contactin-2 (CNTN2), the paranodal region for Caspr and the nodal region for voltage-gated sodium channels (Nav).

Double staining of myelin markers showed that the various markers appear approximately at the same time on myelinating branches (**Figure 17B**). Presence of only one of the markers but not the others was exceedingly rare, though instances of faint MPZ presence without surrounding paranodal structures were observed (**Figure 18B,** hollow arrow-head) – suggesting that this pattern might represent the earliest but short phase of motor axonal myelin formation.

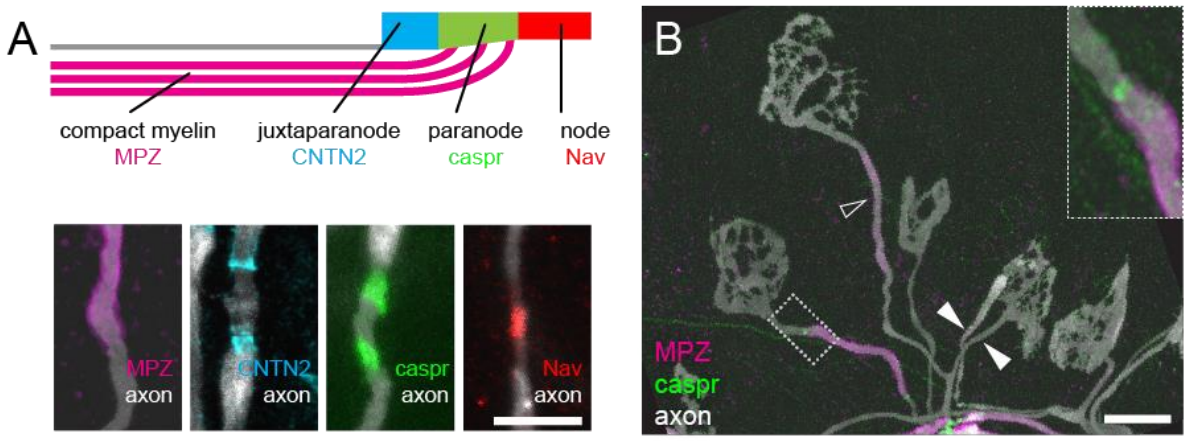

Figure 17: Caspr is a representative marker for nodal formation. **A:** Schematic representation of myelin and Node of Ranvier structure and the representative markers; **B:** Examples of axon branches in the process of myelination and elimination; hollow arrow head indicate faint MPZ presence preceding Caspr staining; white arrow heads indicating doubly innervating branches; enlarged view of dashed box showed a maturing paranode with Caspr staining (green) and MPZ staining of compacted myelin sheath (magenta). Scale bar = 10 µm; Scale bar = 5 µm.

2.2.2.3. Myelination during synapse elimination

The timing of terminal branch myelination on motor axons coincides with the time-frame of NMJ synapse elimination (Wyatt and Balice-Gordon, 2003). Indeed, when I examined immunostainings for myelin / node components for the innervation pattern of the NMJs, I could identify partially myelinated terminal branches that are still engaged in competition, *i.e.* share innervation of an NMJ with another axon branch (**Figure 18B**). I first established the timing of synapse elimination: from P7 to P11, the proportion of doubly innervated NMJs dropped from around 50% to less than 5% (**Figure 18A**). At the same time, the percentage of singly innervating terminal branches

with nodal structures (Caspr staining positive) increased from 23.0 ± 4.0% to 71.1 ± 7.2% (**Figure 18B**, number of animals ≥ 3, number of branches ≥ 50). By the end of the second postnatal week, nearly all the branches innervating the *triangularis sterni* muscle become singly innervated as well as myelinated.

Notably, when comparing innervation and myelination patterns branch by branch, I found that axon branches still engaged in competition (*i.e.* innervating doubly innervated NMJs) lagged in myelination when compared to axon branches that had successfully completed competition (*i.e.* singly innervating branches) – even if they were immediate neighbors or branches of the same motor neuron. This lag was detectable with all four myelin/nodal markers described above (**Figure 18C**, MPZ positive sin = 51.4 ± 6.5%, din = 24.6 ± 5.4%, Mann-Whitney test $p = 0.02$; CNTN2 positive sin = 38.2 ± 3.9%, din = 16.3 ± 1.8%, $p < 0.01$; Caspr positive sin = 42.5 ± 8.4%, din = 18.0 ± 4.4%, $p < 0.01$; Nav positive sin = 44.2 ± 4.7%, din = 25.5 ± 4.0%, $p = 0.03$; number of axon per animal ≥ 50, animal per group ≥ 5).

As development progressed, the fraction of competing branches that showed signs of myelination increased, in parallel to the fraction of branches that already finished competition. Indeed, nodal structures and myelin could even be found on retreating axons that already lost competition and formed so called retraction bulbs (“rebu”; **Figure 18B,** and later in **Figure 25B,** Kruskal-Wallis test P7: $p = 0.03$; P9: $p < 0.01$; P11: $p < 0.01$).

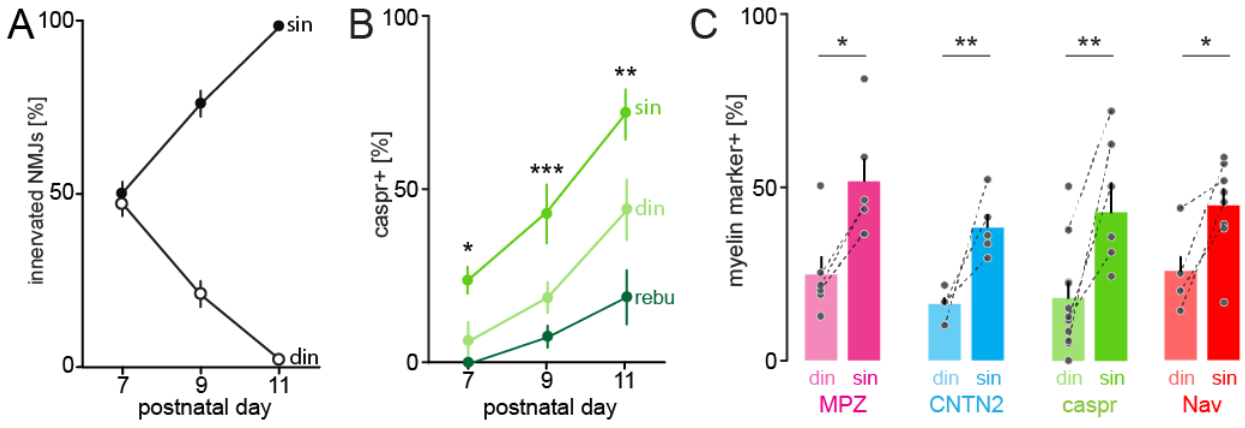

Figure 18: Synapse elimination and myelination coincide during the second postnatal week; **A:** Quantification of on-going synapse elimination from P7 to P11, singly innervated NMJ (sin) vs. doubly innervated NMJ (din); **B:** Quantification of initiation of myelination on terminal branches from P7 to P11, comparing singly / doubly innervating branches (sin / din) and retraction bulbs (rebu); **C:** Quantification of myelin/nodal structure positive terminal branches with immunostaining of MPZ, CNTN2, Caspr and Nav on P9.

2.2.3. Dynamics of molecular components at nascent nodes

Since the initiation of myelination appears to be correlated to the competition status of terminal branches, it is possible that myelin formation is in general delayed on branches still in competition (but advances at normal speed once initiated), or that the accumulation of nodal protein is slower in poly-innervating terminal branches. To differentiate these scenarios, I devised a fluorescence recovery after photobleaching (FRAP) assay on new transgenic mice (provided by P. Brophy, U. Edinburgh) that express GFP-labeled axonal proteins, Caspr and Nav, that are localized at paranodes and nodes respectively. My aim was to characterize the maturation state of nodes with single-branch precision and explore the initiation events that contribute to node formation and hence myelination.

2.2.3.1. Characterization of *Thy1:Caspr-GFP* transgenic mice

Transgenic mice expressing GFP-tagged Caspr protein under the control of *Thy1* promoter were generated by Peter Brophy and colleagues (U.Edinburgh, Brivio *et al.*,

2017). In the spinal cord lysate of the *Thy1:Caspr-GFP* mouse, the Caspr antibody detected a faint band of Caspr-GFP (**Figure 19A** upper panel, black arrow) slightly larger than the wildtype Caspr band (grey arrow), as previously reported (Brivio *et al.*, 2017). The same blot was stripped and restained with a GFP antibody, confirming the GFP positive band (**Figure 19A** lower panel, black arrow). Analysis of motor axon arbors in this mouse showed that – as other *Thy1*-driven transgenic mice (Feng *et al.*, 2000) – the *Thy1:Caspr-GFP* line expressed the transgene in a subset (~70%) of motor neurons at P9 (**Figure 19B,** white arrow pointing to a Caspr-GFP positive paranode, black arrow pointing to a Caspr-positive but GFP-negative paranode). Together this indicates that the overexpression of Caspr-GFP in the transgenic mice is of moderate levels compared to the endogenous Caspr. Caspr-GFP expressing axons showed a similar rate of initiation of myelination at P9 as their wild-type littermates, confirmed with Caspr antibody staining (**Figure 19C**). Therefore, the *Thy1:Caspr-GFP* transgenic mouse line appears to be a suitable model to study the dynamics of emerging paranodal structures – with all the caveats that result from using an overexpressed protein that is not controlled by the endogenous promoter.

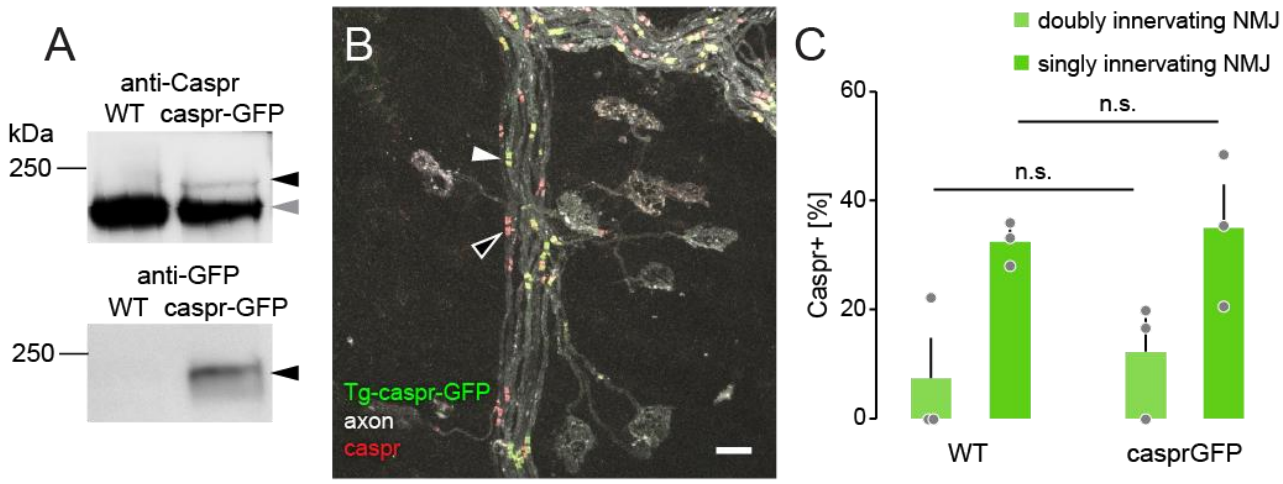

Figure 19: Characterizing the *Thy1:Caspr-GFP* transgenic mice. **A:** Western blot of spinal cord lysate from wild-type control and *Thy1:Caspr-GFP*, stained with antibody against Caspr (above) and antibody against GFP (below). A faint Caspr positive band (black arrowhead) can be observed in the anti-Caspr stained *Thy1:Caspr-GFP* lysate above the endogenous bands (grey arrowhead), which is also GFP positive (below). **B:** Confocal imaging of the triangularis sterni muscle of P9 *Thy1:Caspr-GFP* mouse,

where ~70% of the Caspr positive nodes (red, stained with anti-Caspr antibody), were also GFP positive (native GFP, green); **C:** The initiation frequency of myelination on terminal axon branches is comparable between wild-type and *Thy1:Caspr-GFP* transgenic mice on P9.

2.2.3.2. FRAP assay on *Thy1:Caspr-GFP* and *Thy1:Nav-GFP*

To test whether initiation of myelination is delayed on branches still engaged in competition, and to further understand the protein turn-over process at nodes of Ranvier, I performed FRAP analysis on transgenic mice that express GFP-tagged Caspr. In *triangularis sterni* muscle explants, GFP-labeled nodes were photo-bleached with a 488 nm laser to ~40% of their original intensity, then allowed to recover over the course of 3 h perfused with oxygenized Ringer's solution (**Figure 20A-D**). Interestingly, a significant recovery was observed in young mice with developing myelin after photobleaching, but not in adult mice where myelination is complete (P9 – P11 compared to 6 weeks, Mann-Whitney test $p < 0.01$, number of axons analyzed per group ≥ 13, number of animal per group ≥ 10, **Figure 20E**). Moreover, in early postnatal mice, the recovery rate of paranodal Caspr-GFP on singly innervating terminal branches was significantly faster compared to the recovery rate on contemporary intercostal nerve axons, where the nodes were more fully developed (Kruskal-Wallis test with Dunn's Multiple Comparison Test positive, $p < 0.01$, number of axons analyzed per group ≥ 13, number of animal per group ≥ 10). Together the data indicates that the accumulation of Caspr protein is faster on nascent paranodal structures compared to fully developed paranodes.

When comparing paranodes on terminal axon branches that had either completed or were still engaged in competition, I found a clear dichotomy: the recovery rate of Caspr on branches still engaged in competition ("din") was significantly higher than that measured on singly innervating branches at the same developmental age (Kruskal-Wallis test with Dunn's Multiple Comparison Test positive, $p < 0.01$, **Figure 20E**). Also,

axons innervating NMJs where competition recently resolved (“young sin”), as defined by a singly innervated NMJ associated with a retraction bulb, displayed an intermediate recovery rate when compared to branches that have either resolved competition or are still engaged in it – suggesting that the paranodal structures quickly mature, once the competition-associated “brake” on myelination is lifted.

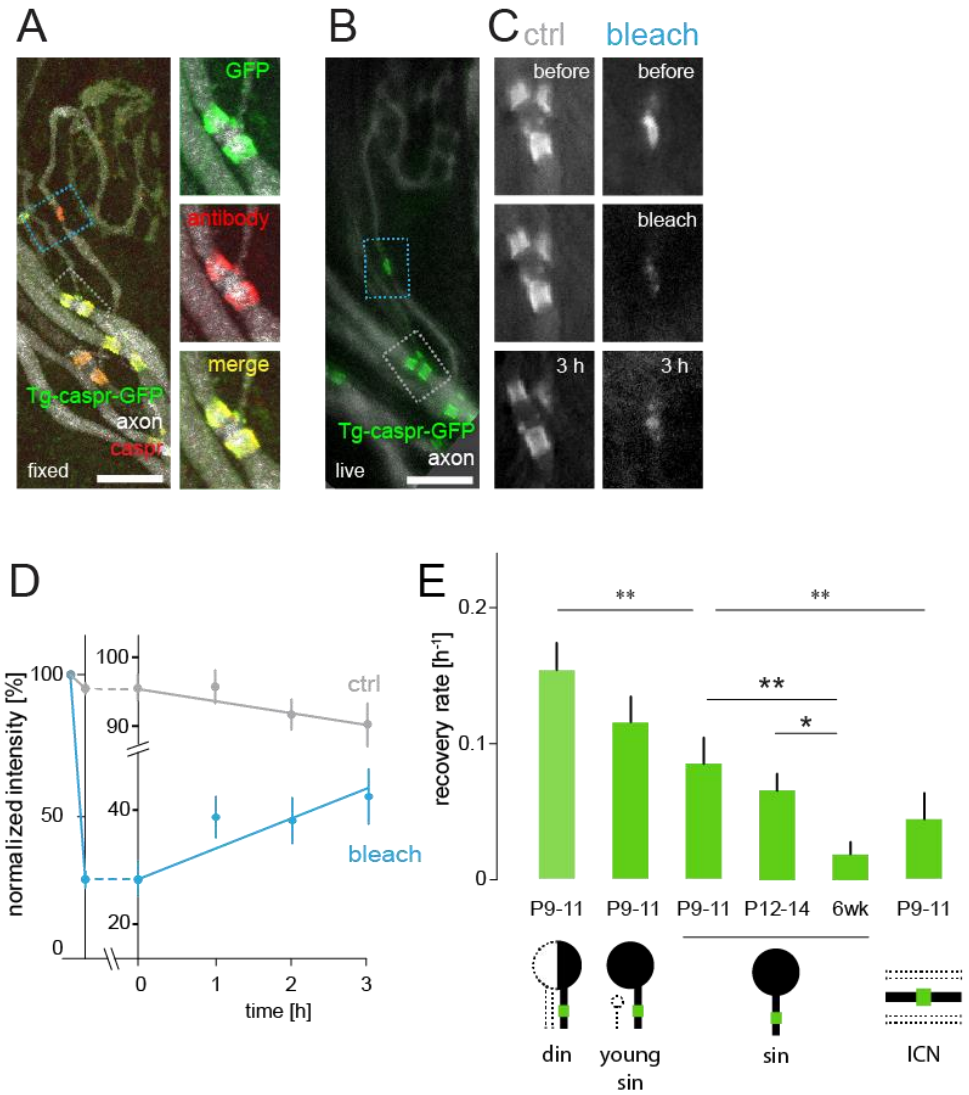

Figure 20: Myelination is delayed in competing branches. **A:** Confocal image of fixed and stained *Thy1:Caspr-GFP* P11 muscle with Caspr antibody staining (red) co-localizing with GFP signals on paranodal structures, GFP in green, axon in white from *Thy1:OFP3*; **B:** The same terminal branch from (**A**) imaged live with wide-field microscopy; **C:** FRAP assay of the paranodes in the dashed boxes in (**A**) and (**B**), gray box marked the control paranode, white the bleached paranode; **D:** Sample bleached and control time-course over 3 h, averaged over 21 pairs of paranodes in 17 animals of P9-P11; **E:** Quantification of recovery rate, comparing singly innervated branches of different developmental ages (P9-P11, P12-P14, 6 weeks), and different competition status at the same developmental age (P9-P11).

We repeated the same assay on *Thy1:Nav-GFP* mice, which showed a similar decrease in recovery rate in adult animals compared to the young pups in their second postnatal week (**Figure 21**). Together, the FRAP experiment showed that the turn-over rate of nodal protein can be an indicator of how recent the myelination started in the terminal branches, and that competing branches are delayed in the initiation of nodal component accumulation, compared to singly innervating branches.

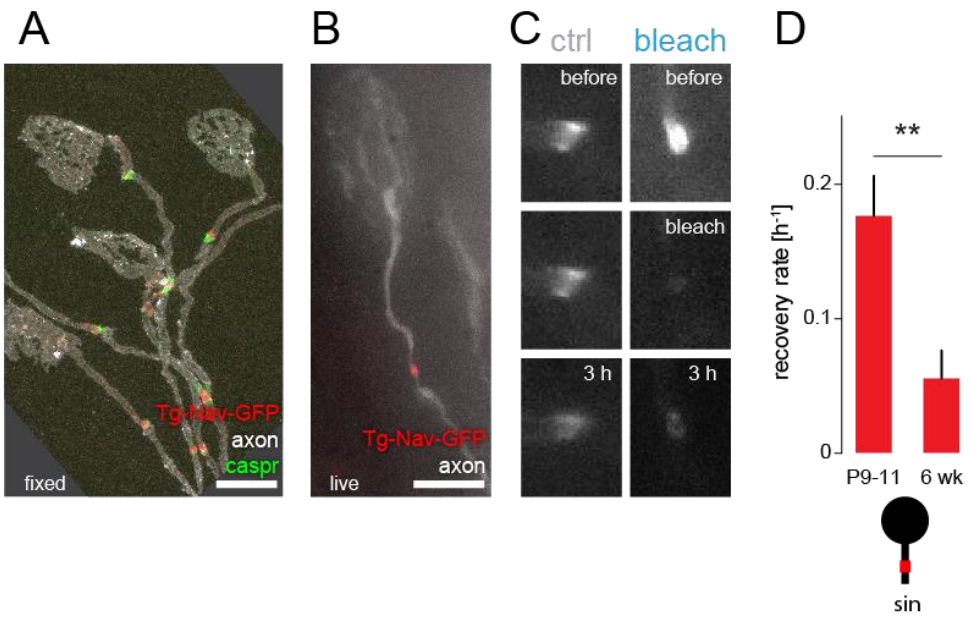

Figure 21: characterization and FRAP assay using *Thy1:Nav-GFP*. **A:** Confocal image of fixed and stained *Thy1:Nav-GFP* P11 muscle with Caspr antibody staining (green) on paranodal structures, Nav-GFP in red on node, axon in white from *Thy1:OFP3*; **B:** Terminal branch of *Thy1:Nav-GFP* P11 imaged live with wide-field microscopy; **C:** FRAP assay of the nodal structure in B with a control node in the same field of view but on a different imaging plane; **D:** Quantification of recovery rate, comparing nodes on singly innervated branches of developing P9 – P11 vs. 6 weeks (10 axons from 5 animals per group, Mann-Whitney test p = 0.0068).

Overall, these FRAP-experiments revealed that the lack of myelination initiation is not due to a slower accumulation rate of nodal proteins on competing branches compared to their winning neighbors, but rather because of a delay in the initiation of myelination on competing branches. Still, it appears that this is a delay, rather than an absolute inability to initiate myelination on competing branches – as axon branches

mature, even if they still compete, increasingly initiate myelination (**Figure 18B**). Next I attempted to test, whether shifting the time course of myelination in relation to competition would alter progress of neuronal remodeling.

2.3. Effects of myelinating factor on synapse elimination: would premature myelination narrow the "window of plasticity"?

Delaying myelination until competition is resolved can be a cost-effective measure for the organism, since it has been shown that in the mature brain, myelination can consolidate neural circuitry by suppressing plasticity (McGee *et al.*, 2005), where the stability of the myelin sheath is crucial to ensure rapid conduction of action potential and axonal integrity. It has been reported that in the delay line axons of barn owl *nucleus laminaris*, where myelination is delayed until after the head reaches the animal's adult width, when the formation of neuronal circuit is finalized (Cheng and Carr, 2007). Therefore it is conceivable that premature myelination can close the plastic window in the PNS, affecting the pruning process.

The myelinating factor Neuregulin 1 type III (Nrg1-III) has been shown to play an important role in controlling the rate and extent of myelin PNS myelination (Taveggia *et al.*, 2005). To find out if myelination had any influence on the competition outcome of the terminal motor neurons, we used genetic manipulation of NRG1-III to visualize the effect *in vivo*.

2.3.1. Effect of premature myelination (*Thy1:Nrg1-III*)

We first studied the effect of NRG1-III overexpression on animals using *Thy1:Nrg1-III* animals, which overexpress NRG1-III in motor neurons and other neuronal populations (Velanac *et al.*, 2012) and indeed found a higher initiation rate of

myelination in terminal axon branches that innervate singly, as well as doubly innervated NMJs at P7 (Mann-Whitney test p = 0.03, **Figure 22A, B, D**). However, increased myelination on branches still in competition did not seem to hinder branch elimination (**Figure 22C**). Indeed, work published in parallel to our efforts, which focused on tSCs in on *soleus* and *sternomastoid* muscles, reported transiently accelerated pruning in *Thy1:Nrg1-III* transgenic mice (Lee *et al.*, 2017). Together, these data refute the hypothesis that premature myelination stabilizes competing branches and hinders synaptic elimination.

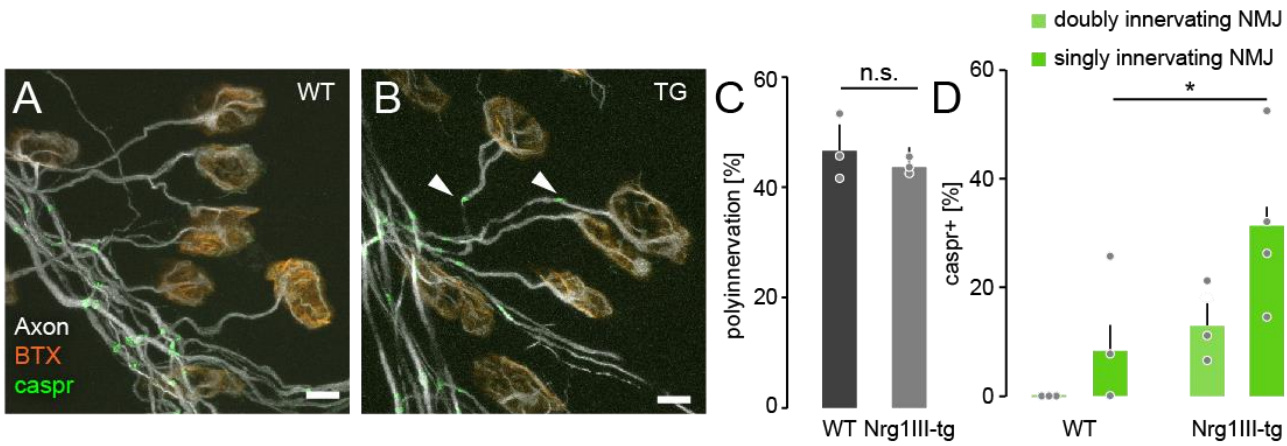

Figure 22: Overexpression of NRG1-III accelerates myelination, but does not affect the pruning process in *triangularis sterni*. **A:** P7 *Trangularis sterni* muscle of wild-type control animal, **B:** littermate control of *Thy1:Nrg1-III* transgenic mouse, arrowhead point to a Caspr positive paranode on one singly and one doubly innervating branch; axon stained with tubulinβ-III in white, Caspr antibody staining in green and NMJ stained with BTX in orange; Scale bar = 10 µm; **C:** Quantification of synaptic elimination status on P7; **D:** Quantification of myelin initiation status on P7.

2.3.2. AAV9-mediated *Nrg1-III* deletion (*Nrg$^{FL/FL}$;TdTomato* + iCre)

Since overexpressing myelin promoting factor did not affect pruning significantly, we also probed the effects of deleting NRG1-III in motor neurons. By neonatal intra-ventricular injection of AAV9-CMV-iCre virus into *Nrg1* conditional knock-out animals (*Nrg$^{FL/FL}$*, Velanac *et al.*, 2012), NRG1-III was deleted in a subset of motor neurons (and other scattered cells in the nervous system). iCre expression was confirmed with a Cre-inducible transgenic *TdTomato* reporter, and the Cre-negative branches served

as internal control (**Figure 23A, B**) – and the expected effect on myelination was clearly apparent on the tdTomato labeled ("Cre+") branches compared to the internal control (Mann-Whitney test p = 0.03, **Figure 23A, B, D**). However, this delay in myelination did not have an obvious influence on pruning at the age investigated (**Figure 23C**).

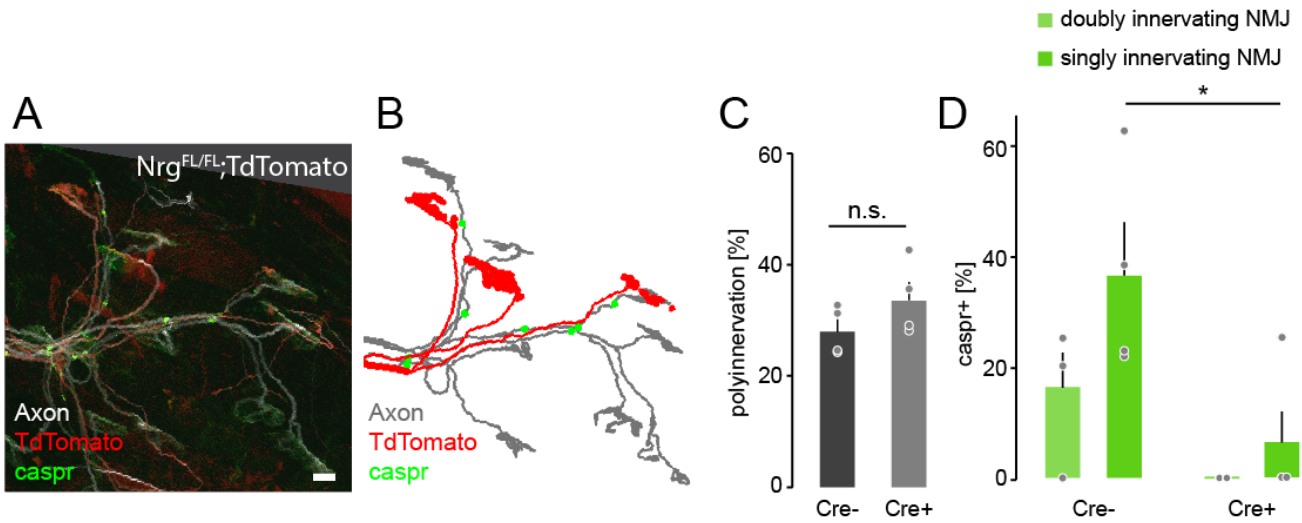

Figure 23: Deletion of Nrg1-III delays myelination, but does not affect the pruning process in *triangularis sterni*. **A:** P9 Nrg$^{FL/FL}$;*TdTomato* animal partially induced by injecting AAV9-CMV-iCre, with the expression of *TdTomato* (red) as indication of Cre expression; **B:** Schematic outline of the *TdTomato* positive (red) and negative axons (grey), and Caspr paranodes in green; **C:** Quantification of synaptic elimination status on P9; **D:** Quantification of myelin initiation status on P9.

Taken together, these genetic manipulations show that synapse elimination in the PNS is not globally affected by premature myelination induced by overexpression of NRG1-III. In fact, both prohibiting and enhancing myelination by genetic manipulation of *Nrg1-III* in competing branches have very limited lasting effect on synapse elimination. Since branches in competition are significantly delayed in the formation of myelin, it appears that in the PNS, competition status influences myelination, but a reverse effect is not apparent at the population level. Still, these experiments involve artificial levels of pro-myelination signaling and could be impacted by remote effects. Thus, I next explored, whether a subtle influence of myelination on competition could be detected at the single axon level under conditions where no artificial manipulation of myelination or competition were undertaken.

2.4. Effects of branch pruning events on myelination: does myelination convey an advantage in competition?

During the process of pruning superfluous inputs, branches terminating on the same NMJ compete for the territory they occupy, typically shifting progressively until one axon completely withdraws, leaving the entire endplate to the winning partner (Walsh and Lichtman, 2003). Axon diameter of the competing branches was found to be proportional to the occupied terminal area as well (Keller-Peck *et al.*, 2001). At the same time, axon diameter in the PNS is influenced by myelination (de Waegh, Lee and Brady, 1992). As axon caliber and myelin together determine the ability of an axon branch to convey action potentials, and *e.g.* branch-point failures could be a mechanism to "shut out" a competing branch (Debanne, 2004), I wanted to explore systematically, whether the precise competition status of an axon branch would influence its propensity to myelinate, and whether myelination would confer a detectable advantage in competition. To explore this, I analyzed the myelination status on competing branches in correlation to their respective terminal area and axon diameter.

2.4.1. Initiation of myelination *vs.* NMJ territory

It is a unique feature of neuromuscular remodelling that morphological features of single axons can be used to predict outcome of synaptic competition – this is true for the synaptic territory (i.e. percentage of postsynaptic membrane) that a branch innervates, as well as for its diameter (Keller-Peck *et al.*, 2001; Buffelli *et al.*, 2003; Walsh and Lichtman, 2003; Brill *et al.*, 2016).To determine the exact correlation between competition status and myelination, I thus measured the proportion of the NMJ area occupied by competing branches – which serves as a predictor of competition outcome, and quantified their myelination state. To this end, I crossed *ChAT:Cre* mice to the *Thy1:Brainbow-1.1* line M (Livet *et al.*, 2007), which though a

“genetic random generator” labels individual motor units with a combination of membrane-targeted fluorescent proteins, enabling the determination of synaptic territory occupied by the terminal branches (**Figure 24A**). Analysis of the corresponding myelination status of the terminal branches (using Caspr immunostaining) shows that myelination was kept at a lower level throughout the double innervation stage (**Figure 24B**), independent of the NMJ area it occupied, suggesting that there is a “brake” on myelination until after competition resolves. As myelinated branches are not enriched amongst predominant putative “winner” braches (χ^2 test, 1-40% vs. 60-99% $p = 0.17$), but only amongst established winners (χ^2 test, $p < 0.0001$). It appears that myelination does not confer a competitive advantage over their unmyelinated counterparts. This is in contrast to other subcellular characteristics of terminal axon branches (such as cytoskeletal stability or organelle transport), which systematically differ between axon branches that are “winning” (>50% territory) or are “losing” (<50%; Brill *et al.*, 2016).

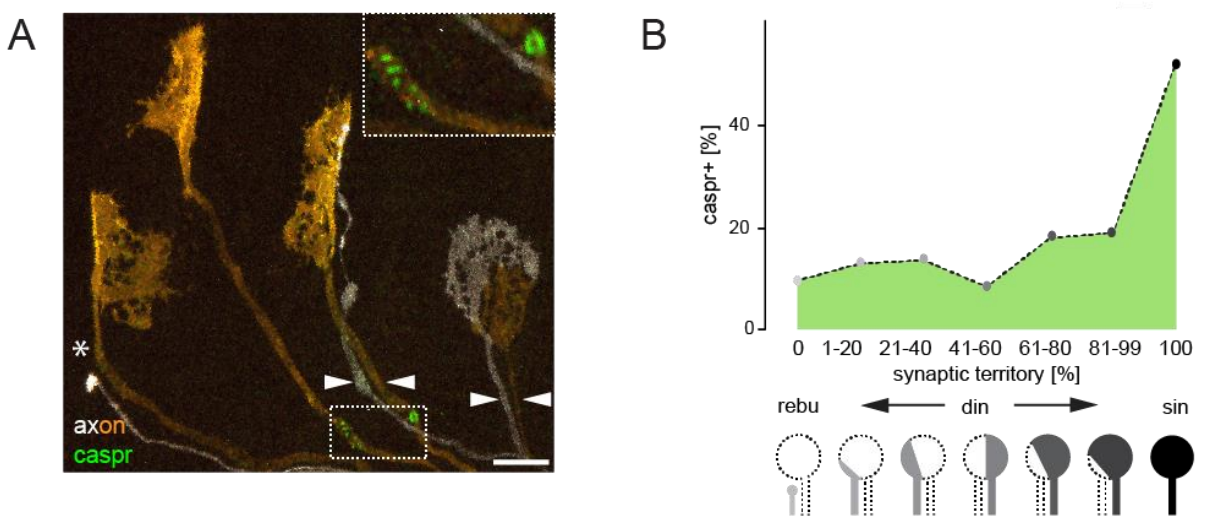

Figure 24: Synaptic territory occupied by competing branches does not correlate with their myelination state. **A:** Example of *ChAT:Cre; Thy1:Brainbow 1.1* Line M labeling, with distinctive fluorescence labeling of motor units (orange and white); arrowheads indicate competing branches, and star marks a retraction bulb (rebu), enlarged dashed box shows example of paranodal accumulation of Caspr staining (green), scale bar = 10 µm; **B:** Quantification of initiation of myelination versus synaptic territory of the input (Axon per group > 70, animals per group ≥ 18).

2.4.2. Initiation of myelination *vs.* axon diameter

Terminal branches still engaged in competition are delayed in myelination, and typically the branches retreat without forming any myelin, while the winning branches initiate the myelination program (**Figure 25A**). However, around 15% of the axons overcome the inhibition and start to myelinate before the competition finishes (**Figure 25C**). Indeed, axons that lose the competition and formed retraction bulbs, although rarely, can also be observed to have myelin residue wrapping around the retreating branches (**Figure 25B**).

Since myelination in the peripheral nervous system is typically occurring on axons with diameter larger than 1 µm (Voyvodic, 1989; Peters, Palay and Webster, 1991), it is possible that the myelination of branches still in competition is dependent on the axonal diameter – and that two signals compete, namely a competition-related brake and a diameter-dependent accelerant on myelination. However, analyzing the presence of nodal structures in relation to axonal diameter showed that the diameter of terminal branches with or without myelin did not differ systematically. In fact, even branches that completed competition (“100%”) showed no jump in thickness, even though it is assume that these branches quickly mature and consolidate their synapses (**Figure 25D**). Only retreating branches with myelin is significantly thicker than the non-myelinated branches (**Figure 25D**, Mann-Whitney test, $p < 0.01$). Within the myelinated branches, the stretches wrapped in myelinating SCs are not significantly different from the non-myelinated stretches, although in retreating branches, myelin seem to preserve the thickness of the axonal stretch underneath (**Figure 25E**). Taken together, the results confirmed previous studies (Voyvodic, 1989; Peters, Palay and Webster, 1991) that myelin on PNS terminal branches is only found on axon stretches with a diameter larger than 1 µm. However, competing branches above this threshold are not invariably myelinated, and the myelinated branches are not significantly thicker than their unmyelinated partners. Moreover, even in these early stages of myelination, the

previously reported local effect of myelinating SCs on local axon diameter is apparent (Black, Waxman and Hildebrand, 1985; Hernández, Blackburn and Alvarez, 1989). Finally, and perhaps most strikingly, even terminal branches that are myelinated can still lose in competition and be pruned back if necessary – suggesting that in addition to developmental axon pruning, developmental myelin degradation is a physiological process also in mammals (Czopka, ffrench-Constant and Lyons, 2013).

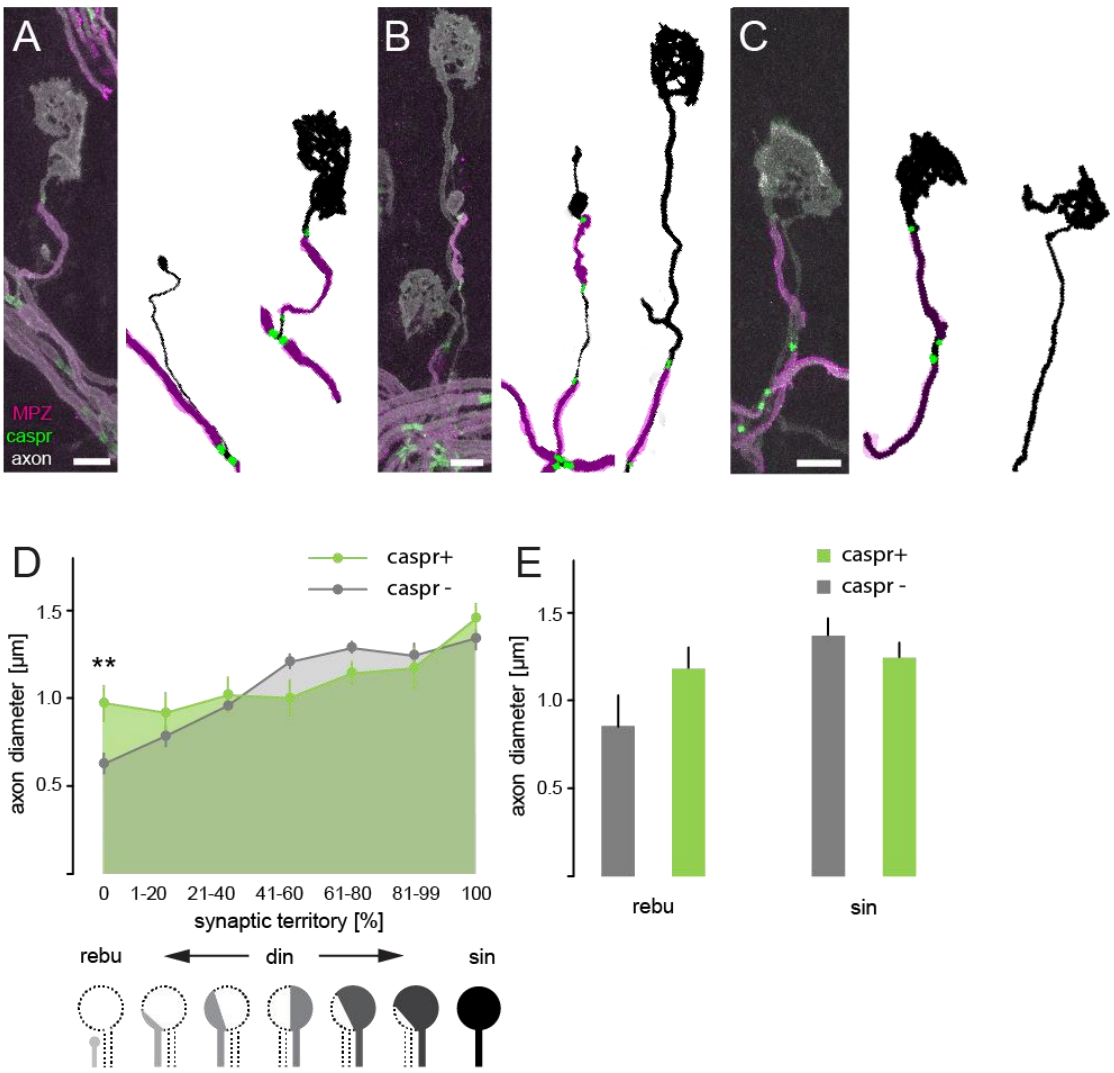

Figure 25: Myelinated branches in competition do not differ from their non-myelinated sister branch in axon diameter. **A:** Example of a myelinating winning branch vs. a retreating axon without any myelin (MPZ staining in magenta and Caspr staining in green); schematic outline of the retreating and surviving axons with their respective myelin and nodal markers; **B:** Example of a myelinated retreating branch and its winning neighbor, in this case unmyelinated; **C:** Example of a pair of competing branches with one of the axons myelinated; **D:** Quantification of axon diameter averaged over the whole length of the terminal branch versus its synaptic territory, with or without initiation of myelination (axon per group ≥ 10, animals per group ≥ 7); **E:** Quantification of axon diameter of the terminal branch stretches with MPZ

staining compared to the stretches without, in retreating branches (rebu) or singly innervating branches (sin, axon per group ≥ 7, animals per group ≥ 7).

2.4.3. Competition status of neighboring branches

Activity-dependent synaptic elimination is considered a local phenomenon, where b competition is resolved by local interactions at each NMJ (Keller-Peck *et al.*, 2001). To analyze if the initiation of myelination is also regulated at each terminal branch independently, *ChAT:Cre; Thy1:Brainbow 1.1* line M mice were used to analyze small sub-arbors composed of three neighboring terminal branches from the same motor-unit (**Figure 26A**). Interestingly, a ~40% decrease in myelination initiation was observed on singly innervating branches with a doubly innervating neighbor (**Figure 26C**, white arrowheads), compared to ones with singly innervating neighbors on either side (**Figure 26B**, black arrowhead).

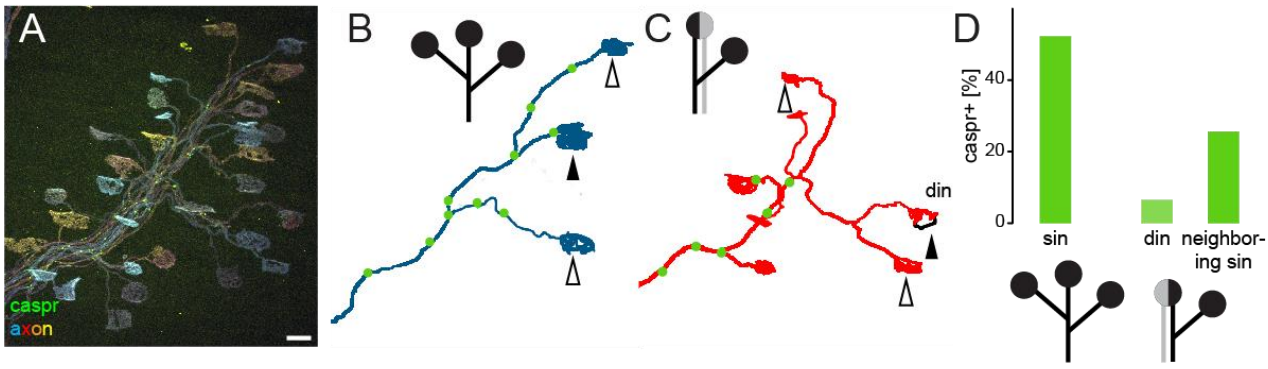

Figure 26: Innervation state may also affect neighboring branches on the same motor-unit. **A:** Example of *ChAT:Cre; Thy1:Brainbow 1.1* Line M labeling, with distinctive combinations of fluorescence labeling of motor units; scale bar = 20 µm; **B, C:** Schematic outline of single motor-units in (**A**); black arrowhead point to a singly innervating terminal branch in (**B**), and a doubly innervating terminal branch in (**C**), with two singly innervating neighbors (white arrowheads); Caspr positive paranodes marked in green; **D:** Quantification of initiation of myelination of singly innervating branch with sin neighbors (e.g. black arrowhead in **B**) versus doubly innervating branches (e.g. black arrowhead in **C**) and singly innervating branch with din neighbors (e.g. white arrowheads in **C**, Axon per group ≥ 40, animals per group ≥ 13).

These results suggest either an intra-axonal or local effect emanating from competing synapses that also delays myelination nearby – the nature of this influence remains unclear, but could be examined, by *e.g.* analyzing local cargo delivery in

relation to nearby competition outcomes. Overall, this raises the question about the mechanism underlying the impact of ongoing completion on local myelination initiation.

2.5. How does synapse elimination delay myelination? Potential mechanisms

Since the branches in competition are delayed in myelin initiation, and promoting myelination did not obviously affect pruning, I then asked whether prolonging the competition process affects myelination instead. The hereditary spastic paraplegia gene, *Spastin*, is a microtubule severing enzyme that targets the stable microtubule segments rich in acetylated or polyglutamylated tubulin (Baas *et al.*, 2016). It has been shown to promote branch formation (Yu *et al.*, 2008), axon outgrowth (Wood *et al.*, 2006), and is linked to synaptic structure and function (Trotta *et al.*, 2004) as well as axon maintenance and transport (Tarrade *et al.*, 2006). Neuron-specific *Spastin* deletion in mice results in a substantial delay in pruning during postnatal development of the NMJs (Brill *et al.*, 2016), which provides an interesting system to study the effect of delayed synapse elimination on myelination.

2.5.1. AAV9-mediated *Spastin* ablation (*Spastin*$^{FL/FL}$*;TdTomato* + iCre)

Deletion of *Spastin* causes a significant delay in synapse elimination during the first postnatal weeks, with double innervation persisting longer compared to the wild-type animals – the likely interpretation is that microtubule dismantling is an important step in the execution of competition outcome and impacts the dismantling speed of "losing" axon branches (Brill *et al.*, 2016). Here we used conditional knock-out *Spastin* animals (*Spastin*$^{FL/FL}$; Brill *et al.*, 2016), which I intraventricularly injected with AAV9-CMV-iCre, to induce subset deletion of *Spastin* in motor neurons (**Figure 27A, B**) – again, recombination was monitored with a Cre-dependent *TdTomato* reporter allele (*i.e.* "Cre positive axon branch" refers to a TdTomato-labeled branch). In accordance with the

findings by Brill *et al.* 2016 in *Spastin* knock-out animals, significantly more doubly innervating terminal branches were found in Cre-positive branches compared to the negative controls (**Figure 27C**, double-innervation in wild-type = 10.5 ± 2.9%, 9 muscle / 5 animals, in Cre-positive branches = 30.9 ± 3.0%, n = 8/12; t-test p = 0.02, both groups passed the D'Agostino & Pearson normality test). Interestingly, initiation of myelination on these competing branches was also significantly more common compared to Cre-negative sister branches (**Figure 27D**; number of animals per group ≥ 3, Mann-Whitney test p = 0.04). However, branches that already finished competition had similar degree of myelination with or without *Spastin*. Together with the results on BTX blockade of synapses (see above, Section 2.2.1), this suggests that artificially extending the competition phase (with BTX), but not the clearance phase (*Spastin* deletion) lengthens the delay in myelination initiation. This is in line with my previous observation that late during physiological competition (P11; **Figure 18**) even axon branches that are still engaged with a doubly innervated junction can be myelinated, and eventually be pruned back if necessary.

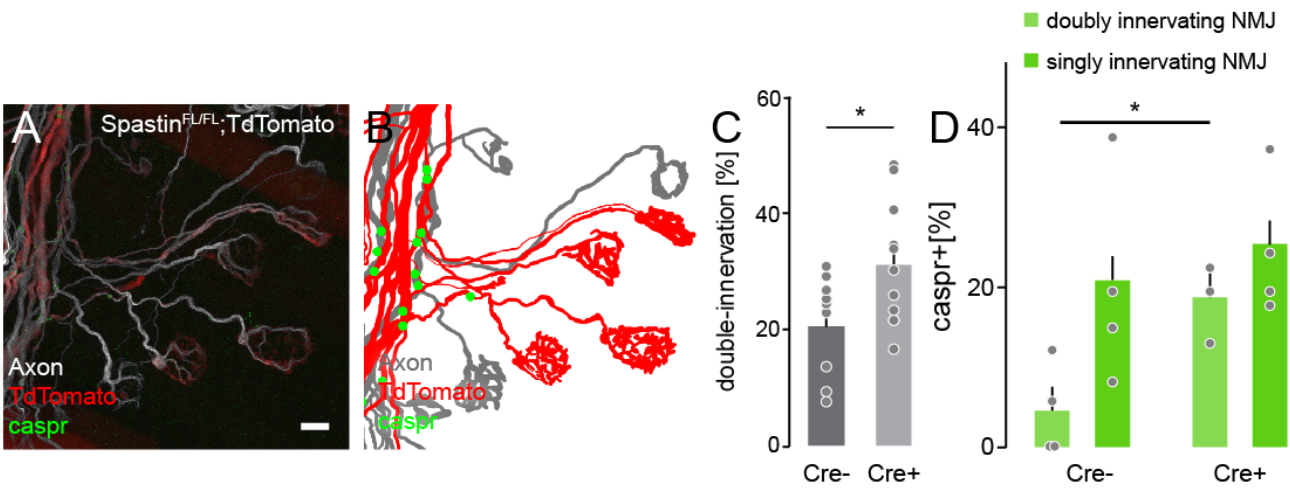

Figure 27: Selective deletion of *Spastin* in motor neurons increase initiation of myelination on competing branches. **A:** *Triangularis sterni* muscle of a *Spastin*$^{FL/FL}$;*TdTomato* injected with AAV9-CMV-iCre, with the expression of *TdTomato* (red) as indication of Cre expression; **B:** Schematic outline of the *TdTomato* positive (red) and negative axons (grey), and Caspr paranodes in green; **C:** Quantification of synaptic elimination status on P9; **D:** Quantification of myelin initiation status on P9.

2.5.2. Spastin deletion combined with postsynaptic activity block

The delayed synapse elimination in Spastin leads to increased myelination on competing branches, in contrast to the BTX-induced delay of both pruning and myelin formation. It is therefore of interest to explore, how activity blockade affects the axoglial remodeling process in Spastin knock-out animals, to dissect how the two manipulations relate to each other.

To enable this, I first repeated the experiments above with a global *Spastin* knock-out mouse line (which shows the same delay in resolving double-innervation as the viral approach above; Brill *et al.*, 2016). Here again, I found a significant increase in myelination on competing branches (**Figure 28A-C**; Caspr positive terminal branches on P9 in WT = 8.7 ± 3.4%, in KO = 22.4 ± 7.1%, animals per group ≥ 7, Mann-Whitney test $p = 0.01$). When P7 *Spastin* KO animals were locally injected with fluorescently-conjugated BTX on one side of the thorax, the injected pups were viable and active after the treatment, not distinguishable from untreated controls. After two days, the injected side of the thorax showed distinct fluorescence at NMJs compared to the uninjected side of the same animal (**Figure 28D, E**). Interestingly, the branches with BTX-positive endplates showed a significant delay in myelination compared to the unaffected branches (**Figure 28F**, double-innervation in BTX-negative control = 21.0 ± 4.8%, in BTX-postive = 6.5 ± 4.9%, Wilcoxon test $p = 0.03$, animal per group = 5). This suggests that blocking neurotransmission supersedes the effect seen above in *Spastin*-deleted pups, where axon branches that cannot be cleared due to a stabilized microtubular cytoskeleton start myelinating.

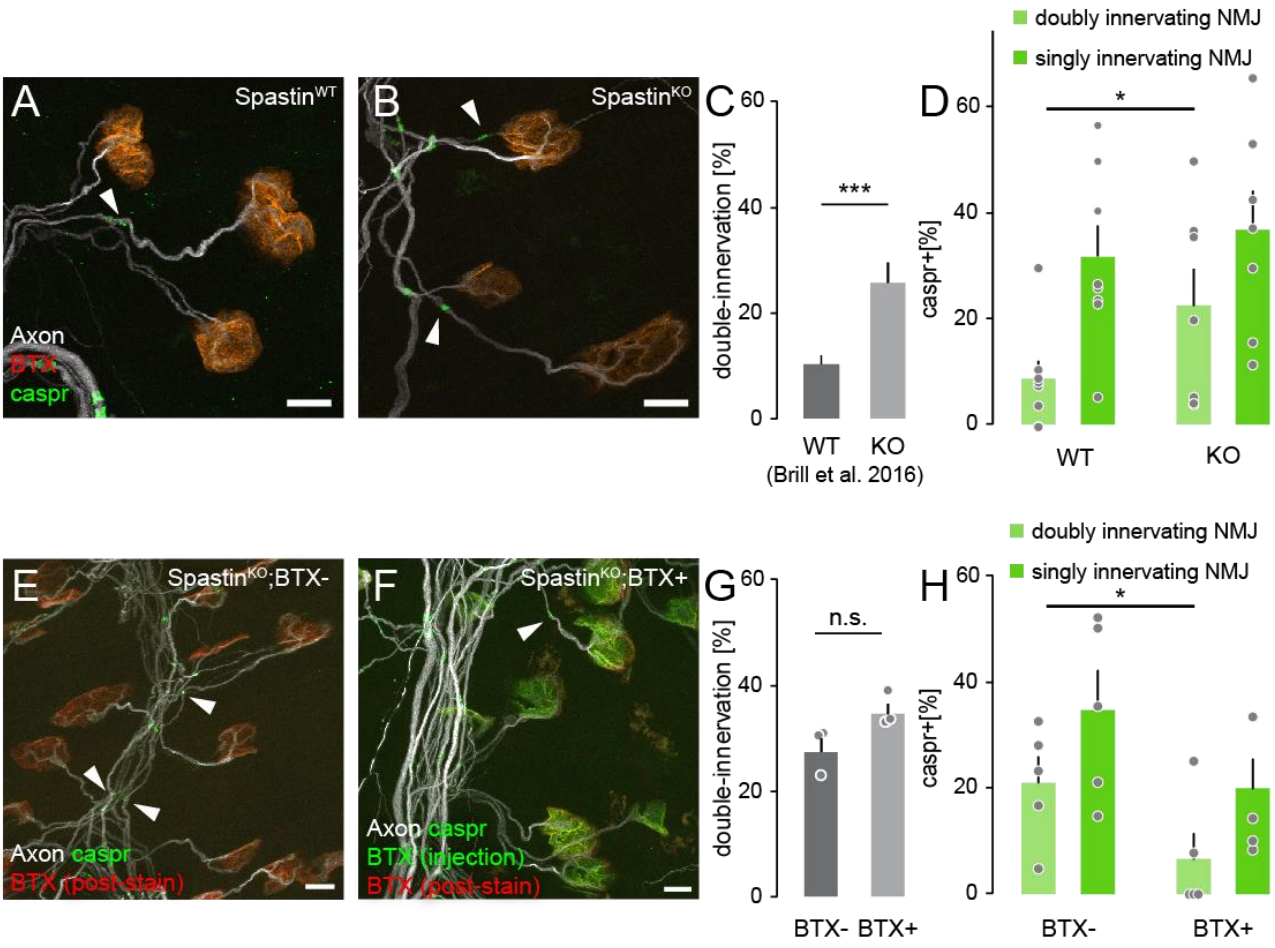

Figure 28: Activity blockade with injected BTX significantly delays myelination in *Spastin* KO. **A:** P9 *Trangularis sterni* muscle of wild-type control animal, arrowhead point to a Caspr positive paranode (green) on a singly innervating branch; **B:** littermate control of *Spastin* KO mouse, arrowhead point to a Caspr positive paranode on one singly and one doubly innervating branch; axon stained with Tubulinβ-III in white, NMJ stained with BTX in orange; **C:** *Spastin* KO animals are significantly delayed in synaptic pruning on P9 compared to wildtype control animals (modified from Brill et al. 2016); **D:** Quantification of myelin initiation status on P9 of *Spastin* KO animals compared to WT; **E:** P9 *Trangularis sterni* muscle on the uninjected side of the *Spastin* KO thorax; **F:** *Trangularis sterni* muscle on the injected side of the thorax, from the same animal as in (**E**), arrowheads point to Caspr positive paranodes (green), and injected BTX is pseudo-colored in green over the post-stained BTX in red. **G:** Quantification of synaptic elimination status on P9 comparing BTX injected to the uninjected muscle in *Spastin* KO animals; **H:** Quantification of myelination initiation status on P9 from the same animals as in (**G**). Scale bar = 10 µm.

2.5.3. Is axonal transport affecting myelination?

During the dismantling of retreating branches, organelle transport was found to be deficient compared to winning branches. This is likely because microtubules, the track for axonal cargo transport, in the retreating branches are highly fragmented and

destabilized. Accordingly, *Spastin* deletion, which stabilizes microtubules and delays pruning, maintains transport in retreating axons (Brill *et al.*, 2016). This raises the intriguing possibility that the competition-associated myelination brake is due to insufficient delivery of axonally transported nodal components, which would delay myelination, or of pro-myelination factors, which are then inserted into the membrane of the axon branch to provide the myelination signal for local SCs. I explored both possibility, but due to methodological and temporal restrictions, I can only report preliminary data here.

2.5.3.1. Caspr-GFP particle movement in young motor-neurons

In young *Thy1:Caspr-GFP* mice, GFP-positive particles moving along the axons could be observed in young animals (**Figure 29A**, arrowheads pointing to examples of such particles), but not in adult animals (**Figure 29B**). The movement of these particles in young animals were directional and predominantly anterograde (**Figure 29C**, number of axons per group ≥ 10, number of animals per group ≥ 3), coinciding with the time-frame of comparably high recovery after photobleaching in the FRAP data from Section 2.2.3. However, such particles were extremely rare (1-2 particles / hour) in terminal branches, so quantification and comparison between singly vs. doubly innervating branches was not possible. I also failed to observe the insertion of such particles into photobleached nascent paranodes – overall, the low amount of Caspr-GFP that seems to be delivered in such particulate form does not chime with the relatively high insertion rate that I measured at these ages. Thus, a regulation of node formation by limiting supply of paranodal or nodal constituents seems unlikely (which according to current models is also not believed to set the pace of myelination, but rather *vice versa*; Zhang *et al.*, 2012).

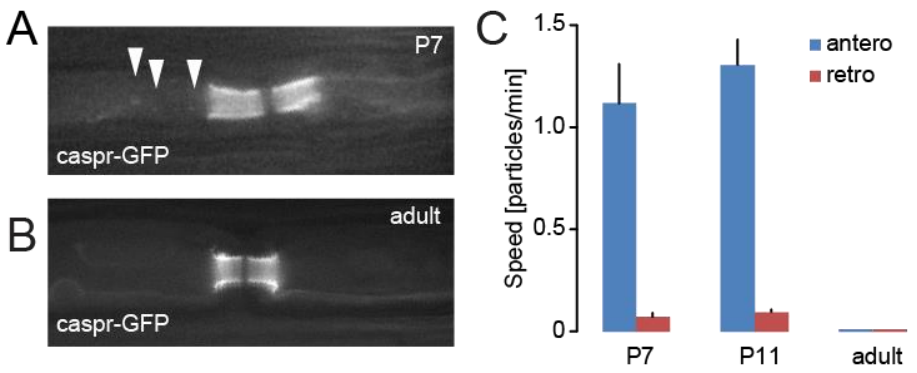

Figure 29: Moving GFP positive particles could be observed in young *Thy1:Caspr-GFP* animals, but not in adult. **A:** Intercostal nerve of P7 *Thy1:Caspr-GFP* animal, arrowhead pointing to floating particles; **B:** Intercostal nerve of 4 month old adult animal; **C:** Quantification of the number of particles moving along the intercostal nerve.

2.5.3.2. *Thy1:Stop-KHC* as a tool for reducing axonal transport

To directly manipulate transport flux in axons, the overexpression of the kinesin heavy chain (KHC) cargo-binding domain (CBD) was used to function as a dominant-negative mutant of KHC (Cai, Gerwin and Sheng, 2005). With a floxed Stop-codon inserted before the KHC-CBD domain, my colleagues (M. Brill) generated a Cre-inducible dominant-negative *Thy1:Stop-KHC* mouse line. We crossed this mouse line to *ChAT*:Cre for selective expression of the mutated KHC isoform in motor axons, and to *Thy1:mito-TagRFP* mice to visualize mitochondrial transport *in vivo.* This approach showed a reduced transport flux of mitochondria in intercostal nerve axons by about half compared to wild-type controls (**Figure 30A**), proving the efficacy of this manipulation on kinesin-dependent transport at least of mitochondria. However, no significant change in synaptic elimination (**Figure 30B**) or myelin initiation (**Figure 30C**) was observed in P9 *Thy1:Stop-KHC*. There are a number of possible reasons for this, other than a refutation of our hypothesis that intra-axonal transport delivers a scalable myelination signal, such as insufficient expression of the dominant-negative inhibitor in distal or immature axons; the usage of non-affected motors by the delivery vesicles for putative pro-myelination signals *etc.* Future work and probably additional

approaches will be needed to put our transport hypothesis for the competition-related myelination brake to a vigorous test.

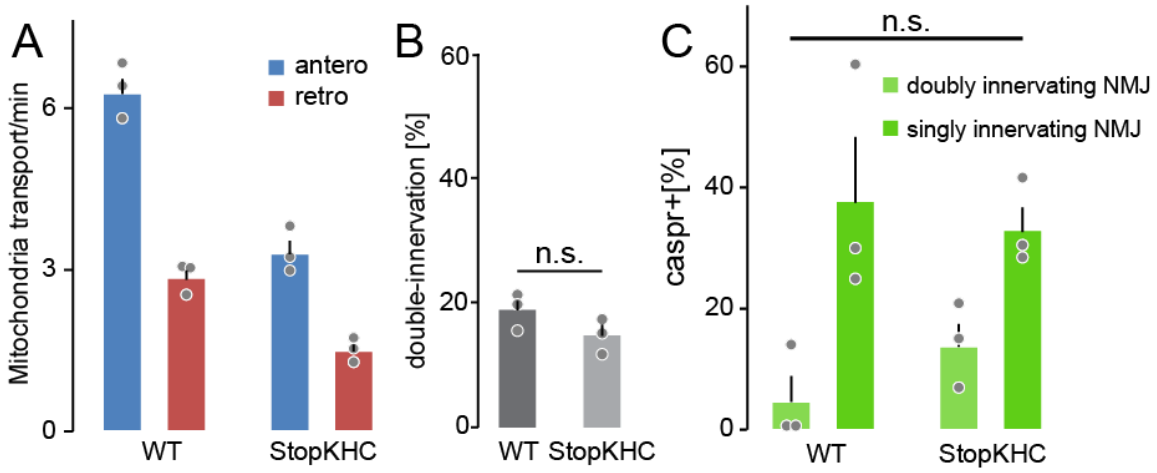

Figure 30: *Thy1:Stop-KHC* as a tool for modifying kinesin dependent transport. **A:** Mitochondria transport rate is reduced in adult *Thy1:Stop-KHC* intercostal nerve; **B:** Quantification of synaptic elimination status on P9; **C:** Quantification of myelin initiation status on P9.

3. DISCUSSION

In the vertebrates, neurons and their surrounding glial cells undergo drastic remodeling during early development: on the one hand, excessive neuronal projections that initially form are eliminated in an activity-dependent manner, until a more precise and efficient network is established (Cohen-Cory, 2002). On the other hand, myelin sheaths form around axons to dramatically increase conduction velocity (Vabnick and Shrager, 1998). Similar modifications can also be observed later in life, where synapse potentiation and depression, as well as myelin synthesis and retraction, reshape neuronal circuits in response to a changing environment (Matsuzaki *et al.*, 2004; Chang, Redmond and Chan, 2016). While we increasingly gain insights into the molecular and cell biological mechanisms of these developmental remodeling processes (Simons and Trotter, 2007; Schafer and Stevens, 2013; Baraban, Koudelka and Lyons, 2017), the "bigger picture" e.g. of how these parallel processes intersect during circuit formation remain elusive. This is in a large part due to the challenges of studying them in the complex and crowded environment of the CNS. These challenges especially limits direct observational tools, such as intravital imaging, which while very powerful to understand cellular interactions remain severely limited in the CNS by constraints of accessibility and resolution (Misgeld and Kerschensteiner, 2006). Hence, to dissect the interaction between synaptic pruning and myelination, the PNS and especially the neuromuscular system offers an accessible model – which I used in this series of studies. At the mouse NMJ, activity-dependent pruning of terminal branches results in a highly stereotypical one to one connection between motor neuron and muscle fiber during the first two postnatal weeks (Balice-Gordon and Lichtman, 1993). During the same time period, all axon branches become fully myelinated (Grove and Brophy, 2014). Together these processes result – over a relatively short period – in the predictable transition of all synapses from a poly-innervated and unmyelinated immature state to the mature and stable pattern of single innervation and consistent

myelination. This robust remodeling process of the axon-glial enables branch-specific observations by time-lapse microscopy, as well as efficient histological assays *e.g.* of genetic or pharmacological manipulations. In the studies described in this thesis, I used such assays to: 1) perform a candidate-based genetic screen for factors that affect various aspects of synaptic pruning and myelination *in vivo*; 2) scrutinize the intersection of pruning and myelination at single terminal branches, during the time when these processes coincide in development; and 3) utilize pharmacological and genetic manipulations to functionally dissect the interaction between synapse competition and myelination. My study demonstrated that pruning and myelination of terminal motor axon branches are connected processes, which are both under the influence of neurotransmission. More specifically, axonal branches still engaged in the process of synapse elimination are delayed in myelination compared to their sister branches that have resolved synaptic competition. In reverse, however, myelinated terminal branches can still be pruned back even under physiological conditions. Thus, while synapse competition gates myelination, a reverse impact is not apparent – a surprising result, given the prevailing notion in the literature that myelination might close “windows of plasticity”. The genetic manipulations I subsequently employed showcased on the one hand that indeed even premature myelination has little effect on the pruning process. On the other hand, prolonging the poly-innervated state by stabilizing microtubules and thus preserving organelle transport increases myelination on competing branches, hinting at a mechanism by which regulation of transport *e.g.* of axonal myelination factors could be the limiting factor to hinder myelination on competing branches – a model that can now be rigorously tested in follow-up studies.

3.1. Molecular factors affecting synapse elimination

In a first series of experiments, I explored the role of glial cells in synapse remodeling by focusing on the last step of the series of events that mediates the

transition from double to single innervation: the final disassembly of the “losing” axonal branch. During this stage of synapse elimination, terminal branches locally fragment and shed material. These so called “axosomes” are immediately engulfed by the SCs that wrap all motor axon branches (Bishop *et al.*, 2004; Brill *et al.*, 2011; Ko and Robitaille, 2015). Based on the literature on post-traumatic axon degeneration, corpse engulfment after apoptosis and studies of axon remodeling in invertebrates – all of which bear some similarities with NMJ synapse elimination in vertebrates – we compiled a list of candidate genes that might be involved in axosome engulfment.

Where possible, we obtained appropriately staged neuromuscular tissue of mouse strains that carry cell type-conditional or general deletions of these genes. I then performed a basic screen for innervation phenotype, where the percentage of poly-innervation in mutant muscles was compared to tissue from littermate controls. The results showed a surprising robustness of the pruning process in the PNS, where depletion of many of the factors did not significantly affect pruning or results only in a transient delay during development.

Together, the screen identified engulfment-related *Megf10/11* as delaying synapse elimination (*unpublished*), and the apoptosis related *Dr6* to promote SC proliferation and myelination (Colombo *et al.*, 2018). However, some technical aspects need to be considered to put these somewhat disappointing results into perspective: (1) While the screening method of quantifying poly-innervation with littermate controlled *triangularis sterni* muscles is a relatively straight-forward assay, it probably only identifies factors strongly affecting the elimination process outcome, but not more subtle phenotypes in engulfment. Indeed, it does not assay axosome engulfment *per se*, which cannot easily be done using immunostainings, because in axosomes many of the antigens used to mark axons (*e.g.* neuron-specific tubulin isoforms) are lost. Axosomes are better identified by genetic labeling of axons; to do this systematically in the number of lines screen here, however, requires an unrealistic breeding effort. (2) In the cell type-

specific, Cre-mediated deletion, a direct confirmation of loss of protein was often not possible. Where possible, I used a Cre-dependent *TdTomato* reporter strain as an indicator of efficient recombination. While this reporter was controlled by the *CAG-TdTomato* reporter that also respond to Cre induction, which indeed indicate presence of Cre in the soma, it does not necessarily guarantee the effectiveness of target gene ablation or of full loss of the protein in the cell over the limited period available between deletion and my developmental time point of interest. (3) In several instances we used heterozygote animals as controls, to avoid overly complicated breeding schemes. While this is a justified approach in many known instances, where a single allele is sufficient to sustain gene function, this pragmatic decision might result in missing some gene dose-dependent phenotypes.

Thus, in conclusion, the presence of a pruning phenotype in this screening assay is a good indicator for an *in vivo* role of the investigated molecule in developmental synaptic elimination. In converse, the *lack* of a phenotype does not definitely exclude the importance of a given actor. With these limitations in mind, I want to discuss the results that I obtained in the genetical manipulation of 10 different factors that might affect the axosome formation and engulfment process during neuromuscular synapse elimination.

3.1.1. *Atg7* deletion did not affect synapse elimination

Autophagy is implicated in response to acute neuronal injury and neurodegenerative diseases, but is also suggested to be constitutively active in neurons for protein and organelle turn-over (Rubinsztein *et al.*, 2005). *Atg7* neuronal ablation in the CNS was reported to cause region-specific neuronal dystrophy (Komatsu *et al.*, 2006, 2007; Friedman *et al.*, 2012), and its deletion in SCs results in delay of myelin clearance after peripheral nerve injury (Jang *et al.*, 2016). Indeed,

previous work from our lab had implicated both SC and axonal autophagy-like processes in axon branch removal (Song *et al.*, 2008).

Given this, we were surprised to find that neither neuronal, nor SC-specific depletion of ATG7 had significant effects on synaptic pruning. One possibility to explain this result on technical grounds, is incomplete deletion in the investigated cell types. In this case, Cre-mediated excision could not be confirmed by the TdTomato reporter in homozygous floxed *Atg7* animals as *Atg7* and the *TdTomato* insertion locus (Rosa26) are both located on the 6th chromosome (Li *et al.*, 1995; Smith *et al.*, 2018). Unfortunately, we also had no suitable antibodies for detecting ATG7 *in vivo*. In addition, the strain for neuronal deletion that we used (SLICK-3; Young *et al.*, 2008), expresses an estrogen-dependent form of Cre and hence depends on tamoxifen induction, which is particularly problematic in such a “blind” setting. Therefore while my results do not support a role of ATG7-dependent autophagy in synapse elimination, given prior evidence, it might be worth to perform further analysis with more robust neuronal delete strain, *e.g. ChAT:Cre*, and would be more conclusive compared to the SLICK-3 / tamoxifen-based induction used here. Moreover, ATG7 likely affects neuronal maintenance and SC-mediated clearance later in development. For instance, ATG7 deletion in the CNS causes observable deficits starting at P14 to P21 (Komatsu *et al.*, 2006). Similarly, the effect on post-traumatic SC-mediated axon clearance was observed in adult.

Thus, it would be interesting to investigate the effect of ATG7 depletion on PNS neurons in a later stages of NMJ development, when pruning is completed, but axon homeostasis needs to be stablished and maintained (Misgeld and Schwarz, 2017). Indeed, such studies are now underway in our and other labs (Israelson *et al.*, 2015; Jang *et al.*, 2016).

3.1.2. Wallerian degeneration and caspase mediated pruning

The fact that Wallerian degeneration and developmental axon loss share some morphological similarities and both seem to represent endogenous programs of axon regression prompted the speculation that common molecular mechanisms might underlie these two processes (Gillingwater and Ribchester, 2001). Indeed, the cytoplasmic expression of Nmnat1, the enzymatically active part of the Wld^S protein, was found to delay axonal degeneration induced by mitochondrial dysfunction (Press and Milbrandt, 2008), while mitochondria transport is abolished selectively in branches retracted during synapse elimination (Brill et al., 2016). To these known similarities, my work now adds the observation that also developmental removal of axons can involve the degradation of myelin sheath – suggesting that as during Wallerian degeneration also developmental axon loss has to be accompanied by active mechanisms to remove leftover myelin. Still, my effort to directly reexamine the involvement of the Wallerian-like mechanism using a stronger allele (*ΔNLS-WLD*^{S}; Beirowski et al., 2009) than employed earlier, only confirmed and strengthened the notion that blocking Wallerian-like axon degeneration does not affect axonal pruning (Parson, Mackintosh and Ribchester, 1997). In this context interesting follow-up experiments could probe, whether expression of a WLD^S fusion protein would affect organelle transport rates in retreating branches (as has been suggested in mature axons in the fly; Avery *et al.*, 2012), and whether the local mitochondria transport deficits seen during development lead to local oxidative stress – tools to address these questions are now available (Breckwoldt *et al.*, 2014).

Since caspases are also candidate-mediators of axon pruning, (Watts, Hoopfer and Luo, 2003; Campbell and Okamoto, 2013), I analyzed the muscles of *Bax*-KO mice, where a major pathway leading to caspase activation is globally blocked. Quantitative analysis did not show a change in synapse innervation patterns, excluding a major effect of this allele alone on axon pruning. Neither was activated Caspase-3 detectable

in the motor neurons innervating neonatal *triangularis sterni* muscle, which is consistent with previous observations in the developing sciatic nerve (Grinspan *et al.*, 1996; Syroid *et al.*, 1996). The effect of *Bax* deletion on removal of glial cells will be discussed in Section 3.1.4.

3.1.3. Engulfment-related factors

Previous studies demonstrated the importance of phagocytic glia engulfment for establishing synaptic connectivity during CNS development (Schafer and Stevens, 2013). These studies confirmed previous observations in fly models of pruning (Watts, Hoopfer and Luo, 2003; Awasaki and Ito, 2004) and in the mammalian PNS (Bishop *et al.*, 2004; Song *et al.*, 2008). The mammalian engulfment receptors, however, remained elusive. It was only in work published in parallel to my own efforts that the *Draper* homologue, MEGF10 and other engulfment receptors (such as MerTK; Wu *et al.*, 2009; Chung *et al.*, 2013) were identified important glial engulfment receptors in the mammalian CNS.

Indeed, while genetic deletion of many engulfment-related factors (including ELMO1, GAS6 and PrS) had no discernible effect on NMJ innervation, deletion of MEGF10/11 resulted in a transient delay of establishing single innervation on P7 *triangularis sterni* but not on P9. In contrast to the clearance of satellite glial cell precursors, where MEGF11 did not have an effect and was not detected by Wu *et al.*, 2009, MEGF11 and MEGF10 seem to have additive effect during NMJ synapse elimination compared to single KO. A third CED-1 homolog, Jedi-1 is also present in the mammalian PNS, and it has been reported that MEGF10 and Jedi-1 are found in satellite glial cell precursors, and are important for the clearing of apoptotic dorsal root ganglion neurons (Wu *et al.*, 2009). Whether a more prominent effect could be detected with Jedi-1 remains to be investigated (the required knock-out was not available to us on the time-scale of this thesis). In the *Megf10/11* deletion setting, there was no

obvious increase in the number of retraction bulbs, which raises the question whether engulfment signaling not only regulates clearance of axonal debris, but is also directly involved in the axosome shedding process. In any case, the effect of *Megf10/11* depletion was weak and transient, for this reason, we chose to not further pursue this lead, also given the emerging literature on this molecule in the CNS (Chung *et al.*, 2013).

Overall, the weakness of this phenotype points to apparent redundancies of the engulfment system, which should be explored in the future. For example, it seems that the axon debris engulfment system could be redundant on multiple levels: like MEGF10/11/12, ELMO1 also has immediate homologues, such as ELMO2 / ELMO3, with at least ELMO2 also being widely expressed and promoting similar phagocytic functions as ELMO1 (Gumienny *et al.*, 2001).

Moreover, beyond the pathways probed, other unrelated engulfment pathways could contribute. For instance, the phosphatidylserine-binding soluble bridging molecules include, in addition to GAS6 and PrS, molecules such as milk fat globule EGF factor 8 (MFGE8). MFGE8 was found to be secreted by macrophages and required for phagocytosis after lipopolysaccharide-induced neuronal death in the striatum (Hanayama *et al.*, 2002; Fricker *et al.*, 2012). Phosphatidylserine could also be detected by phagosome surface receptors in its naked form by brain angiogenesis inhibitor 1 (BAI1), which has also been implicated in microglial engulfment of apoptotic neurons (Park *et al.*, 2007; Mazaheri *et al.*, 2014).

What one should also consider is the fact that SCs and the retreating axon branch are in direct proximity to each other, thus the shed axosomes may not require any specific marker to recruit the phagocytic glia in this case, as it is literally released into the SCs embrace (Ravichandran and Lorenz, 2007). Indeed, it is not even clear, whether phosphatidylserine or similar “eat-me” markers are expressed on axosomes during developmental pruning. While the tools to examine this question have long been

insufficient, recent advances (such as genetically encoded “phosphatidylserine-exposure” sensors; Yeung *et al.*, 2008) may enable a worthwhile direct investigation of this question. To further confirm the importance of phagocytic SC engulfment on developmental axon pruning, more detailed analysis on the exact morphology of the competing axons are needed.

3.1.4. Apoptosis-related factors

The series of SC bleaching experiments that I performed to characterize the morphology of SCs on retreating axon branches showed tSCs extending long and tube-like structures along the atrophic branch. Numerical analysis revealed that singly innervated NMJ and NMJ with a recently retracted branch have approximately one tSC less than the contemporary doubly innervated NMJ, suggesting that one of the tSCs might be transferred to the retreating branch and thus disappear from the synapse. Thus, although tSCs are not assigned to the territories occupied by individual competing branches (Brill *et al.*, 2011), it seems that when competition resolves, one of the tSCs gets sorted to assist the retraction of the losing branch, while its territory is rapidly covered by the remaining tSCs. This phenomenon could be specific to muscles with multiple tSCs covering an endplate, since in some muscles innervated by the sciatic nerve NMJs are often covered by single SC – and still manage to resolve multiple-innervation (Riley, 1981; Reynolds and Woolf, 1992; Son and Thompson, 1995). What is the eventual fate of these excess SCs that associate with the retreating axons?

I probed the possibility of apoptotic clearance of these cells. As in the developing sciatic nerve (Grinspan *et al.*, 1996; Syroid *et al.*, 1996), I rarely found apoptotic SCs positive for cleaved Caspase-3 in the neonatal *triangularis sterni* muscle, which is surprising considering the massive terminal branch retraction during pruning. It indicates either that tSCs are not removed by classical apoptosis, or that this process

is very swift. To disambiguate these possibilities, I studied the muscles of *Bax* KO mice, where a major apoptotic pathway is globally blocked. I did not observe aberrant SCs unassociated with axons, excluding a major effect of this allele on SC clearance. Combining with the data of unchanged innervation patterns at the NMJ discussed in Section 3.1.2, it suggests that neither on the glial nor on the axonal side, global *Bax* deletion exerts a major influence. In contrast, in the *Dr6* knock-out mice – another candidate signaling factor regulating pruning and glial development (Nikolaev *et al.*, 2009; Mi *et al.*, 2011), I found evidence for increased SC numbers at the NMJ and its innervating axons, accompanied by slightly accelerated myelination. This confirmed in vitro results of colleagues that showed increased SC proliferation and myelination in the absence of DR6 signaling, and suggests that DR6 acts as a brake during glial development in the PNS. Moreover, our collaborative study identified an unusual mode of paracrine signaling of DR6, which does not require its cytoplasmic death domain and depends on regulated shedding of this receptor via proteases of the ADAM10 family (Colombo *et al.*, 2018).

Together my results on the fate and apoptotic signaling in tSCs favor the hypothesis that apoptosis is not the prevailing mechanism for the reorganization of excessive SCs. It is therefore meaningful to explore other possibilities, such as SCs translocating to surviving branches after synapse elimination, or loss of SCs without apoptosis. The time-lapse imaging of *Brainbow* mice, some of which show multicolor tSC labeling ("Schwannbow"), could be useful to help unraveling the SC reorganizing mechanism (Livet *et al.*, 2007). Moreover, means to selectively delete genes in tSCs would be very helpful, but are currently not available. To this end, we have mapped the insertion site of above-mentioned "Schwannbow" mice, and found the transgene to be located on Chromosome 10 (locus: Chr10: 52,700,653- 52,693,225, in the intronic region of the *Slc35f1* gene; mapping performed by Cergentis). To enable follow-up projects, we are

currently generating knock-in mice that carry a Cre-recombinase allele inserted into this putatively tSC-specific locus.

3.2. Competition status delays initiation of myelination

The next part of my PhD thesis focused on the possible interaction between synapse elimination and myelination. The screen detailed above provided a hint of the robustness of the stereotypical axon pruning and myelination pattern in the PNS, where activity dependent pruning of terminal branches leads to a strict one to one connection between motor neuron and muscle fiber in the adult (Balice-Gordon and Lichtman, 1993). In parallel, all the branches eventually become fully myelinated (Grove and Brophy, 2014). This system thus provides a stable and reproducible system that allows exploring how the parallel processes of synapse remodeling and myelination unfold with single axon-branch resolution.

3.2.1. Activity blockade delays both synapse elimination and myelination

In this study, local injection of α-bungarotoxin, which irreversibly binds and blocks AChRs, was used to reduce synaptic activity in parts of neonatal *triangularis sterni* muscles. Such treatment is expected to delay synapse elimination (Loeb *et al.*, 2002; Misgeld *et al.*, 2002; Buffelli *et al.*, 2003). Indeed, my innervation counts confirmed this expectation; notably, however, myelination of the terminal branches was also delayed (see **Figure 15**). A similar procedure was performed using curare which also binds AChR, though reversibly, resulting in excessive axonal sprouting, an increase in the number of smaller AChR clusters, and a reduction in synaptic neuregulin expression (Loeb *et al.*, 2002; Loeb, 2003). Another model to alter synaptic activity using the genetic depletion ChAT also delayed synapse elimination, though here premature myelination was observed in the mutant (Misgeld *et al.*, 2002; Buffelli *et al.*, 2003). The

discrepancies between the results likely reflect the differential cellular site of action or the timing of the various manipulations. This can potentially be further investigated using electrophysiological or opto-physiological assays to determine the level of activity in the axonal branches in response to these various manipulations.

Still my results indicate that synapse elimination and myelination are probably interlinked; one possible explanation is that both processes depend on neurotransmission – however, while myelination is generally thought to be controlled by axonal activity (Hines *et al.*, 2015; Chang, Redmond and Chan, 2016), there is little evidence so far that blocking postsynaptic nAChRs would interrupt axon-to-SC signaling directly (Ko and Robitaille, 2015). Another is that the delay in resolving poly-innervation, and hence an expanded time window of remodeling *per se* delays myelination, since its initiation might require a certain level of axonal maturity and signaling that competing branches do not provide. My detailed examination of the relative timing of remodeling and myelination along single developing axon branches strongly favors the latter interpretation.

3.2.2. Competing branches shows less initiation of myelination

To investigate the progress of myelination on single motor axon branches, I chose Caspr immunostainings, for which a very robust antibody is available, and a detailed comparison with various markers for the different myelin and nodal domains showed that all components of the axoglial unit assembled almost in synchrony. The exception was the occasional faint presence of the myelin-marker, MPZ, marking the earliest stage of myelination, when a few SC membrane wraps have not yet resulted in immuno-histochemically detectable paranodal differentiation. Still, either marker yielded the same result: at terminal branches (*e.g.* on postnatal day P9), I found a significant delay of myelination on branches still engaged in competition, compared to

their sister branches nearby that had already finished competing. This delaying effect was also found on P7 and P11, while the percentage of myelin initiation increases with age for both competing and singly innervating branches. On P7, around 50% of the NMJs are poly-innervated, though only 5% of the competing branches shows signs of myelin initiation; while on P11 less than 5% the branches remain doubly innervated, among which >40% have started to myelinate. From P7 to 11, the frequency of Caspr-positive singly innervating branches is consistently about 20 ~ 30% higher than the doubly innervating ones (see **Figure 18**). This amounts to a delay of myelination on competing branches by about 2 ~ 3 days, which is very significant, given that at this point myelination of terminal branches has only been initiated two days earlier (around P5). This delay was also confirmed with other myelin and nodal protein markers on P9 (see **Figure 18**). The phenomenon indicates existence of mechanisms preventing competing branches from starting myelination, which could be due to either reduced pro-myelination signaling, or limited availability of components needed to assemble the axoglial unit on the competing branches – also, irrespective of availability, the latter could either start accumulating later or simply accumulate more slowly. To explore these possibilities, I established an assay to measure the nodal assembly rate with single-branch resolution.

3.2.3. Myelination initiation is delayed on competing branches

I devised a FRAP assay using *Thy1:Caspr-GFP* transgenic mice (Brivio *et al.*, 2017) provided to us by P. Brophy at U. Edinburgh to analyze the early dynamics of nascent paranodal structures. The GFP-tagged Caspr was found to colocalize with endogenous Caspr, similarly distributed on terminal branches during development, and can rescue the Caspr knock-out phenotype (see **Figure 19** and Brivio et al., 2017). Moreover, the overexpression level seems moderate by Western blot analysis (see **Figure 19** and Brivio *et al.*, 2017). Interestingly, when I performed FRAP experiments

the recovery rate was significantly higher in young mice with developing myelin, compared to adult mice where myelination is complete. In the latter case, recovery was essentially not measurable over a two-hour observation window, in tune with the known long life-time of mature paranodal structures (Zhang *et al.*, 2012). Moreover, in young mice, the recovery rate on singly innervating terminal branches was significantly faster, compared to contemporary nodes in the intercostal nerves, where the nodes are more fully developed (see **Figure 20**; in line with the known maturation gradient of myelination along peripheral nerves, Hildebrand, Bowe and Remahl, 1994). Thus, there appears to be a correlation between the measured recovery rate and the maturation stage of the paranodal structure – with Caspr protein accumulation being faster on nascent compared to fully mature paranodes. Strikingly, the recovery rate of Caspr on branches still engaged in competition was significantly higher than that measured on nearby singly innervating branches (see **Figure 20**). Branches identified as recent winners in synaptic competition by a nearby retraction bulb, displays an intermediate recovery rate. These observations suggest that the main reason for the delay in nodal assembly is not delayed assembly or lack of availability of nodal components (which are believed to be delivered either by targeted exocytotic provision or lateral diffusion and trapping in the axon, see below; Zhang *et al.*, 2012). Instead, my data favor a model, where initiation of myelination is selectively delayed on competing branches, *e.g.* because signaling that initiates myelination is missing or weak.

3.2.4. Myelinated axon branches are not favored in competition

Current literature on roles of myelination beyond facilitating fast action potential conduction, stresses the idea that myelination might contribute to terminate axonal plasticity, by “cementing” axons in place (Geoffroy and Zheng, 2014). For example, in

the visual cortex, myelination coincides with closure of a critical period of remodelling; an effect that seems to be mediated by *Nogo*-signaling – the same myelin-associated pathway that also represses CNS regeneration (McGee *et al.*, 2005). This notion led us to ask directly, whether myelination – which despite the delay still takes place on remodeling axon branches – would convey a competitive advantage, or whether myelination would be a substantial impediment to subsequent retraction. To our surprise, a more detailed analysis on axonal branches still engaged in competition revealed that myelination does not seem to provide a decisive advantage during competition, nor does it preclude retraction. The percentage of territory occupied by individual innervating branches is predictor of likely competition outcome (Walsh and Lichtman, 2003), which is also correlated with the axon diameter of the terminal axons (Keller-Peck *et al.*, 2001). However, analysis of the corresponding myelination status of the terminal branches showed that the myelination status was relatively even across the occupied NMJ area (see **Figure 24**), and the axon diameter, though increases proportionally to the terminal territory, did not differ between myelinated and unmyelinated competing branches (see **Figure 25**). The latter analysis also excluded the interpretation that the delay in myelination of competing branches is simply due to their lower caliber. In the PNS, myelination occurs only in axons with diameter larger than 1 µm (Voyvodic, 1989; Peters, Palay and Webster, 1991), a diameter that axon branches typically acquire at 50% innervation territory (Keller-Peck *et al.*, 2001; and **Figure 25**); but my analysis of axon diameter vs. myelination did not reveal any discontinuity in myelination probability at this diameter. It appears that competing terminal branches can achieve the diameter required for PNS myelination, but myelination is still repressed until after competition resolves. In convers, my data also suggests that myelinated fibers are not systematically superior in competition. Indeed, I found some examples of partly myelinated terminal branches in the process of being pruned. Here, the myelinated axon stretches seemed to preserve axon diameter

compared to neighboring atrophic segments (**Figure 25**) – in tune with previous analysis of partially myelinated axons, e.g. in the optic nerves, where myelinated segments of the same axon were thicker than non-myelinated parts (Black, Waxman and Hildebrand, 1985; Hernández, Blackburn and Alvarez, 1989). Controlled manipulation of axon caliber (*e.g.* using PTEN deletion; Fraser *et al.*, 2008) could be an informative follow-up here to see whether the delaying impact of competition could be overridden by providing axons of larger caliber that tend to present stronger myelination signals (*e.g.* neuregulin, see below; Michailov *et al.*, 2004). The corresponding experiment is currently underway.

An interesting and surprising observation was that the delay in myelination due to ongoing competition also seemed to extend to neighboring branches. Singly innervating branches with a neighboring doubly innervated branch on the same motor unit were delayed compared to branches with only singly innervated neighbors (see **Figure 26**). Previous studies showed that synaptic elimination is dependent on local activity at each NMJ, and the competition status of sibling branches sharing a bifurcation is random (Keller-Peck *et al.*, 2001). However, the difference in myelin initiation implies a possible regional maturation gradient, where induction of myelination was affected by the competition status of direct neighbors. Further analysis of regional effect on myelination with different motor-units would be an interesting extension of my study for understanding the locally linking competition to myelination.

3.3. Mechanism of synapse elimination and myelination interaction

Since myelin is a stable structure that can suppress plasticity and consolidate neuronal connections, and also is a metabolically and cell biologically “expensive” structure to build and dismantle, it seems economical for the organism to delay myelination until competition resolves (McGee *et al.*, 2005; Cheng and Carr, 2007). To

probe the directionality of this intersection, I performed genetic manipulations that affect onset and speed of myelination on the one hand and the resolution phase of synaptic pruning on the other hand.

3.3.1. Premature myelination does not affect synaptic pruning

Although examples of myelinated retraction bulbs were observed during development, it was found to be an exceedingly rare phenomenon. The occasional pruned myelinated branches did not preclude the possibility that premature myelination closes the plastic window of synaptic elimination, as was shown in the CNS for oligodendrocytes (McGee *et al.*, 2005). However, overexpression of NRG1-III, which significantly increased myelination during early development on both competing and non-competing branches, did not consolidate the competing branches or result in a delay in synapse elimination (see **Figure 22**). On the contrary, it has been reported that in the soleus and sternomastoid muscles, that overexpression of NRG1-III leads to acceleration of pruning, which could possibly be explained by speculative function of NRG1-III in the non-myelinating tSCs (Lee *et al.*, 2016). In converse, neuronal deletion of *Nrg1-III* significantly delayed myelin formation on terminal branches, confirming previous reports that NRG1-III expression is required for myelination in the PNS even in the late stages of distal myelination (Taveggia *et al.*, 2005). The deletion did not affect synaptic pruning either (see **Figure 23**), in line with our general notion that myelination is not a pacemaker for synapse remodeling.

Together with the data presented in Section 3.2.4, it appears that terminal branch myelination in the PNS has little influence on the synaptic pruning process, but is rather repressed by the competition status in general. Thus, complete myelination of terminal branches does not seem to convey a structural, metabolic or functional advantage in competition (with action potential conduction being able to skip across minor gaps in

the myelination pattern by electrotonic mechanisms; Kandel, 2014), and removal mechanisms for the occasional myelin sheath formed on a losing branches exist in the developing motor system.

3.3.2. Modulated synaptic pruning affect myelination

Since the previous data suggested that altering myelination did not obviously affect pruning, I undertook manipulation to the reverse, *i.e.* that affect the synaptic elimination process and especially the ability of axon branches to mature cell biologically, *e.g.* with regards to their cytoskeletal organization and axonal transport. Using deletion of the microtubule severing enzyme Spastin, which has been shown to promote branch formation (Yu *et al.*, 2008), axon outgrowth (Wood *et al.*, 2006), and substantially delay pruning during postnatal NMJ development (**Figure 27**, **Figure 28** and Brill *et al.*, 2016). I observed a significant increase in myelination on competing branches. This was true, whether I used global knock-out mice or conditional genetics that restricted deletion to single cells and the postnatal period (**Figure 27, Figure 28**). Since in our previous work, we found that *Spastin* deletion stabilizes microtubules and preserves axonal transport in retreating axonal branches (Brill *et al.*, 2016), the hypothesis emerged that delayed synaptic pruning allowed sufficient transport of myelinating factors for the eventual formation of nodal structures on competing branches. The observation is in accordance with previous observation that branches still in competition on P11 can also become myelinated. This shows that ongoing maturation even of competing axons can eventually trigger the formation of myelin.

Interestingly, when *Spastin* deletion was combined with BTX-induced activity block, the branches with BTX-positive endplates still showed a significant delay in myelination compared to the unaffected branches (see **Figure 28**). This suggests that branches with stabilized microtubule can still be affected by the bungarotoxin blockade of AChR,

therefore neurotransmission might be the permissive upstream factor regulating both synaptic pruning and myelination.

Overall, our model points to the possibility that maturation of axon branches, which accelerates once competition is complete, also lifts the transient “brake” on myelination. Our previous work has shown that this maturation coincides with an increase in axonal transport into the “winner” branches (Brill *et al.*, 2016). If so, what is the relevant cargo?

3.3.3. Tools for modulating axonal transport

In the *Thy1:Caspr-GFP* mice, I observed motile GFP-positive particles in neonates coincident with a high insertion rate of Caspr as measured by FRAP. In contrast, in adult animals, when no FRAP recovery could be detected, such particles were absent. It is intriguing to speculate about a possible correlation between these particles and the insertion rate of Caspr-GFP at the paranodes. Mostly based on *in vitro* experiments, current models posit that the transmembrane proteins, which contribute to nodal and paranodal structures in axons, appear to assemble at their proper sites via two different mechanism: nodal sodium and paranodal potassium channels are reported to be locally inserted by exocytosis; while adhesion molecules (including Caspr) appear to diffuse laterally in the axonal membrane before being trapped at nascent nodes (Zhang *et al.*, 2012).

However, while this predominantly anterograde transport of Caspr-GFP could be measured in the intercostal nerve, it is almost undetectable in terminal branches, in line with the general drop in flux rates of particles along branching axon arbors (Misgeld and Schwarz, 2017). And since the FRAP data show that – once node formation is initiated in competing branches – the accumulation rate is as high as in all other early nascent nodes, and even higher than in the average singly innervating branches, it is unlikely that lack of nodal components due to reduced axonal transport underlies the

reduced nodal formation on competing branches. Indeed, appearance of faint MPZ staining – *i.e.* an assembly process on the SC side – appears to be the earliest step of myelination in my assays, and clearly would not be expected to be impacted by a lack of Caspr or Nav. Hence, rather than transport of structural components, transport of signaling molecules that initiate node formation seems like a plausible explanation for the delay in myelination on competing branches. For example, cleaved Nrg1-III, the upstream myelination determining factor, was shown to be transported in vesicles (Velanac, 2009).

I tried to test this possibility, based on the prediction that blocking cargo transport in a subset of axons should delay their myelination. To this end, I characterized newly generated transgenic mice in which *Thy1*-driven overexpression of a kinesin heavy chain cargo-binding domain can be induced by Cre recombinase. Overexpression of this dominant-negative repressor of transport complex assembly has been used to reduce intracellular transport *e.g.* of mitochondria in vitro (Cai, Gerwin and Sheng, 2005). By crossing this mouse to a *ChAT:Cre* strain for induction in motor neurons, I could induce a ~50% reduction of mitochondrial transport in adult intercostal nerves. However, in my further analysis, these mice did not show any myelination and innervation phenotype – which either refutes my hypothesis, or points to technical shortcomings of this difficult experiment, as the transport complex of the putative Nrg1-III vesicles are not known and the expression levels of *Thy1*-driven gene expression can be insufficient in early postnatal ages, which remains to be tested for the *Thy1:Stop-KHC* strain. Despite this inconclusive outcome, the potential of using these new mice for studying the effect of decreased transport on distal axonal homeostasis remains an intriguing outlook emerging from my thesis.

3.4. Model: Activity coordinated myelination following competition

Establishment of the invariant one-to-one innervation pattern at the NMJ (Keller-Peck *et al.*, 2001; Wyatt and Balice-Gordon, 2003) with parallel complete myelination of the terminal axons (Salzer, Brophy and Peles, 2008) is a highly stereotypical developmental outcome, which nevertheless is driven by activity-dependent competition. The apparent contradiction between an adaptive process achieving an invariable outcome is probably explained by the need to fine-tune innervation patterns to create an efficient and adapted network (*e.g.* motor unit size distribution) and to ensure reliable neuromuscular transmission at this most important of all synapses – which after all forms the sole output channel of the nervous system. In parallel, rapid myelination of the established connections is beneficial for increasing conduction speed and stabilizing axonal structures (Vabnick and Shrager, 1998; Simons and Trotter, 2007). However, why delay myelin formation on competing branches?

One simple reason might be that, if substantial myelination occurred on axon branches that are later pruned back, the myelin sheaths would have to be dismantled and digested – a degradative step that is possible (see **Figure 25**), but likely costly, as seen by the various aberrant immune and glial effects that myelin degradation can have in later life (Safaiyan *et al.*, 2016; Cantuti-Castelvetri *et al.*, 2018). Thus, a mechanism to coordinate the progress of synaptic / axonal remodeling and myelination seems like a beneficial addition to the developmental programs that shape complex nervous systems. And while the intersection between neuronal remodeling and myelination in the CNS is only emerging as a topic (Hughes *et al.*, 2018). just as for other aspects of neural development, the events at the peripheral NMJ might serve as a guiding model.

Based on my combined data as detailed above, I can propose a model for the coordinated progress of synapse elimination and myelination in the PNS (**Figure 31**), that – while speculative – explains the data I obtained and can guide the experiments

still to be done. During competition of the motor units innervating muscle fibers (**Figure 31A**), as part of activity-driven remodeling, microtubule stability and organelle transport are reduced in “losing branches” (**Figure 31B**). These branch-specific changes in vesicular transport results in differentiate Nrg1-III (or other pro-myelination factor) accumulation on the neuronal membrane, as the territory occupied by each innervating branch shifts, and the axon diameter expands or shrinks accordingly (**Figure 31C**). Myelin and nodal components only assemble as the Nrg1-III amount passes a certain threshold, which takes place only after competition resolves in most terminal axons (**Figure 31D**). On the other hand, if the accumulated Nrg1-III reaches this threshold before single innervation is established, the myelination status does not affect the competition outcome, and if the myelinated branch loses, the terminal branch will be pruned back and the formed myelin sheath dismantled. In the end, a single-innervating pattern on muscle fiber is established, and all the branches become completely myelinated (**Figure 31E**). The model ensured a simple and straightforward prohibition of myelination during competition, balancing efficiency of fast myelination and the cost of disassembling myelinated losing branches – and “uses” the axon-autonomous remodeling of the intra-axonal transport machinery as a readout to coordinate intercellular events.

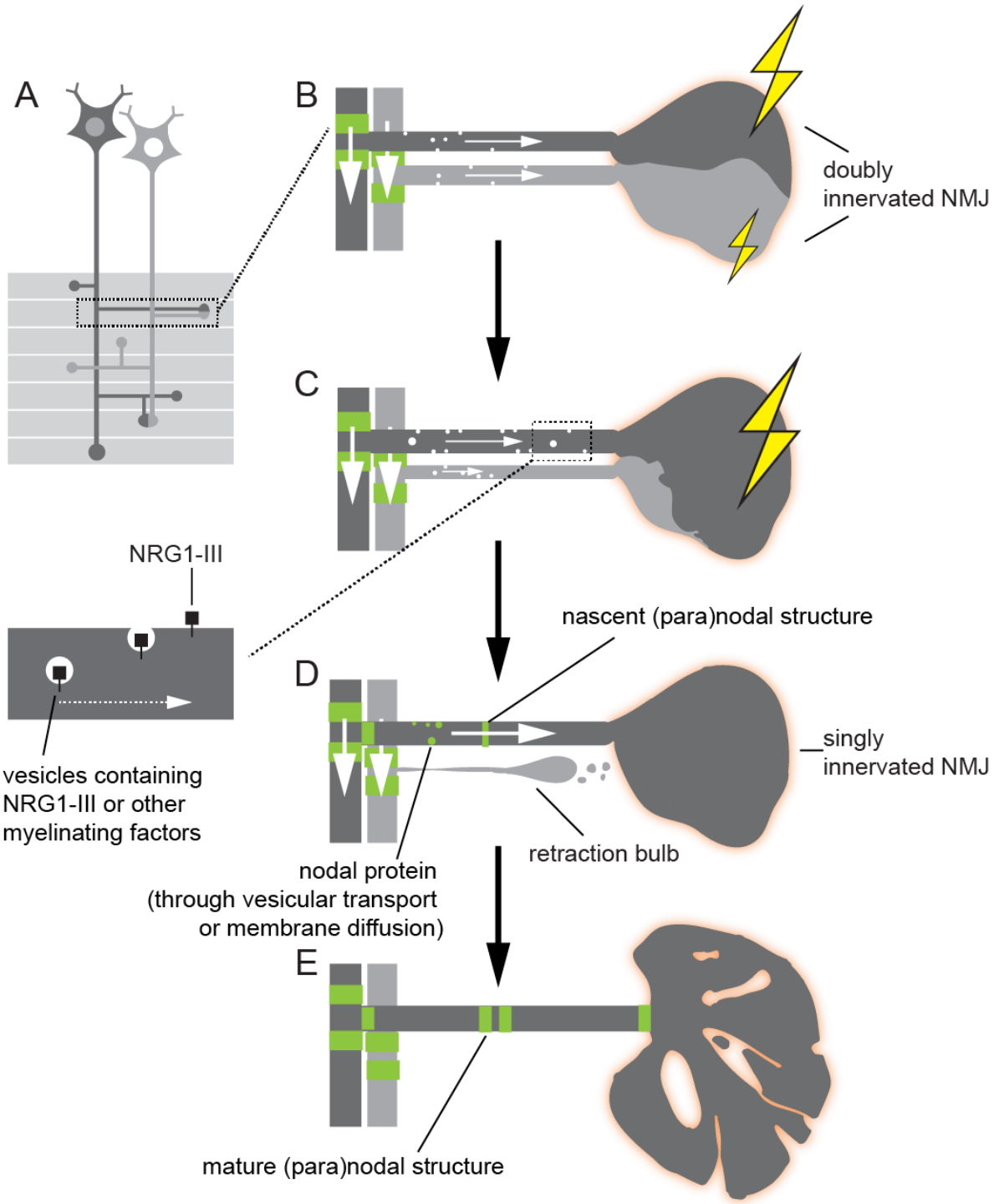

Figure 31: Model of the activity coordinated synapse elimination and subsequent myelination. **A:** Schematic illustration of two developing motor neurons innervating muscle fibers; **B:** Two branches innervating the same NMJ, the upper terminal with stronger activity than the lower one, arrows and white dots indicate transport of vesicles with myelinating factors in both axons (*e.g.* Nrg1-III); **C:** The branch with stronger neurotransmission enlarges its terminal territory and axon diameter, though both branches can accumulate Nrg1-III insertion into the cell membrane; **D:** The losing branch forms a retraction bulb, while the surviving branch overcomes the threshold for myelination and start accumulation of myelin and nodal proteins (green); **E:** The losing branch is completely eliminated, while the surviving branch consolidates the terminal connection, and becomes fully myelinated.

3.5. Outlook: Further experiments to consolidate the model

The model implicates that activity-dependent and branch-specific Nrg1-III transport is the key to the coordinated myelination after synapse elimination. Therefore modulating activity, transport and Nrg1-III expression on the single-branch level would be the next step to confirming the proposed mechanisms.

Local activity blockage with α-bungarotoxin injection induced a delay in both synaptic pruning and myelination, without inducing denervation in the two days before analysis and after application (see **Figure 15**), confirming the delaying effect on synaptic pruning achieved by curare injection and genetic ChAT ablation (Loeb *et al.*, 2002; Buffelli *et al.*, 2003). Further analysis could be performed to determine if this treatment affects axonal transport and microtubule composition at the terminal branches. Selective inhibition of activity by subset genetic manipulation could also be helpful in illustrating the branch-specific effect of activity on myelination, and indeed the expression of tetanus neurotoxin light chain was found to reduce myelination (Hines *et al.*, 2015). Genetic ablation of ChAT however, was found to increase myelination (Misgeld *et al.*, 2002), where electrophysiological measurement of the branch activity would be helpful to determine the exact axonal activity change under such circumstances. I undertook pilot experiments with chemo-genetic DREADD-based modulation of neurotransmission (Nichols, 2009), but unfortunately the expression levels of these chemo-genetic modulator channels detected in motor-neurons appeared to be insufficient in the postnatal period of the knock-in animals available.

Modulation of transport is possible with the *Thy1:Stop-KHC* transgenic animals, where I found mitochondrial transport to decrease by about half in adult. Whether the transport rate is also reduced in young animals remains to be tested. Although expression of this dominant-negative version of KHC with *ChAT:Cre* in all motor neurons did not result in altered synaptic pruning, it remains to be tested if subset

induction would have any effect on these two processes, since the branch-specific modulation depends largely on the relative synaptic strength compared to each other (Buffelli *et al.*, 2003; Darabid, Arbour and Robitaille, 2013). However, for myelination – the process of interest here – the results were negative, but this could be explained by a variety of technical shortcomings as detailed above. Conceiving a better experiment to manipulate axonal transport and study putative effects on distal myelination is possible, e.g. based on recent opto-chemic or opto-genetic modulators of transport (Borowiak *et al.*, 2015; Van Bergeijk *et al.*, 2015), but will be challenging as long as we do not have a clear understanding of the relevant cargo.

Distribution of Nrg1-III is difficult to measure in the wild-type terminal branches without a sensitive antibody, and even in the HA-tag labeled transgenic Nrg1-III mice used here, the available Nrg1 protein was still largely below the detectable threshold of HA-antibody (Velanac, 2009). AAV induced Nrg1-III expression could be helpful for illustration of the Nrg1-III distribution, although to reach the detection threshold probably also requires a high titer of viral infection, which could in turn affect the physiological conditions of the transfected neurons. Another possibility is to generate a Cre-inducible *Nrg1-III* overexpressing mouse-line, which in combination with the CAG-*TdTomato* reporter and AAV-CMV-iCre could result in branch-specific overexpression of NRG1-III, proving the branch-specific NRG1-III accumulation could indeed promote local myelination without affecting pruning – such mice, however, were not available to us.

Since myelination on singly innervating branches also appears to be affected by its immediate competing neighbor on the same motor-unit, it is interesting to test if microtubule and transport are likewise affected by the competition status of neighboring synapses, to see whether there is a consistent relationship between local cytoskeletal stability, transport and myelination. Neighboring branches that do not belong to the same motor unit, but are in the spatial vicinity of the competing branch,

should also be analyzed, as a control for possible diffusible rather than intra-axonal spread of the relevant signals.

It would also be intriguing to test whether this model applies for other systems in the CNS. Evidence shows that CNS myelin can also undergo drastic remodeling during developmental pruning. In the metamorphic phase of *Xenopus laevis*, intact myelin detaches, protrudes from the axons and is engulfed by astrocytes as the optic nerves shorten to accommodate the much smaller head of the adult animal (Mills *et al.*, 2015). A further example of delayed myelination, until a neuronal circuit structure is finalized, was found in the delay line axons of barn owl *nucleus laminaris*, where myelination is delayed until after the head reaches the animal's adult width (Cheng and Carr, 2007). Activity-regulated myelin formation was also discovered in zebrafish with tetanus toxin in the reticulospinal or commissural primary ascending neurons, where diminished activity can reduce myelin formation within specific neuronal circuits (Koudelka *et al.*, 2016). Similar mechanisms of delayed myelination and disassembly of formed myelin on axons to be pruned or altered may also apply here – indeed retractions of myelin sheets have been directly observed in zebrafish (Baraban, Koudelka and Lyons, 2017; Almeida *et al.*, 2018; Auer, Vagionitis and Czopka, 2018). Since myelination thickness and composition can affect action potential transduction in subtle ways, and is therefore relevant for CNS activity and remodeling, myelin plasticity could be subject to even more fine-tuned regulations, and aberrations in such mechanism could contribute to pathological conditions (Pajevic, Basser and Fields, 2014; Stogsdill and Eroglu, 2017).

3.6. General conclusions

The aim of this study was to gain insights into the process and mechanism of axon-glial remodeling with single-branch resolution, using the developing mouse NMJ as a model. The interaction between synaptic elimination and axonal myelination, two major

events during development of the nervous system, could be underlying important adaptation and plasticity phenomena to optimize neuronal transmission. Through genetic manipulation with transgenic mice, I screened for molecules possibly influencing the remodeling process. Among factors involved in neuronal maintenance and maturation, disassembling of retreating axonal structures, SC engulfment of debris and apoptosis, the engulfment-related factor *Megf10/11* was identified to delay synaptic pruning transiently, and the apoptosis-related *Dr6* to reduce SC proliferation and myelination. I further demonstrated that myelination is delayed selectively on competing branches. Detailed analysis showed that myelination on competing branches did not increase the chance that a branch won during synaptic competition; indeed, in rare instances, even a myelinated branch can be pruned. Genetically induced premature myelination using Nrg1-III overexpressing mice does not significantly affect pruning. At the same time, prolonging the competition phase with genetic ablation of the microtubule-severing enzyme Spastin resulted in increased myelination on competing branches, suggesting the possible effect of microtubule dynamics and axonal transport on the coordinated myelination by competition status.

Based on these experimental results, I propose a first model for the coordinated succession of myelination after resolving synaptic competition. In this model, activity-dependent synapse competition regulates branch-specific microtubule dynamics and transport rates, which in turn determines the accumulation rate of myelin-promoting factors (such as Nrg1-III) on the terminal branches, resulting in differential onset and speed of myelination. Shortly after competition resolves, the transport-dependent pro-myelination signal reaches its threshold in a “winner” axon branch, and the sheathing SCs initiate myelination of this terminal branches.

4. MATERIALS AND METHODS

4.1. Animals

For screening synapse elimination related factors, *plpCreERT* mice (Leone *et al.*, 2003) were used to mediate tamoxifen-inducible Cre expression in oligodendrocytes and SCs, and SLICK-3 animals (Young *et al.*, 2008) for tamoxifen-dependent neuronal expression. For both combinations, 5 mg/ml tamoxifen dissolved in corn oil was subcutaneously injected on postnatal Day 3 to induce gene deletion in the respective cell types. A CAG-*TdTomato* mouse line with the reporter sequence inserted in the ROSA locus and controlled by a floxed Stop-codon, therefore expressing *TdTomato* fluorescence following Cre-mediated recombination (Madisen *et al.*, 2010) were crossed in to control for Cre expression.

For SC deletion, *Elmo1*^{FL} (Elliott *et al.*, 2010) and *Atg7*^{FL} mice (Komatsu *et al.*, 2005) were crossed to the *plpCreERT* line and CAG-*TdTomato* reporter line. *Atg7*^{FL} mice was also analyzed when crossed to SLICK-3 animals. *Megf10* and 11 knockout mice (Kay, Chu and Sanes, 2012) were crossed to generate littermate controlled WT/KO and double KO animals. *Bax*$^{KO/WT}$ animals (Jackson Laboratory #002994, Knudson *et al.*, 1995) were crossed to generate general *Bax*$^{WT/WT}$ and *Bax*$^{KO/KO}$ animals. DR6 knock-out mice (Zhao *et al.*, 2001) were crossed to *plpGFP* mice (Mallon *et al.*, 2002) for SC labeling and DR6 deletion. Total Spastin deletion was achieved in *Spastin*^{KO} mice, and subset deletion by crossing *Spastin*^{FL} to the *CAG-tdTomato* line and neonatally injected with AAV9-CMV-iCre. *ΔNLS-Wld*^{S} heterozygous animals were compared to homozygous wildtype to analyze the effect of the Wld^{S} on synapse elimination (Beirowski *et al.*, 2009). *PrS* (Burstyn-Cohen, Heeb and Lemke, 2009) and *Gas6* (Angelillo-Scherrer *et al.*, 2001) knock-out animals were crossed to produce the double knock-out animals and provided by Dr. Vered Shacham, from the lab of Prof. Dr. Avraham Yaron, Department of Biomolecular Sciences, Weizmann Institute of Science, Israel. Dr. Monika Brill obtained the KHC-CBD plasmid from the authors (Cai, Gerwin

and Sheng, 2005) and cloned it into the *Thy1:Stop-YFP* vector for ES cell injection at the MPI of Molecular Cell Biology and Genetics, Dresden, to generate the *Thy1:Stop-KHC* transgenic mice. The *Thy1:Stop-KHC* lines were screened and the Line 352 was crossed to *Thy1:mitoRFP-H* with neuronal mitochondria expressing RFP (Misgeld *et al.*, 2007) for developmental and transport measurement. Manipulation of NRG1-III level was achieved either with overexpressing *Thy1:Nrg1-III* line (Velanac *et al.*, 2012) or crossing the conditional knock-out $Nrg^{FL/FL}$ (Velanac *et al.*, 2012) to *CAG-tdTomato* and inject with AAV9-CMV-iCre (produced by the Engelhardt lab).

For labeling motor neurons, *Thy1:YFP-16* or *Thy1:OFP-3* mice with cytoplasmic YFP or OFP expression (Feng *et al.*, 2000; Brill *et al.*, 2011), or the membrane-tethering *Thy1:Brainbow-1.1* line M (Livet *et al.*, 2007) crossed to ChATCre (Rossi *et al.*, 2011) were used.

Thy1:Caspr-GFP and *Thy1:Nav-GFP* (Brivio *et al.*, 2017) were generate by Prof. Peter Brophy and Dr. Diana Sherman (U. Edinburgh). They were crossed to *Thy1:OFP-3* mice for the FRAP assays.

All studies were performed in accordance with the approval by the responsible regulatory agencies.

4.2. Mouse genotyping

Transgenic animals were genotyped by PCR from tail biopsies. Animals are either marked by tattooing on the paws (before weaning) or with numbered ear marks (after weaning) by animal care takers Manuela Budak and Nebahat Budak. DNA isolation with lysis buffer, PCR with GoTaq Green Master Mix (M712, Promega) and gel electrophoresis were performed by Kristina Wullimann. The mouse tails were collected in PCR tubes and DNA was isolated using a standard protocol.

4.3. Neonatal AAV-injection (Az55.2-1-54-2532-58-2016)

Postnatal Day 2/3 pups were anaesthetized with isoflurane and injected with 3µl AAV9-CMV-iCre (titer adjusted to 0.5-5x10^{13} copies/ml, produced by Engelhardt lab) into the right lateral ventricle at a rate of 30 nl/s using a fine glass pipette (3.5" Drummond #3-000-203-G/X) attached to a nanoliter injector (Micro4™ MicroSyringe Pump Controller connected with Nanoliter 2000, World Precision Instruments) with ultrasound guidance (Vevo1100 Imaging System, with a Microscan MS550D transducer, Visualsonics). 0.05% (wt/vol) trypan blue was added to the virus at to visualize the solution. The pups were allowed to recover on a heating mat until fully awake before returning to the mother, and sacrificed on P9 for immunohistochemistry.

Bungarotoxin injection on P7 was administered in a similar manner, where the needle was inserted laterally under the skin of the right thorax, and 1 µl 50 mg/µl Alexa488- or 594- conjugated α-bungarotoxin (Invitrogen, B13422, B13423) was injected instead.

4.4. Western blot

Mouse spinal cord was isolated in 1x PBS and homogenized on ice, washed in 1xPBS, pH 7.4 and pelleted, before resuspended in 300 µl lysis buffer for 30 minutes (50 mM Tris-HCl, pH 8.0, 1% Tx100, 0.25% NP-40, 150 mM NaCl, 0.1 mM EDTA + 1:50 protease inhibitor). The pellet was resuspended in 200 µl lysis buffer + protease inhibitor and the concentration determined with BCA assay (Pierce™ BCA Protein Assay Kit, #23225, Thermo Scientific). 20 µg protein with 4x LDS sample buffer and 200 mM DTT was heated at 70°C for 10 minutes, loaded on the precast NuPAGE® SDS-PAGE gel (Thermo Scientific) and electrophoresed. The separated proteins were then transferred onto a methanol-activated PVDF membrane by electrophoresis with 15V constant, max. 0.4 A for 45 minutes (Towbin, Staehelin and Gordon, 1979). The blotted membrane was then blocked with 1% BSA (Sigma, A7030) in PBS-T at RT for

30 minutes and incubated with the primary antibody (anti-Caspr 1:1000, polyclonal rabbit, Abcam, 1 mg/ml) at 4°C overnight. The membrane was washed and incubated with HRP coupled secondary antibody 1:5000 at room temperature for 1 – 2 hours, washed and incubated with mixed ECL reagent for 2 – 5 min, before developed with Fusion FX7 Spectra (Vilber). The blot was then stripped with SDS containing buffer for 30 minutes at room temperature, washed and blocked, before repeating the process with anti-GFP 1:10000 (polyclonal chicken, Abcam, 10mg/ml).

4.5. Immunohistochemistry and confocal microscopy

The thorax was extracted and fixed in 4% paraformaldehyde (PFA) for 1hr in 0.1M phosphate buffer (PB). The triangularis muscle was dissected as previously described (Kerschensteiner *et al.*, 2008; Brill *et al.*, 2011) and incubated overnight (4°C) in the respective primary antibodies diluted in blocking solution (5% BSA, 0.5% Triton X-100 in 0.1M PB): anti-βIII-tubulin conjugated to Alexa488 (BioLegend, 1:200; mouse IgG2a #657403), Alexa555 (mouse monoclonal, 1:200; BD Pharmingen, #560339), Alexa647 (BioLegend, 1:200; mouse IgG2a # 657405). To label postsynaptic nicotinic acetylcholine receptors, Alexa 488-, Alexa 594- or Alexa 647-conjugated α-bungarotoxin (Invitrogen, B13422, B13423, B35450, 50µg/ml, 1:50 in 0.1M PB) were added to the primary antibody mixture. For labeling of nodal components, antibodies against Caspr (polyclonal rabbit from Trimmer or ab34151, Abcam, 1 mg/ml diluted 1:400), MPZ (combined chicken IgY, PZO, Aves Labs, 200 µg/ml 1:200); CNTN2 (polyclonal goat IgG, AF4439, R&D Systems); pan Nav subunit α (polyclonal rabbit, AG1392, Abgent, 1.0 mg/ml diluted 1:400). Muscles were washed in 0.1M PB, incubated for 1hr at room temperature with corresponding secondary antibodies coupled to Alexa 488, Alexa 594 or Alexa 647 (Invitrogen), and washed again in 0.1M PB. In the end, *triangularis sterni* muscle whole-mounts were placed in Vectashield (Vector Laboratories). Image stacks were recorded using a confocal microscope

(Olympus FV1000) equipped with x20/0.8 N.A., x40/1.35 and x60/1.42 N.A. oil-immersion objectives, and maximum intensity projections were generated using the open source software ImageJ/Fiji (Schindelin *et al.*, 2012).

4.6. *Ex vivo* imaging of the *triangularis sterni* explant

The *triangularis sterni* explant were prepared from young or adult mice respectively. Mice were either lethally anesthetized with isoflurane (Abbot, adult) or decapitated (2^{nd} postnatal week), before isolating the entire anterior thoracic wall. The explant was then fixed on a Sylgard-coated 3.5 cm plastic Petri dish using shortened insect pins (Fine Science Tools), exposing the *triangularis sterni* muscle and the intercostal nerves. During imaging, the explant was kept at 31-33℃ with a heating ring connected to an automatic temperature controller (TC-344C, Warner Instruments) and steadily perfused with Ringer's solution (125 mM NaCl, 2.5 mM KCl, 1.25 mM NaH_2PO_4, 26 mM $NaHCO_3$, 2 mM $CaCl_2$, 1 mM $MgCl_2$, 20 mM glucose, oxygenated with 95% O2/ 5% CO2).(Kerschensteiner *et al.*, 2008)

The FRAP assay and mitochondrial trafficking measurements were performed with an Olympus BX51WI microscope equipped with ×20/0.5 N.A. and ×100/1.0 N.A. water-immersion objectives, an automated filter wheel (Lambda 10-3, Sutter Instrument) and a CCD camera (CoolSnap HQ2, Visitron Systems). All devices were controlled by μManager 1.4 (Edelstein et al., 2010). To measure mitochondria trafficking in the intercostal nerve, CFP ET filter set (AHF Analysentechnik) was used and 150 images per movie were acquired at 1 Hz using an exposure time of 400 ms.

4.7. Fluorescence recovery after photobleaching (FRAP)

Ex vivo thoracic preparations were extracted as previously described (Brill *et al.*, 2011) from *Thy1:Caspr-GFP* mice. FRAP analysis (modified from Axelrod, Koppel, Schlessinger, Elson, & Webb, 1976) and time-lapse recording were performed on an

Olympus BX51WZ microscope with 100x/1.0 N.A. water immersion objective. The laser (473nm, DL-473, Rapp OptoElectronic) for photobleaching was manually focused on the bleaching area (μm^2) and the sample was bleached for 1~3 s. The GFP signal were imaged before and immediately after photobleaching with a GFP/mCherry dualband ET filter set (AHF Analysentechnik), then in one-hour interval for three hours with 800ms exposure time. The intensity of the bleached area was measured with the polygon tool in imageJ and another GFP-positive paranode in the same field of view was used as control to correct the recovery rate.

4.8. Image processing and analysis

Neuromuscular junction analysis: Extracted *triangularis sterni* muscle was fixed and stained as described. Innervation pattern was determined by counting the number of innervating branches ending on each bungarotoxin stained endplate in ImageJ/Fiji. The myelination status on terminal branches was determined by any presence of nodal markers on the respective stretches between the last branching point and the NMJ, excluding any possible staining at the branching point, where it was difficult to discern from the more prominent nodal structures on the stem. Synaptic territory was determined by converting the maximum intensity Z-projection of the confocal stack into binary image with the “Otsu” or “Huang” auto-threshold algorithm in ImageJ/Fiji. NMJ endplate size was determined by measuring the binarized bungarotoxin staining with the same technique. Muscle fiber was stained with Alexa647 phalloidin (Invitrogen, A22287, diluted 1:50 in 0.1 M PB) and the confocal stacks were rotated using the “reslice” function of ImageJ/Fiji, to measure the area and diameter of individual fibers.

Image representation: Maximum intensity projections were generated from confocal image stacks with ImageJ/Fiji, then further processed in Adobe Photoshop. The individual channels were adjusted in level and sometimes non-linearly in gamma for optimal visual effect, then pseudo-colored with the “screen” blend mode.

4.9. Statistics

Statistical tests were performed using the GraphPad PRISM software. Statistical significance was determined using the Mann-Whitney test (non-parametric test for two groups), Wilcoxon text (non-parametric test for paired two groups) or the Kruskal-Wallis test with *post hoc* Dunn's multiple comparisons test (non-parametric test for three or more groups) respectively. Unpaired t-test was used when the data-set passed the D'Agostino & Pearson normality test. χ^2 test was used for comparing expected frequencies between groups, and the *p*-value calculated from the test was shown. $p < 0.05$ was considered to be significant, and indicated by "*"; $p < 0.01$ by "**"; and $p < 0.001$ by "***". Bar-graphs show mean ± standard error of the mean.

4.10. Buffers and solutions

Gitocher Buffer

Reagent	Quantity	Concentration	Source
Tris pH 8.8	25 ml	1.43 M	Roth, 4855.1
$(NH_4)_2SO_4$	5 ml	1.66 M	Sigma-Aldrich, M3148
$MgCl_2$	5 ml	0.65 M	
Gelatine	0.05 g		Roth, 4275.3
H_2O	15 ml		
Total	50 ml		

Lysis Buffer

Reagent	Quantity
Gitocher Buffer	15 µl
β-mercaptoethanol	1.5 µl
Proteinase K	0.75 µl
H_2O	125.25 µl
Total	150 µl

10x Ringer's solution

Reagent	Quantity	Concentration	Source
$NaHCO_3$	21.84 g	260 mM	Sigma-Aldrich, S6297
$NaH_2PO_4 \cdot H_2O$	1.72 g	12.5 mM	Riedel de Hän; 04270
KCl	1.86 g	25 mM	
NaCl	73.05 g	1.2 mM	
H_2O	up to 1 l		
Total	1 l		

1x Ringer's solution

Reagent	Quantity	Concentration	Source
1M $CaCl_2$	2 ml	2 mM	Sigma-Aldrich, C1016
1M $MgCl_2$	1 ml	1 mM	
H_2O	900 ml		
10x Ringer's solution	100 ml	20 mM	
Glucose	3.6 g		Sigma-Aldrich, 16301
Total	1 l		

1x Ringer's solution is prepared on the day of the experiment (by Christine Karrer). Glucose was added and the solution was oxygenized with carbogen gas (95% O_2 and 5% CO_2) for at least 15 min before use.

Agarose gel

Reagent	Quantity	Source
50 x TAE buffer	2 ml	Roth, CL86.1
Agarose	1 g	SeaKem, 50004
Gel Red nucleic acid stain	10 µl	VWR International,730-2957
H_2O	up to 100 ml	
Total	100 ml	

0.1 M Phosphate buffer

Reagent	Quantity
0.1M NaH_2PO4	500 ml
0.1 M Na_2HPO_4	500 ml
Total	1 l

0.1 M PB (pH 7.4) was used for all experiments (prepared by Alexandra Graupner).

4% Paraformaldehyde (PFA) in 0.1 M PB

Reagent	Quantity	Source
PFA	40 g	Sigma-Aldrich, P6148
NaOH	125 µl	Roth, KK71.1
0.1 M PB	up to 1 l	
Total	1 l	

PFA, NaOH and 0.1 M PB were mixed on a heating plate at 50-60°C until the solution is clear, then filtered and stored at -20°C before use (prepared by Alexandra Graupner).

Blocking solution

Reagent	Quantity
BSA	5 g
Triton X-100	500 µl
0.1 M PB	up to 100 ml
Total	100 ml

Blocking solution was filtered and aliquoted before storing at -20°C until use.

5. PUBLICATIONS

Wang, M., Kleele, T., Brophy, P., Brill, M.S., Misgeld, T. (2015) Assembly and disassembly of the axon-glial unit during neuromuscular synapse elimination. *European Conference on Axon Guidance, Circuit Development and Regeneration.* Vienna, Austria.

Wang, M., Kleele, T., Brophy, P., Brill, M.S., Misgeld, T. (2016) Assembly of the axon-glial unit during neuromuscular synapse elimination. *Mechanisms of neuronal remodeling.* Seeon, Germany.

Brill, M. S., Kleele, T., Ruschkies, L., **Wang, M.**, Marahori, N. A., Reuter, M. S., Hausrat, T. J., Weigand, E., Fisher, M., Ahles, A., Engelhardt, S., Bishop, D. L., Kneussel, M., Misgeld, T. (2016). Branch-Specific Microtubule Destabilization Mediates Axon Branch Loss during Neuromuscular Synapse Elimination. *Neuron,* 92(4), 845–856.

Colombo, A., Hsia, H.-E., **Wang, M.**, Kuhn, P.-H., Brill, M. S., Canevazzi, P., Feederle, R., Taveggia, C., Misgeld, T., Lichtenthaler, S. F. (2018). Non-cell-autonomous function of DR6 in SC proliferation. *The EMBO Journal,* 1–14.

Wang, M., Kleele, T., Schwab, M., Engelhardt, S., Shermann, D., Brophy, P., Misgeld, T., Brill, M.S. Nodal development during synapse elimination (*in preparation*).

6. CONTRIBUTIONS TO EXPERIMENTAL WORK

Together with Prof. Thomas Misgeld and Dr. Monika Brill, I was involved in devising the experimental plan for this project. I performed all experiments regarding the intersection of synapse elimination and myelination, which included trouble shooting and executing the experiments, especially mouse breeding, time-lapse imaging, FRAP, neonatal injection, immunohistochemistry and confocal microscopy, and data analysis. I am writing the first outline and designing all the display items for the manuscript in preparation for this project (Wang *et al.*, *in preparation*) together with Prof. Thomas Misgeld and Dr. Monika Brill. The early characterization of the *Thy1:Caspr-GFP* and *Thy1:Nav-GFP* mice was done by my colleague, Dr. Tatjana Kleele and were generate by Prof. Peter Brophy and Dr. Diana Sherman (U. Edinburgh). The *Thy1:Stop-KHC* mice were generated by Dr. Monika Brill, who also performed most of the mouse breeding for the screen detailed in Section 2.1. The AAV9-CMV-iCre virus was provided by Andrea Ahles with the support Prof. Stefan Engelhardt.

For Colombo *et al.,* 2018, I performed and analyzed immunohistochemistry and confocal microscopy experiments, which were summarized in Figure 4, which I designed. For Brill *et al.,* 2016, I contributed to time-lapse imaging, neonatal injection, confocal imaging and data analysis, mostly contained in Figure 7, Supplementary Figure 4 and 6.

7. REFERENCES

Abraham, W. C. (2008) ‘Metaplasticity: Tuning synapses and networks for plasticity’, *Nature Reviews Neuroscience*. doi: 10.1038/nrn2356.

Abraham, W. C. and Bear, M. F. (1996) ‘Metaplasticity: The plasticity of synaptic plasticity’, *Trends in Neurosciences*. doi: 10.1016/S0166-2236(96)80018-X.

Almeida, R. G. *et al.* (2018) ‘Myelination of Neuronal Cell Bodies when Myelin Supply Exceeds Axonal Demand’, *Current Biology*. Elsevier Ltd., 28(8), p. 1296–1305.e5. doi: 10.1016/j.cub.2018.02.068.

Angelillo-Scherrer, A. *et al.* (2001) ‘Deficiency or inhibition of Gas6 causes platelet dysfunction and protects mice against thrombosis’, *Nature Medicine*. doi: 10.1038/84667.

Auer, F., Vagionitis, S. and Czopka, T. (2018) ‘Evidence for Myelin Sheath Remodeling in the CNS Revealed by In Vivo Imaging’, *Current Biology*. Elsevier Ltd., 28(4), p. 549–559.e3. doi: 10.1016/j.cub.2018.01.017.

Avery, M. A. *et al.* (2012) ‘Wld S prevents axon degeneration through increased mitochondrial flux and enhanced mitochondrial Ca 2+ buffering’, *Current Biology*. doi: 10.1016/j.cub.2012.02.043.

Awasaki, T. *et al.* (2006) ‘Essential Role of the Apoptotic Cell Engulfment Genes draper and ced-6 in Programmed Axon Pruning during Drosophila Metamorphosis’, *Neuron*, 50(6), pp. 855–867. doi: 10.1016/j.neuron.2006.04.027.

Awasaki, T. and Ito, K. (2004) ‘Engulfing action of glial cells is required for programmed axon pruning during Drosophila metamorphosis’, *Current Biology*. doi: 10.1016/j.cub.2004.04.001.

Axelrod, D. *et al.* (1976) ‘Mobility measurement by analysis of fluorescence photobleaching recovery kinetics’, *Biophysical Journal*, 16(9), pp. 1055–1069. doi: 10.1016/S0006-3495(76)85755-4.

Baas, P. W. *et al.* (2016) ‘Stability properties of neuronal microtubules’, *Cytoskeleton*,

73(9), pp. 442–460. doi: 10.1002/cm.21286.

Balice-Gordon, R. J. and Lichtman, J. W. (1993) ‘In vivo observations of pre- and postsynaptic changes during the transition from multiple to single innervation at developing neuromuscular junctions.’, *The Journal of neuroscience : the official journal of the Society for Neuroscience*, 13(2), pp. 834–855. doi: 10.1523/JNEUROSCI.13-02-00834.1993.

Balice-Gordon, R. J. and Lichtman, J. W. (1994) ‘Long-term synapse loss induced by focal blockade of postsynaptlc receptors’, *Nature*, pp. 519–524. doi: 10.1038/372519a0.

Baraban, M., Koudelka, S. and Lyons, D. A. (2017) ‘Ca 2+ activity signatures of myelin sheath formation and growth in vivo’, *Nature Neuroscience*. Springer US, 21(January). doi: 10.1038/s41593-017-0040-x.

Barres, B. A. *et al.* (1992) ‘Cell death and control of cell survival in the oligodendrocyte lineage.’, *Cell*, 70(1), pp. 31–46. doi: 10.1016/0092-8674(92)90531-G.

Beirowski, B. *et al.* (2009) ‘Non-Nuclear WldS Determines Its Neuroprotective Efficacy for Axons and Synapses In Vivo’, *Journal of Neuroscience*. doi: 10.1523/JNEUROSCI.3814-08.2009.

Bengtsson, S. L. *et al.* (2005) ‘Extensive piano practicing has regionally specific effects on white matter development’, *Nature Neuroscience*. doi: 10.1038/nn1516.

Van Bergeijk, P. *et al.* (2015) ‘Optogenetic control of organelle transport and positioning’, *Nature*. Nature Publishing Group, 518(7537), pp. 111–114. doi: 10.1038/nature14128.

Bishop, D. L. *et al.* (2004) ‘Axon branch removal at developing synapses by axosome shedding’, *Neuron*, 44(4), pp. 651–661. doi: 10.1016/j.neuron.2004.10.026.

Black, J. A., Waxman, S. G. and Hildebrand, C. (1985) ‘Axo-glial relations in the retina-optic nerve junction of the adult rat: freeze-fracture observations on axon membrane structure’, *Journal of Neurocytology*. doi: 10.1007/BF01224803.

Bliss, T. V. P. and Lømo, T. (1973) ‘Long-lasting potentiation of synaptic transmission in the dentate area of the anaesthetized rabbit following stimulation of the perforant path’, *The Journal of Physiology*. doi: 10.1113/jphysiol.1973.sp010273.

Bliss, T. V and Gardner-Medwin, a R. (1973) ‘Long-lasting potentiation of synaptic transmission in the dentate area of the unanaestetized rabbit following stimulation of the perforant path.’, *The Journal of physiology*. doi: 4727084.

Borowiak, M. *et al.* (2015) ‘Photoswitchable Inhibitors of Microtubule Dynamics Optically Control Mitosis and Cell Death’, *Cell*. Elsevier Ltd, 162(2), pp. 402–411. doi: 10.1016/j.cell.2015.06.049.

Breckwoldt, M. O. *et al.* (2014) ‘Multiparametric optical analysis of mitochondrial redox signals during neuronal physiology and pathology in vivo’, *Nature Medicine*, 20(5), pp. 555–560. doi: 10.1038/nm.3520.

Brill, M. S. *et al.* (2011) ‘Spatial constraints dictate glial territories at murine neuromuscular junctions’, *Journal of Cell Biology*, 195(2), pp. 293–305. doi: 10.1083/jcb.201108005.

Brill, M. S. *et al.* (2016) ‘Branch-Specific Microtubule Destabilization Mediates Axon Branch Loss during Neuromuscular Synapse Elimination’, *Neuron*. Elsevier Inc., 92(4), pp. 845–856. doi: 10.1016/j.neuron.2016.09.049.

Brivio, V. *et al.* (2017) ‘Assembly of CNS Nodes of Ranvier in Myelinated Nerves Is Promoted by the Axon Cytoskeleton’, *Current Biology*. Elsevier Ltd., 27(7), pp. 1068–1073. doi: 10.1016/j.cub.2017.01.025.

Brugnera, E. *et al.* (2002) ‘Unconventional Rac-GEF activity is mediated through the Dock180-ELMO complex’, *Nature Cell Biology*, 4(8), pp. 574–582. doi: 10.1038/ncb824.

Buffelli, M. *et al.* (2003) ‘Genetic evidence that relative synaptic efficacy biases the outcome of synaptic competition’, *Nature*, 424(6947), pp. 430–434. doi: 10.1038/nature01836.1.

Burstyn-Cohen, T., Heeb, M. J. and Lemke, G. (2009) 'Lack of Protein S in mice causes embryonic lethal coagulopathy and vascular dysgenesis', *Journal of Clinical Investigation*. doi: 10.1172/JCI39325.

Cai, Q., Gerwin, C. and Sheng, Z. H. (2005) 'Syntabulin-mediated anterograde transport of mitochondria along neuronal processes', *Journal of Cell Biology*, 170(6), pp. 959–969. doi: 10.1083/jcb.200506042.

Cajal, S. R. y (1911) 'Histologie du Systeme Nerveux de l'Homme et des Vertebres', *Instituto Ramon y Cajal, Madrid*, 2.

Campbell, D. S. and Okamoto, H. (2013) 'Local caspase activation interacts with Slit-Robo signaling to restrict axonal arborization', *Journal of Cell Biology*, 203(4), pp. 657–672. doi: 10.1083/jcb.201303072.

Cantuti-Castelvetri, L. *et al.* (2018) 'Defective cholesterol clearance limits remyelination in the aged central nervous system', *Science*. doi: 10.1126/science.aan4183.

Chang, K.-J., Redmond, S. A. and Chan, J. R. (2016) 'Remodeling myelination: implications for mechanisms of neural plasticity', *Nature Neuroscience*, 19(2), pp. 190–197. doi: 10.1038/nn.4200.

Charles, P. *et al.* (2002) 'Neurofascin is a glial receptor for the paranodin/Caspr-contactin axonal complex at the axoglial junction', *Current Biology*, 12(3), pp. 217–220. doi: 10.1016/S0960-9822(01)00680-7.

Cheng, S. M. and Carr, C. E. (2007) 'Functional delay of myelination of auditory delay lines in the nucleus laminaris of the barn owl', *Developmental Neurobiology*. doi: 10.1002/dneu.20541.

Chung, W.-S. *et al.* (2013) 'Astrocytes mediate synapse elimination through MEGF10 and MERTK pathways.', *Nature*, 504(7480), pp. 394–400. doi: 10.1038/nature12776.

Cohen-Cory, S. (2002) 'The Developing Synapse: Construction and Modulation of Synaptic Structures and Circuits Synaptogenesis: A Microscopic View', 298(October), pp. 770–777.

Coleman, M. P. and Freeman, M. R. (2010) 'Wallerian Degeneration, Wld, and Nmnat', *Annual Review Neuroscience*, 33(Coleman 2005), pp. 245–267. doi: 10.1146/annurev-neuro-060909-153248.Wallerian.

Colombo, A. *et al.* (2018) 'Non-cell-autonomous function of DR6 in Schwann cell proliferation', *The EMBO Journal*, 37(12). doi: 10.15252/embj.

Czopka, T., ffrench-Constant, C. and Lyons, D. A. (2013) 'Individual oligodendrocytes have only a few hours in which to generate new myelin sheaths invivo', *Developmental Cell*. doi: 10.1016/j.devcel.2013.05.013.

Darabid, H., Arbour, D. and Robitaille, R. (2013) 'Glial cells decipher synaptic competition at the mammalian neuromuscular junction', *The Journal of Neuroscience*, 33(4), pp. 1297–313. doi: 10.1523/JNEUROSCI.2935-12.2013.

Darabid, H., Perez-Gonzalez, A. P. and Robitaille, R. (2014) 'Neuromuscular synaptogenesis: coordinating partners with multiple functions', *Nature Reviews Neuroscience*. Nature Publishing Group, (October), pp. 1–16. doi: 10.1038/nrn3821.

Debanne, D. (2004) 'Information processing in the axon', *Nature Reviews Neuroscience*. doi: 10.1038/nrn1397.

Deckwerth, T. L. *et al.* (1996) 'BAX is required for neuronal death after trophic factor deprivation and during development', *Neuron*. doi: 10.1016/S0896-6273(00)80173-7.

Elliott, M. R. *et al.* (2010) 'Unexpected requirement for ELMO1 in clearance of apoptotic germ cells in vivo', *Nature*. doi: 10.1038/nature09356.

Elmore, S. (2007) 'Apoptosis: A Review of Programmed Cell Death', *Toxicologic Pathology*, 35(4), pp. 495–516. doi: 10.1080/01926230701320337.

Fan, H., Favero, M. and Vogel, M. W. (2001) 'Elimination of Bax expression in mice increases cerebellar Purkinje cell numbers but not the number of granule cells', *Journal of Comparative Neurology*. doi: 10.1002/cne.1055.

Favero, M. *et al.* (2009) 'On the mechanism of action of muscle fibre activity in synapse competition and elimination at the mammalian neuromuscular junction', *European*

Journal of Neuroscience, 29(12), pp. 2327–2334. doi: 10.1111/j.1460-9568.2009.06779.x.

Feller, M. B. (2002) 'The role of nAChR-mediated spontaneous retinal activity in visual system development', *Journal of Neurobiology*. doi: 10.1002/neu.10140.

Feng, G. *et al.* (2000) 'Imaging neuronal subsets in transgenic mice expressing multiple spectral variants of GFP', *Neuron*. doi: 10.1016/S0896-6273(00)00084-2.

Fields, R. D. (2015) 'A new mechanism of nervous system plasticity: activity-dependent myelination.', *Nature reviews. Neuroscience*. Nature Publishing Group, 16(12), pp. 756–67. doi: 10.1038/nrn4023.

Fraser, M. M. *et al.* (2008) 'Phosphatase and tensin homolog, deleted on chromosome 10 deficiency in brain causes defects in synaptic structure, transmission and plasticity, and myelination abnormalities', *Neuroscience*. doi: 10.1016/j.neuroscience.2007.10.048.

Fricker, M. *et al.* (2012) 'MFG-E8 Mediates Primary Phagocytosis of Viable Neurons during Neuroinflammation', *Journal of Neuroscience*, 32(8), pp. 2657–2666. doi: 10.1523/JNEUROSCI.4837-11.2012.

Friedman, L. G. *et al.* (2012) 'Disrupted Autophagy Leads to Dopaminergic Axon and Dendrite Degeneration and Promotes Presynaptic Accumulation of -Synuclein and LRRK2 in the Brain', *Journal of Neuroscience*, 32(22), pp. 7585–7593. doi: 10.1523/JNEUROSCI.5809-11.2012.

Gamage, K. K. *et al.* (2017) 'Death Receptor 6 Promotes Wallerian Degeneration in Peripheral Axons', *Current Biology*. Elsevier Ltd., 27(6), pp. 890–896. doi: 10.1016/j.cub.2017.01.062.

Garratt, A. N. *et al.* (2000) 'A dual role of erbB2 in myelination and in expansion of the Schwann cell precursor pool', *Journal of Cell Biology*, 148(5), pp. 1035–1046. doi: 10.1083/jcb.148.5.1035.

Geoffroy, C. G. and Zheng, B. (2014) 'Myelin-associated inhibitors in axonal growth

after CNS injury', *Current Opinion in Neurobiology*. doi: 10.1016/j.conb.2014.02.012.

Gibson, E. M. *et al.* (2014) 'Neuronal activity promotes oligodendrogenesis and adaptive myelination in the mammalian brain', *Science*. doi: 10.1126/science.1252304.

Giese, K. P. *et al.* (1992) 'Mouse P0gene disruption leads to hypomyelination, abnormal expression of recognition molecules, and degeneration of myelin and axons', *Cell*, 71(4), pp. 565–576. doi: 10.1016/0092-8674(92)90591-Y.

Gillingwater, T. H. and Ribchester, R. R. (2001) 'Compartmental neurodegeneration and synaptic plasticity in the Wlds mutant mouse', *Journal of Physiology*, 534(3), pp. 627–639. doi: 10.1111/j.1469-7793.2001.00627.x.

Green, D. R. and Levine, B. (2014) 'To be or not to be? How selective autophagy and cell death govern cell fate', *Cell*. doi: 10.1016/j.cell.2014.02.049.

Grinspan, J. B. *et al.* (1996) 'Axonal interactions regulate Schwann cell apoptosis in developing peripheral nerve: neuregulin receptors and the role of neuregulins.', *The Journal of neuroscience : the official journal of the Society for Neuroscience*, 16(19), pp. 6107–6118.

Grove, M. and Brophy, P. J. (2014) 'FAK Is Required for Schwann Cell Spreading on Immature Basal Lamina to Coordinate the Radial Sorting of Peripheral Axons with Myelination.', *The Journal of neuroscience : the official journal of the Society for Neuroscience*, 34(40), pp. 13422–34. doi: 10.1523/JNEUROSCI.1764-14.2014.

Gumienny, T. L. *et al.* (2001) 'CED-12 / ELMO , a Novel Member of the CrkII / Dock180 / Rac Pathway , Is Required for Phagocytosis and Cell Migration State University of New York at Stony Brook', *October*, 107, pp. 27–41.

Hafizi, S. and Dahlbäck, B. (2006) 'Gas6 and protein S: Vitamin K-dependent ligands for the Axl receptor tyrosine kinase subfamily', *FEBS Journal*, 273(23), pp. 5231–5244. doi: 10.1111/j.1742-4658.2006.05529.x.

Hanayama, R. *et al.* (2002) 'Identification of a factor that links apoptotic cells to phagocytes', *Nature*, 417(6885), pp. 182–187. doi: 10.1038/417182a.

Hara, T. *et al.* (2006) ‘Suppression of basal autophagy in neural cells causes neurodegenerative disease in mice’, *Nature*. doi: 10.1038/nature04724.

Hebb, D. O. (1949) ‘The organization of behavior: A Neuropsychological Approach’, *The American Journal of Psychology*. doi: 10.2307/1418888.

Hernández, C., Blackburn, E. and Alvarez, J. (1989) ‘Calibre and Microtubule Content of the Non-Medullated and Myelinated Domains of Optic Nerve Axons of Rats’, *European Journal of Neuroscience*. doi: 10.1111/j.1460-9568.1989.tb00371.x.

Hildebrand, C., Bowe, C. M. and Remahl, I. N. (1994) ‘Myelination and myelin sheath remodelling in normal and pathological PNS nerve fibres’, *Progress in Neurobiology*, 43, pp. 85–141.

Hille, B. (2001) *Ion channels of excitable membranes. Edition 3*, *Ion channels of excitable membranes. Edition 3*. doi: 10.1007/3-540-29623-9_5640.

Hines, J. H. *et al.* (2015) ‘Neuronal activity biases axon selection for myelination in vivo’, *Nature Neuroscience*, 18(5), pp. 683–689. doi: 10.1038/nn.3992.

Hodgkin, A. L. and Huxley, A. F. (1952) ‘A Quantitative Description of Membrane Current and its Application to Conduction and Excitation in Nerves’, *J. Physiol.* doi: 10.1016/S0092-8240(05)80004-7.

Hoopfer, E. D. *et al.* (2006) ‘Wlds Protection Distinguishes Axon Degeneration following Injury from Naturally Occurring Developmental Pruning’, *Neuron*, 50(6), pp. 883–895. doi: 10.1016/j.neuron.2006.05.013.

de Hoz, L. and Simons, M. (2015) ‘The emerging functions of oligodendrocytes in regulating neuronal network behaviour’, *BioEssays*, 37(1), pp. 60–69. doi: 10.1002/bies.201400127.

Hubel, D. H. and Wiesel, T. N. (1970) ‘The period of susceptibility to the physiological effects of unilateral eye closure in kittens’, *The Journal of Physiology*. doi: 10.1113/jphysiol.1970.sp009022.

Hughes, E. G. *et al.* (2018) ‘Myelin remodeling through experience-dependent

oligodendrogenesis in the adult somatosensory cortex', *Nature Neuroscience*. Springer US, 21(5), pp. 696–706. doi: 10.1038/s41593-018-0121-5.

Huxley, A. F. and Stämpeli, R. (1949) 'Evidence for saltatory conduction in peripheral myelinated nerve fibres', *The Journal of Physiology*. doi: 10.1113/jphysiol.1949.sp004335.

Israelson, A. *et al.* (2015) 'Macrophage migration inhibitory factor as a chaperone inhibiting accumulation of misfolded SOD1', *Neuron*. Elsevier Inc., 86(1), pp. 218–232. doi: 10.1016/j.neuron.2015.02.034.

Jang, S. Y. *et al.* (2016) 'Autophagic myelin destruction by schwann cells during wallerian degeneration and segmental demyelination', *Glia*, 64(5), pp. 730–742. doi: 10.1002/glia.22957.

Kandel (2014) 'Principles of neural science', *Igarss 2014*. doi: 10.1007/s13398-014-0173-7.2.

Kandel, E. R., Schwartz, J. M. and Jessell, T. M. (2013) *Principles of Neural Science*, *Principles of Neural Science*. doi: 10.1036/0838577016.

Karbowski, M. *et al.* (2006) 'Role of Bax and Bak in mitochondrial morphogenesis', *Nature*. doi: 10.1038/nature05111.

Kasthuri, N. and Lichtman, J. W. (2003) 'The role of neuronal identity in synaptic competition', *Nature*. doi: 10.1038/nature01836.

Kay, J. N., Chu, M. W. and Sanes, J. R. (2012) 'MEGF10 and MEGF11 mediate homotypic interactions required for mosaic spacing of retinal neurons', *Nature*, 483(7390), pp. 465–469. doi: nature10877 [pii]\r10.1038/nature10877.

Keller-Peck, C. R. *et al.* (2001) 'Asynchronous synapse elimination in neonatal motor units: Studies using GFP transgenic mice', *Neuron*, 31(3), pp. 381–394. doi: 10.1016/S0896-6273(01)00383-X.

Kerschensteiner, M. *et al.* (2008) 'Ex vivo imaging of motor axon dynamics in murine triangularis sterni explants', *Nature Protocols*, 3(10), pp. 1645–1653. doi:

10.1038/nprot.2008.160.

Knudson, C. M. *et al.* (1995) ‘Bax-deficient mice with lymphoid hyperplasia and male germ cell death.’, *Science*.

Ko, C.-P. and Robitaille, R. (2015) ‘Perisynaptic Schwann Cells at the Neuromuscular Synapse: Adaptable, Multitasking Glial Cells’, *Cold Spring Harbor Perspectives in Biology*, pp. 1–20.

Komatsu, M. *et al.* (2005) ‘Impairment of starvation-induced and constitutive autophagy in Atg7-deficient mice’, *Journal of Cell Biology*, 169(3), pp. 425–434. doi: 10.1083/jcb.200412022.

Komatsu, M. *et al.* (2006) ‘Loss of autophagy in the central nervous system causes neurodegeneration in mice’, *Nature*, 441(7095), pp. 880–884. doi: 10.1038/nature04723.

Komatsu, M. *et al.* (2007) ‘Essential role for autophagy protein Atg7 in the maintenance of axonal homeostasis and the prevention of axonal degeneration.’, *Proceedings of the National Academy of Sciences of the United States of America*, 104(36), pp. 14489–14494. doi: 10.1073/pnas.0701311104.

Koudelka, S. *et al.* (2016) ‘Individual Neuronal Subtypes Exhibit Diversity in CNS Myelination Mediated by Synaptic Vesicle Release’, *Current Biology*. The Authors, 26(11), pp. 1–9. doi: 10.1016/j.cub.2016.03.070.

Kudo, W. *et al.* (2012) ‘Inhibition of Bax protects neuronal cells from oligomeric Aβ neurotoxicity’, *Cell Death and Disease*. doi: 10.1038/cddis.2012.43.

Kuma, A. *et al.* (2004) ‘The role of autophagy during the early neonatal starvation period’, *Nature*, 432(7020), pp. 1032–1036. doi: 10.1038/nature03029.

Kuo, C. T. *et al.* (2006) ‘Identification of E2/E3 Ubiquitinating Enzymes and Caspase Activity Regulating Drosophila Sensory Neuron Dendrite Pruning’, *Neuron*, 51(3), pp. 283–290. doi: 10.1016/j.neuron.2006.07.014.

Lee, B. *et al.* (2010) ‘White matter neuroplastic changes in long-term trained players of

the game of “Baduk” (GO): A voxel-based diffusion-tensor imaging study’, *NeuroImage*. doi: 10.1016/j.neuroimage.2010.04.014.

Lee, J. Y. *et al.* (2017) ‘Activity-Induced Synaptic Structural Modifications by an Activator of Integrin Signaling at the *Drosophila* Neuromuscular Junction’, *The Journal of Neuroscience*, 37(12), pp. 3246–3263. doi: 10.1523/JNEUROSCI.3128-16.2017.

Lee, S. *et al.* (2012) ‘A culture system to study oligodendrocyte myelination processes using engineered nanofibers.’, *Nature methods*, 9(9), pp. 917–22. doi: 10.1038/nmeth.2105.

Lee, Y. il *et al.* (2016) ‘Neuregulin1 displayed on motor axons regulates terminal Schwann cell-mediated synapse elimination at developing neuromuscular junctions’, *Proceedings of the National Academy of Sciences*, 113(4), pp. E479–E487. doi: 10.1073/pnas.1519156113.

Leone, D. P. *et al.* (2003) ‘Tamoxifen-inducible glia-specific Cre mice for somatic mutagenesis in oligodendrocytes and Schwann cells’, *Molecular and Cellular Neuroscience*, 22(4), pp. 430–440. doi: 10.1016/S1044-7431(03)00029-0.

Levine, B. and Klionsky, D. J. (2004) ‘Development by self-digestion: Molecular mechanisms and biological functions of autophagy’, *Developmental Cell*, 6(4), pp. 463–477. doi: 10.1016/S1534-5807(04)00099-1.

Li, X. *et al.* (1995) ‘Mapping of synapsin II (SYN2) genes to human chromosome 3p and mouse chromosome 6 band F’, *Cytogenet Cell Genet*.

Lichtman, J. W. and Balice-Gordon, R. J. (1990) ‘Understanding synaptic competition in theory and in practice’, *Journal of Neurobiology*. doi: 10.1046/j.1440-1789.2001.00370.x.

Lindsten, T. *et al.* (2000) ‘The combined functions of proapoptotic Bcl-2 family members Bak and Bax are essential for normal development of multiple tissues’, *Molecular Cell*. doi: 10.1016/S1097-2765(00)00136-2.

Liu, J. *et al.* (2012) ‘Impaired adult myelination in the prefrontal cortex of socially

isolated mice', *Nature Neuroscience*, 15(12), pp. 1621–1623. doi: 10.1038/nn.3263.

Livet, J. *et al.* (2007) 'Transgenic strategies for combinatorial expression of fluorescent proteins in the nervous system', *Nature*, 450(7166), pp. 56–62. doi: 10.1038/nature06293.

Loeb, J. A. (2003) 'Neuregulin: An activity-dependent synaptic modulator at the neuromuscular junction', *Journal of Neurocytology*, 32(5–8), pp. 649–664. doi: 10.1023/B:NEUR.0000020640.84708.35.

Loeb, J. a *et al.* (2002) 'Neuregulin expression at neuromuscular synapses is modulated by synaptic activity and neurotrophic factors.', *The Journal of neuroscience : the official journal of the Society for Neuroscience*, 22(6), pp. 2206–2214. doi: 22/6/2206 [pii].

Luo, L. and O'Leary, D. D. M. (2005) 'Axon Retraction and Degeneration in Development and Disease', *Annual Review of Neuroscience*, 28(1), pp. 127–156. doi: 10.1146/annurev.neuro.28.061604.135632.

Madisen, L. *et al.* (2010) 'A robust and high-throughput Cre reporting and characterization system for the whole mouse brain', *Nature Neuroscience*. doi: 10.1038/nn.2467.

Makinodan, M. *et al.* (2012) 'A Critical Period for Social Experience–Dependent Oligodendrocyte Maturation and Myelination', *Science (New York, N.Y.)*, 337(September), pp. 1357–1360. doi: 10.1126/science.1220845.

Mallon, B. S. *et al.* (2002) 'Proteolipid promoter activity distinguishes two populations of NG2-positive cells throughout neonatal cortical development.', *The Journal of neuroscience : the official journal of the Society for Neuroscience*, 22(3), pp. 876–885. doi: 22/3/876 [pii].

Matsuzaki, M. *et al.* (2004) 'Structural basis of long-trm potentiation in single dendritic spines', *Nature*, 429(June), pp. 761–766. doi: 10.1038/nature02594.1.

Mazaheri, F. *et al.* (2014) 'Distinct roles for BAI1 and TIM-4 in the engulfment of dying

neurons by microglia.', *Nature communications*. Nature Publishing Group, 5(May), p. 4046. doi: 10.1038/ncomms5046.

McGee, A. W. *et al.* (2005) 'Experience-driven plasticity of visual cortex limited by myelin and Nogo receptor.', *Science (New York, N.Y.)*, 309(5744), pp. 2222–6. doi: 10.1126/science.1114362.

Mi, S. *et al.* (2011) 'Death receptor 6 negatively regulates oligodendrocyte survival, maturation and myelination', *Nature Medicine*. Nature Publishing Group, 17(7), pp. 816–821. doi: 10.1038/nm.2373.

Michailov, G. V *et al.* (2004) 'Axonal Neuregulin-1 Regulates Myelin Sheath Thickness', *Science*, 304(700 (2004)), pp. 700–703.

Mills, E. A. *et al.* (2015) 'Astrocytes phagocytose focal dystrophies from shortening myelin segments in the optic nerve of Xenopus laevis at metamorphosis.', *Proceedings of the National Academy of Sciences of the United States of America*, 112(33), pp. 10509–14. doi: 10.1073/pnas.1506486112.

Misgeld, T. *et al.* (2002) 'Roles of Neurotransmitter in Synapse Formation', *Neuron*, 36(4), pp. 635–648. doi: 10.1016/S0896-6273(02)01020-6.

Misgeld, T. *et al.* (2007) 'Imaging axonal transport of mitochondria in vivo', *Nature Methods*. doi: 10.1038/nmeth1055.

Misgeld, T. and Kerschensteiner, M. (2006) 'In vivo imaging of the diseased nervous system', *Nature Reviews Neuroscience*, 7(6), pp. 449–463. doi: 10.1038/nrn1905.

Misgeld, T. and Schwarz, T. L. (2017) 'Mitostasis in Neurons: Maintaining Mitochondria in an Extended Cellular Architecture', *Neuron*. Elsevier Inc., 96(3), pp. 651–666. doi: 10.1016/j.neuron.2017.09.055.

Miura, M. (2016) 'Apoptotic and nonapoptotic Caspase function in animal development', *Cold Spring Harbor perspectives in biology*, 4(10), p. a008664. doi: 10.1101/cshperspect.a008664.

Mizushima, N., Yoshimori, T. and Ohsumi, Y. (2011) 'The Role of Atg Proteins in

Autophagosome Formation', *Annual Review of Cell and Developmental Biology*, 27(1), pp. 107–132. doi: 10.1146/annurev-cellbio-092910-154005.

Monk, K. R., Feltri, M. L. and Taveggia, C. (2015) 'New insights on schwann cell development', *Glia*, pp. 1–18. doi: 10.1002/glia.22852.

Mount, C. W. and Monje, M. (2017) 'Wrapped to Adapt: Experience-Dependent Myelination', *Neuron*. Elsevier Inc., 95(4), pp. 743–756. doi: 10.1016/j.neuron.2017.07.009.

Nave, K.-A. and Werner, H. B. (2014) 'Myelination of the Nervous System: Mechanisms and Functions', *Annual Review of Cell and Developmental Biology*, 30, pp. 503–33. doi: 10.1146/annurev-cellbio-100913-013101.

Nichols, C. D. (2009) 'Engineered G-protein coupled receptors are powerful tools to investigate biological processes and behaviors', *Frontiers in Molecular Neuroscience*, 2(October). doi: 10.3389/neuro.02.016.2009.

Nikolaev, A. *et al.* (2009) 'APP binds DR6 to trigger axon pruning and neuron death via distinct caspases', *Nature*. Nature Publishing Group, 457(7232), pp. 981–989. doi: 10.1038/nature07767.

Oztürk, a H. *et al.* (2002) 'Morphometric comparison of the human corpus callosum in professional musicians and non-musicians by using in vivo magnetic resonance imaging.', *Journal of neuroradiology. Journal de neuroradiologie*. doi: JNR-03-2002-29-1-0150-9861-101019-ART6.

Pajevic, S., Basser, P. J. and Fields, R. D. (2014) 'Role of myelin plasticity in oscillations and synchrony of neuronal activity', *Neuroscience*. doi: 10.1016/j.neuroscience.2013.11.007.

Pan, G. *et al.* (1998) 'Identification and functional characterization of DR6, a novel death domain-containing TNF receptor', *FEBS Letters*. doi: 10.1016/S0014-5793(98)00791-1.

Park, D. *et al.* (2007) 'BAI1 is an engulfment receptor for apoptotic cells upstream of

the ELMO/Dock180/Rac module', *Nature*, 450(7168), pp. 430–434. doi: 10.1038/nature06329.

Parson, S. H., Mackintosh, C. L. and Ribchester, R. R. (1997) 'Elimination of Motor Nerve Terminals in Neonatal Mice Expressing a Gene for Slow Wallerian Degeneration (C57Bl/ Wld s)', *European Journal of Neuroscience*, 9(8), pp. 1586–1592. doi: 10.1111/j.1460-9568.1997.tb01516.x.

Peles, E. and Salzer, J. L. (2000) 'Molecular domains of myelinated axons', *Current Opinion in Neurobiology*, 10(5), pp. 558–565. doi: 10.1016/S0959-4388(00)00122-7.

Peters, A., Palay, S. L. and Webster, H. D. F. (1991) *The neurones and supporting cells, in The Fine Structure of the Nervous System*. Third Edit. New York : Oxford University Press, 1991.

Poliak, S. *et al.* (2003) 'Juxtaparanodal clustering of Shaker-like K+channels in myelinated axons depends on Caspr2 and TAG-1', *Journal of Cell Biology*, 162(6), pp. 1149–1160. doi: 10.1083/jcb.200305018.

Press, C. and Milbrandt, J. (2008) 'Nmnat Delays Axonal Degeneration Caused by Mitochondrial and Oxidative Stress', *Journal of Neuroscience*, 28(19), pp. 4861–4871. doi: 10.1523/JNEUROSCI.0525-08.2008.

Pujol, J. *et al.* (2004) 'Delayed myelination in children with developmental delay detected by volumetric MRI', *NeuroImage*, 22(2), pp. 897–903. doi: 10.1016/j.neuroimage.2004.01.029.

Qu, X. *et al.* (2003) 'Promotion of tumorigenesis by heterozygous disruption of the beclin 1 autophagy gene', *Journal of Clinical Investigation*, 112(12), pp. 1809–1820. doi: 10.1172/JCI200320039.

Raff, M. C. *et al.* (1993) 'Programmed cell death and the control of cell survival: lessons from the nervous system.', *Science*.

Raff, M. C., Whitmore, A. V. and Finn, J. T. (2002) 'Neuroscience: Axonal self-destruction and neurodegeneration', *Science*. doi: 10.1126/science.1068613.

Rasband, M. N. and Peles, E. (2016) ‘The nodes of Ranvier: Molecular assembly and maintenance’, *Cold Spring Harbor Perspectives in Biology*, 8(3), pp. 1–16. doi: 10.1101/cshperspect.a020495.

Rasband, M. N. and Shrager, P. (2000) ‘Ion channel sequestration in central nervous system axons.’, *The Journal of Physiology*, 525(1), pp. 63–73. doi: 10.1111/j.1469-7793.2000.00063.x.

Ravichandran, K. S. and Lorenz, U. (2007) ‘Engulfment of apoptotic cells: signals for a good meal’, *Nat. Rev. Immunol.*, 7(12), pp. 964–974. doi: 10.1038/nri2214.

Reynolds, M. L. and Woolf, C. J. (1992) ‘Terminal Schwann cells elaborate extensive processes following denervation of the motor endplate’, *Journal of Neurocytology*, 21(1), pp. 50–66. doi: 10.1007/BF01206897.

Ribchester, R. R. (1993) ‘Co-existence and elimination of convergent motor nerve terminals in reinnervated and paralysed adult rat skeletal muscle.’, *The Journal of Physiology*. doi: 10.1113/jphysiol.1993.sp019728.

Richardson, W. D. *et al.* (2011) ‘NG2-glia as multipotent neural stem cells-fact or fantasy?’, *Neuron*, 70(4), pp. 661–673. doi: 10.1016/j.neuron.2011.05.013.NG2-glia.

Riley, D. A. (1981) ‘Ultrastructural evidence for axon retraction during the spontaneous elimination of polyneuronal innervation of the rat soleus muscle.’, *Journal of neurocytology*, 10(3), pp. 425–40. Available at: http://www.ncbi.nlm.nih.gov/pubmed/7310460.

Rossi, J. *et al.* (2011) ‘Melanocortin-4 receptors expressed by cholinergic neurons regulate energy balance and glucose homeostasis’, *Cell Metabolism*. doi: 10.1016/j.cmet.2011.01.010.

Rubinsztein, D. C. *et al.* (2005) ‘Autophagy and its possible roles in nervous system diseases, damage and repair.’, *Autophagy*, 1(1), pp. 11–22. doi: 10.4161/auto.1.1.1513.

Safaiyan, S. *et al.* (2016) ‘Age-related myelin degradation burdens the clearance

function of microglia during aging', *Nature Neuroscience*. doi: 10.1038/nn.4325.

Salzer, J. L. (2003) 'Polarized domains of myelinated axons', *Neuron*, 40(2), pp. 297–318. doi: 10.1016/S0896-6273(03)00628-7.

Salzer, J. L., Brophy, P. J. and Peles, E. (2008) 'Molecular domains of myelinated axons in the peripheral nervous system', *Glia*, 56(14), pp. 1532–1540. doi: 10.1002/glia.20750.

Sanes, J. R. and Lichtman, J. W. (1999) 'Development of the Vertebrate Neuromuscular Junction', *Annual Review of Neuroscience*, 22(1), pp. 389–442. doi: 10.1146/annurev.neuro.22.1.389.

Schafer, D. P. and Stevens, B. (2013) 'Phagocytic glial cells: Sculpting synaptic circuits in the developing nervous system', *Current Opinion in Neurobiology*. Elsevier Ltd, 23(6), pp. 1034–1040. doi: 10.1016/j.conb.2013.09.012.

Schindelin, J. *et al.* (2012) 'Fiji: An open-source platform for biological-image analysis', *Nature Methods*, 9(7), pp. 676–682. doi: 10.1038/nmeth.2019.

Schlegel, A. A., Rudelson, J. J. and Tse, P. U. (2012) 'White matter structure changes as adults learn a second language', *J Cogn Neurosci*. doi: 10.1162/jocn_a_00240.

Schoenmann, Z. *et al.* (2010) 'Axonal Degeneration Is Regulated by the Apoptotic Machinery or a NAD+-Sensitive Pathway in Insects and Mammals', *Journal of Neuroscience*, 30(18), pp. 6375–6386. doi: 10.1523/JNEUROSCI.0922-10.2010.

Scholz, J. *et al.* (2009) 'Training induces changes in white-matter architecture', *Nature Neuroscience*. doi: 10.1038/nn.2412.

Schuldiner, O. and Yaron, A. (2015) 'Mechanisms of developmental neurite pruning', *Cellular and molecular life sciences : CMLS*, 72(1), pp. 101–119. doi: 10.1007/s00018-014-1729-6.

Seidl, A. H. and Rubel, E. W. (2016) 'Systematic and differential myelination of axon collaterals in the mammalian auditory brainstem', *Glia*, 64(4), pp. 487–494. doi: 10.1002/glia.22941.

Seidl, A. H., Rubel, E. W. and Harris, D. M. (2010) 'Mechanisms for Adjusting Interaural Time Differences to Achieve Binaural Coincidence Detection', *Journal of Neuroscience*, 30(1), pp. 70–80. doi: 10.1523/JNEUROSCI.3464-09.2010.

Seiradake, E., Jones, E. Y. and Klein, R. (2016) *Structural Perspectives on Axon Guidance*, *Annual Review of Cell and Developmental Biology*. doi: 10.1146/annurev-cellbio-111315-125008.

Sengpiel, F. and Kind, P. C. (2002) 'The role of activity in development of the visual system', *Current Biology*, 12(23), pp. 818–826. doi: 10.1016/S0960-9822(02)01318-0.

Simons, M. and Trotter, J. (2007) 'Wrapping it up: the cell biology of myelination', *Current Opinion in Neurobiology*, 17(5), pp. 533–540. doi: 10.1016/j.conb.2007.08.003.

Sirevaag, A. M. and Greenough, W. T. (1987) 'Differential rearing effects on rat visual cortex synapses. III. Neuronal and glial nuclei, boutons, dendrites, and capillaries', *Brain Research*. doi: 10.1016/0006-8993(87)91477-6.

Smith, C. L. *et al.* (2018) 'Mouse Genome Database (MGD)-2018: Knowledgebase for the laboratory mouse', *Nucleic Acids Research*. doi: 10.1093/nar/gkx1006.

Son, Y. J. and Thompson, W. J. (1995) 'Nerve sprouting in muscle is induced and guided by processes extended by schwann cells', *Neuron*, 14(1), pp. 133–141. doi: 10.1016/0896-6273(95)90247-3.

Song, J. W. *et al.* (2008) 'Lysosomal activity associated with developmental axon pruning.', *The Journal of neuroscience : the official journal of the Society for Neuroscience*, 28(36), pp. 8993–9001. doi: 10.1523/JNEUROSCI.0720-08.2008.

Sperry, R. W. (1963) 'Chemoaffinity in the Orderly Growth of Nerve Fiber Patterns and Connections', *Proceedings of the National Academy of Sciences*, 50(4), pp. 703–710. doi: 10.1073/pnas.50.4.703.

Stitt, T. N. *et al.* (1995) 'The anticoagulation factor protein S and its relative, Gas6, are ligands for the Tyro 3/Axl family of receptor tyrosine kinases', *Cell*. doi: 10.1016/0092-8674(95)90520-0.

Stogsdill, J. A. and Eroglu, C. (2017) ‘The interplay between neurons and glia in synapse development and plasticity’, *Current Opinion in Neurobiology*. Elsevier Ltd, 42, pp. 1–8. doi: 10.1016/j.conb.2016.09.016.

Sun, W. (2004) ‘Programmed Cell Death of Adult-Generated Hippocampal Neurons Is Mediated by the Proapoptotic Gene Bax’, *Journal of Neuroscience*. doi: 10.1523/JNEUROSCI.1436-04.2004.

Suzuki, E. and Nakayama, M. (2007) ‘MEGF10 is a mammalian ortholog of CED-1 that interacts with clathrin assembly protein complex 2 medium chain and induces large vacuole formation’, *Experimental Cell Research*, 313(17), pp. 3729–3742. doi: 10.1016/j.yexcr.2007.06.015.

Syroid, D. E. *et al.* (1996) ‘Cell death in the Schwann cell lineage and its regulation by neuregulin.’, *Proceedings of the National Academy of Sciences of the United States of America*, 93(17), pp. 9229–34. doi: 10.1073/pnas.93.17.9229.

Szeligo, F. and Leblond, C. P. (1977) ‘Response of the three main types of glial cells of cortex nad corpus callosum in rats handled during suckling or exposed to enriched, control and impoverished environments following weaning’, *Journal of Comparative Neurology*. doi: 10.1002/cne.901720205.

Tang, G. *et al.* (2014) ‘Loss of mTOR-Dependent Macroautophagy Causes Autistic-like Synaptic Pruning Deficits’, *Neuron*. Elsevier Inc., 83(5), pp. 1131–1143. doi: 10.1016/j.neuron.2014.07.040.

Tapia, J. C. *et al.* (2012) ‘Pervasive Synaptic Branch Removal in the Mammalian Neuromuscular System at Birth’, *Neuron*. Elsevier Inc., 74(5), pp. 816–829. doi: 10.1016/j.neuron.2012.04.017.

Tarrade, A. *et al.* (2006) ‘A mutation of spastin is responsible for swellings and impairment of transport in a region of axon characterized by changes in microtubule composition’, *Human Molecular Genetics*, 15(24), pp. 3544–3558. doi: 10.1093/hmg/ddl431.

Taveggia, C. *et al.* (2005) ‘Neuregulin-1 type III determines the ensheathment fate of axons’, *Neuron*, 47(5), pp. 681–694. doi: 10.1016/j.neuron.2005.08.017.

Tomassy, G. S. *et al.* (2014) ‘Distinct profiles of myelin distribution along single axons of pyramidal neurons in the neocortex’, *Science*. doi: 10.1126/science.1249766.

Towbin, H., Staehelin, T. and Gordon, J. (1979) ‘Electrophoretic transfer of proteins from polyacrylamide gels to nitrocellulose sheets: procedure and some applications.’, *Proceedings of the National Academy of Sciences*. doi: 10.1073/pnas.76.9.4350.

Trachtenberg, J. T. and Thompson, W. J. (1996) ‘Schwann cell apoptosis at developing neuromuscular junctions is regulated by glial growth factor.’, *Nature*, pp. 174–177. doi: 10.1038/379174a0.

Trachtenberg, J. T. and Thompson, W. J. (1997) ‘Nerve terminal withdrawal from rat neuromuscular junctions induced by neuregulin and Schwann cells’, *The Journal of neuroscience : the official journal of the Society for Neuroscience*, 17(16), pp. 6243–6255. Available at: http://www.ncbi.nlm.nih.gov/entrez/query.fcgi?db=pubmed&cmd=Retrieve&dopt=AbstractPlus&list_uids=9236235.

Trotta, N. *et al.* (2004) ‘The hereditary spastic paraplegia gene, spastin, regulates microtubule stability to modulate synaptic structure and function’, *Current Biology*. doi: 10.1016/j.cub.2004.06.058.

Turrigiano, G. G. (1999) ‘Homeostatic plasticity in neuronal networks: The more things change, the more they stay the same’, *Trends in Neurosciences*. doi: 10.1016/S0166-2236(98)01341-1.

Turrigiano, G. G. (2008) ‘The Self-Tuning Neuron: Synaptic Scaling of Excitatory Synapses’, *Cell*. doi: 10.1016/j.cell.2008.10.008.

Vabnick, L. and Shrager, P. (1998) ‘Ion channel redistribution and function during development of the myelinated axon’, *Journal of Neurobiology*, 37(1), pp. 80–96. doi: 10.1002/(SICI)1097-4695(199810)37:1<80::AID-NEU7>3.0.CO;2-4.

Velanac, V. (2009) ‘BACE1 dependent function of Neuregulin1 in peripheral nervous system myelination’.

Velanac, V. *et al.* (2012) ‘Bace1 processing of NRG1 type III produces a myelin-inducing signal but is not essential for the stimulation of myelination’, *Glia*, 60(2), pp. 203–217. doi: 10.1002/glia.21255.

Voyvodic, J. T. (1989) ‘Target size regulates calibre and myelination of sympathetic axons.’, *Nature*, 342(6248), pp. 430–433. doi: 10.1038/342430a0.

de Waegh, S. M., Lee, V. M. Y. and Brady, S. T. (1992) ‘Local modulation of neurofilament phosphorylation, axonal caliber, and slow axonal transport by myelinating Schwann cells’, *Cell*. doi: 10.1016/0092-8674(92)90183-D.

Waller, A. (1850) ‘Experiments on the Section of the Glossopharyngeal and Hypoglossal Nerves of the Frog, and Observations of the Alterations Produced Thereby in the Structure of Their Primitive Fibres’, *Philosophical Transactions of the Royal Society of London*. doi: 10.1098/rstl.1850.0021.

Walsh, M. K. and Lichtman, J. W. (2003) ‘In vivo time-lapse imaging of synaptic takeover associated with naturally occurring synapse elimination’, *Neuron*, 37(1), pp. 67–73. doi: 10.1016/S0896-6273(02)01142-X.

Watts, R. J. *et al.* (2004) ‘Glia engulf degenerating axons during developmental axon pruning’, *Current Biology*. doi: 10.1016/j.cub.2004.03.035.

Watts, R. J., Hoopfer, E. D. and Luo, L. (2003) ‘Axon pruning during Drosophila metamorphosis: Evidence for local degeneration and requirement of the ubiquitin-proteasome system’, *Neuron*, 38(6), pp. 871–885. doi: 10.1016/S0896-6273(03)00295-2.

White, F. a *et al.* (1998) ‘Widespread elimination of naturally occurring neuronal death in Bax-deficient mice.’, *The Journal of neuroscience : the official journal of the Society for Neuroscience*. doi: 10.1523/jneurosci.1446-05.2005.

Wiesel, T. N. *et al.* (1963) ‘Receptive Fields of Cells in Striate Cortex of Very Young,

Visually Inexperienced Kittens.', *Journal of neurophysiology*. doi: citeulike-article-id:7746240.

Williams, D. W. *et al.* (2006) 'Local caspase activity directs engulfment of dendrites during pruning', *Nature Neuroscience*, 9(10), pp. 1234–1236. doi: 10.1038/nn1774.

Wood, J. D. *et al.* (2006) 'The microtubule-severing protein Spastin is essential for axon outgrowth in the zebrafish embryo', *Human Molecular Genetics*, 15(18), pp. 2763–2771. doi: 10.1093/hmg/ddl212.

Wu, H. H. *et al.* (2009) 'Glial precursors clear sensory neuron corpses during development via Jedi-1, an engulfment receptor', *Nature Neuroscience*, 12(12), pp. 1534–1541. doi: 10.1038/nn.2446.

Wu, Y. *et al.* (2005) 'A role for Mer tyrosine kinase in αvβ5 integrin-mediated phagocytosis of apoptotic cells', *Journal of Cell Science*. doi: 10.1242/jcs.01632.

Wyatt, R. M. and Balice-Gordon, R. J. (2003) 'Activity-dependent elimination of neuromuscular synapses', *Journal of Neurocytology*, 32(5–8), pp. 777–794. doi: 10.1023/B:NEUR.0000020623.62043.33.

Yakovlev, P. I. and Lecours, A.-R. (1967) 'The myelogenetic cycles of regional maturation of the brain.', in *Regional Development of Brain in Early Life*. doi: 10.1002/ana.410220408/full.

Yeung, T. *et al.* (2008) 'Membrane phosphatidylserine regulates surface charge and protein localization', *Science*. doi: 10.1126/science.1152066.

Young, P. *et al.* (2008) 'Single-neuron labeling with inducible Cre-mediated knockout in transgenic mice', *Nature Neuroscience*. doi: 10.1038/nn.2118.

Yu, W. *et al.* (2008) 'The Microtubule-severing Proteins Spastin and Katanin Participate Differently in the Formation of Axonal Branches', *Molecular Biology of the Cell*. doi: 10.1091/mbc.E07-09-0878.

Yue, Z. *et al.* (2003) 'Beclin 1, an autophagy gene essential for early embryonic development, is a haploinsufficient tumor suppressor.', *Proceedings of the National*

Academy of Sciences of the United States of America, 100(25), pp. 15077–82. doi: 10.1073/pnas.2436255100.

Yue, Z., Qing, J. W. and Komatsu, M. (2008) 'Neuronal autophagy: Going the distance to the axon', *Autophagy*, 4(1), pp. 94–96. doi: 5202 [pii].

Zalc, B., Goujet, D. and Colman, D. (2008) 'The origin of the myelination program in vertebrates', *Current Biology*, 18(12), pp. 511–512. doi: 10.1016/j.cub.2008.04.010.

Zeng, L. *et al.* (2012) 'Death receptor 6 induces apoptosis not through type I or type II pathways, but via a unique mitochondria-dependent pathway by interacting with bax protein', *Journal of Biological Chemistry*, 287(34), pp. 29125–29133. doi: 10.1074/jbc.M112.362038.

Zhang, Y. *et al.* (2012) 'Assembly and Maintenance of Nodes of Ranvier Rely on Distinct Sources of Proteins and Targeting Mechanisms', *Neuron*, 73(1), pp. 92–107. doi: 10.1016/j.neuron.2011.10.016.

Zhao, H. *et al.* (2001) 'Impaired c-Jun amino terminal kinase activity and T cell differentiation in death receptor 6-deficient mice.', *The Journal of experimental medicine*. doi: 10.1084/jem.194.10.1441.

Zhao, Y.-Y. *et al.* (2012) 'Enriched environment increases the myelinated nerve fibers of aged rat corpus callosum', *Anatomical record*. doi: 10.1002/ar.22446.